THESIS

RAINFALL MONITORING
OF FLOOD EVENTS IN INDONESIA
USING GSMAP AND RAIN GAUGE DATA

NYOMAN SUGIARTHA

POSTGRADUATE PROGRAM
UDAYANA UNIVERSITY
DENPASAR
2013

THESIS

RAINFALL MONITORING
OF FLOOD EVENTS IN INDONESIA
USING GSMAP AND RAIN GAUGE DATA

NYOMAN SUGIARTHA
NIM 1191261007

MASTER DEGREE PROGRAM
GRADUATE STUDY OF ENVIRONMENTAL SCIENCE
POSTGRADUATE PROGRAM
UDAYANA UNIVERSITY
DENPASAR
2013

THESIS

RAINFALL MONITORING
OF FLOOD EVENTS IN INDONESIA
USING GSMAP AND RAIN GAUGE DATA

Thesis to get Master Degree
at Graduate Study of Environmental Science
Postgraduate Program Udayana University

NYOMAN SUGIARTHA
NIM 1191261007

MASTER DEGREE PROGRAM
GRADUATE STUDY OF ENVIRONMENTAL SCIENCE
POSTGRADUATE PROGRAM
UDAYANA UNIVERSITY
DENPASAR
2013

AGREEMENT SHEET

THIS THESIS HAS BEEN APPROVED
ON 5 SEPTEMBER 2013

Knowing

Director of
Postgraduate Program
Udayana University

Head of Graduate Study
of Environmental Science
Postgraduate Program
Udayana University

Prof. Dr. dr. A.A. Raka Sudewi, Sp.S (K).
NIP. 195902151985102001

Prof. Made Sudiana Mahendra, PhD.
NIP. 195611021983031001

RAINFALL MONITORING OF FLOOD EVENTS IN INDONESIA USING GSMAP AND RAIN GAUGE DATA

Thesis

Thesis to get Master Degree
at Graduate Study of Environmental Science
Postgraduate Program Udayana University

By:
NYOMAN SUGIARTHA

Approved by Committee

Committee Member

Committee Member

Ass. Prof. Dr. Takahiro Osawa

Dr. Ir. I Wayan Nuarsa, MSi.
NIP. 196805111993031003

Committee Member

Committee Member

Prof. Ir. I Wayan Arthana, MS, PhD.
NIP. 196007281986091001

Prof. Dr. I Wayan Budiarsa Suyasa, MS.
NIP. 196703031994031002

Head of Committee

Prof. Made Sudiana Mahendra, PhD.
NIP. 195611021983031001

This Thesis Has Been Examined and Assessed

by the Examiner Committees of Postgraduate Program Udayana University

on 19 August 2013

Based on Letter of Agreement from Rector of Udayana University

Number   : 1498/UN.14.4/HK/2013

Date   : 16 August 2013

The Examiner Committees are:

Head of Examiner: Prof. Made Sudiana Mahendra, PhD.

Members:

1. Prof. Dr. I Wayan Budiarsa Suyasa, MS.
2. Prof. Ir. I Wayan Arthana, MS, PhD.
3. Dr. Ir. I Wayan Nuarsa, MSi.
4. Ass. Prof. Dr. Takahiro Osawa

STATEMENT FREE FROM PLAGIARISM

The undersigned below:

NAME	: Nyoman Sugiartha
NIM	: 1191261007
DATE OF BIRTH	: Singaraja, 26 October 1970
ADDRESS	: Perumahan Tegal Jaya Permai I/28, Dalung, Kec. Kuta Utara, Kab. Badung, Bali
THESIS TITLE	: Rainfall Monitoring of Flood Events in Indonesia Using GSMaP and Rain Gauge Data

Hereby declare that the scientific work is plagiarism free. If in the future prove to have plagiarism in scientific work, and then I am willing to accept sanctions in accordance with the regulations of the Minister of Republic Indonesia number 17 in 2010 and regulations applicable in the Republic of Indonesia.

Denpasar, August 2013

I respectfully,

Nyoman Sugiartha

ACKNOWLEDGEMENTS

Denpasar, August 2013
Author

ABSTRACT

Indonesia which lies in equatorial region is recognised having potential of large rainfall amount during rainy season. As a consequence, the rainfall related natural disaster, such as flood is prominent and spreading in many places throughout the country. Study on the rainfall as well as its accurate monitoring is therefore one of fundamental importance for understanding flood mechanism and early warning.

This study evaluates rainfall intensity variation and patterns preceding flood events in Indonesia for the period of 2003-2010 using the GSMaP_MVK satellite-based rainfall product with one hour and 0.1^{o} x 0.1^{o} resolutions and rain gauge station data as a benchmark. The analysed data are 3-hourly average and daily accumulation time steps. The chosen research locations are Medan City, Pekanbaru City, Indragiri Hulu Regency, Samarinda City and Manado City.

The study also verifies accuracy of the GSMaP_MVK in detecting rain/no-rain conditions with respect to the rain gauge data for the flood events over the research locations using continuous and categorical verification statistics. Visual comparison of the two observation data have been made in the forms of time-series and scatter plots based on point to point analysis method.

Graphical comparisons of the GSMaP_MVK with the rain gauge data show discrepancies in capturing rainfall events and intensity. The GSMaP_MVK performs underestimation for the most areas, except Samarinda City, which is overestimated. Short-term period rainfall pattern is the most frequent occurred preceding flood events for the entire study areas which indicate that the areas are more susceptible to flash floods and river overflows.

Overall, the GSMaP_MVK product provides promising potentiality for the application of monitoring rainfall conditions preceding flood events over the research locations. Statistical verifications reveal that on average, correlation coefficients are (0.22-0.54) and (0.65-0.83) for 3-hourly and daily scale, respectively. While, probability of rain detections (PODs) are (0.57-0.75) and (0.93-0.99), accordingly.

Keywords: rainfall, monitoring, accuracy, GSMaP_MVK, rain gauge, flood events

ABSTRAK

Indonesia yang berada di daerah ekuator dikenal memiliki potensi jumlah curah hujan yang besar pada musim hujan. Sebagai konsekuensinya, bencana alam yang berhubungan dengan curah hujan menjadi menonjol dan tersebar di banyak tempat. Studi tentang curah hujan dan juga akurasi dalam pemantauannya, oleh karena itu merupakan salah satu hal mendasar yang penting untuk memahami mekanisme banjir dan peringatan dini.

Studi ini mengevaluasi variasi intensitas dan pola curah hujan yang terjadi sebelum kejadian banjir di Indonesia untuk periode tahun 2003-2010 dengan menggunakan produk curah hujan dari satelit yaitu GSMaP_MVK yang memiliki resolusi 1 jam dan 0.1^o x 0.1^o dan dengan data penakar curah hujan sebagai pembanding. Data yang dianalisis adalah rata-rata interval 3 jam-an dan akumulasi harian. Lokasi penelitian adalah Kota Medan, Kota Pekanbaru, Kabupaten Indragiri Hulu, Kota Samarinda dan Kota Manado.

Studi ini juga memverifikasi akurasi dari GSMaP_MVK dalam mendeteksi kondisi adanya hujan atau tidak ada hujan terhadap data dari penakar curah hujan untuk kejadian banjir di lokasi penelitian dengan menggunakan verifikasi statistik kontinu dan kategori. Perbandingan visual dari kedua data pengamatan disajikan dalam bentuk runut waktu dan diagram hambur berdasarkan metode analisis titik ke titik.

Perbandingan secara grafis dari data GSMaP_MVK dan data penakar curah hujan menunjukkan adanya perbedaan dalam memantau kejadian curah hujan dan intensitasnya. Data GSMaP_MVK menunjukkan estimasi lebih kecil dibandingkan dengan data penakar curah hujan untuk sebagian besar lokasi, kecuali Kota Samarinda yang menunjukkan estimasi lebih besar. Pola curah hujan dengan interval singkat adalah paling sering terjadi sebelum kejadian banjir untuk semua lokasi yang mengindikasikan bahwa lokasi tersebut lebih rentan terhadap banjir bandang dan banjir oleh luapan sungai.

Secara keseluruhan, produk GSMaP_MVK memberikan potensi yang menjanjikan dalam aplikasi untuk memantau kondisi curah hujan sebelum kejadian banjir di lokasi penelitian. Verifikasi statistik menunjukkan bahwa secara rata-rata koefisien korelasi adalah 0.22-0.54 untuk data 3 jam-an dan 0.65-0.83 untuk data harian. Sementara itu, angka probabilitas pemantauan terjadinya hujan adalah 0.55-0.75 untuk data 3 jam-an dan 0.93-0.99 untuk data harian.

Kata kunci: curah hujan, pemantauan, akurasi, GSMaP_MVK, penakar curah hujan, kejadian banjir

SUMMARY

Nyoman Sugiartha: Rainfall Monitoring of Flood Events in Indonesia Using GSMaP and Rain Gauge Data

Indonesia which lies in equatorial region is recognised having potential of large rainfall amount during rainy season. As a consequence, the rainfall related natural disaster, such as flood is prominent and spreading in many places throughout the country. Study on the rainfall as well as its accurate monitoring is therefore one of fundamental importance for understanding flood mechanism and designing reliable flood disaster mitigation and early warning.

Ground-based rain gauge is a conventional device to measure rainfall amount and considered as a point measurement. While, satellite-based rainfall estimates provides complement measurement over wide coverage area having few or even no in situ data. The combination of the two measurement systems is necessary for monitoring rainfall condition of the flood events, especially for the purpose of understanding accuracy of the satellite data.

Previous study by Aryastana (2012) noted that the GSMaP_MVK satellite-based rainfall product detected irregular rainfall pattern with no heavy rain before floods occur in the regency of Medan City (2 events), Indragiri Hulu (2 events), Samarinda City (2 events), Manado City (1 event) and Jambi City (2 events). Hence, further investigations are needed to verify that the rainfall events were correctly captured by the GSMaP_MVK algorithm. The rain gauge data are then used for comparison in terms of rain/no-rain detection capability with the GSMaP_MVK estimates for those areas, except Jambi City due to no continuous rain gauge data available.

The main objective of this study is to evaluate potentiality of the GSMaP_MVK product for monitoring rainfall condition of the flood events in Indonesia, especially in Medan City, Indragiri Hulu Regency, Pekanbaru City, Samarinda City and Manado City. The specific objectives include (1) to compare variations of rainfall intensity of the flood events as observed by the GSMaP_MVK product with that measured by rain gauge station, (2) to identify pattern of rainfall preceding flood events based on the GSMaP_MVK product estimates and the rain gauge measurements, and (3) to verify accuracy of the GSMaP_MVK product estimates versus the rain gauge measurements using continuous and categorical verification statistic scores (i.e. ME, MAE, RMSE, correlation coefficient, POD, FAR and TS).

This study used data of the flood events for the period of 2003-2010, the GSMaP_MVK satellite data with hourly and 0.1^{o} x 0.1^{o} resolutions and the rain gauge station data as a benchmark. The analysed data are 3-hourly average and daily accumulation time steps. Comparison of the GSMaP_MVK with rain gauge data is made in an attempt to understand the difference of the two measurements in capturing rainfall event fluctuations before and after the floods occur.

Visual comparisons between the GSMaP_MVK and rain gauge data show discrepancies in capturing rainfall events and intensity of preceding and following the flood events over Medan City, Pekanbaru City & Indragiri Hulu Regency, Samarinda City and Manado City. However, the GSMaP_MVK product quite match in detecting rainfall occurrences but were less match in estimating the 3-hourly rainfall intensity. The daily observations show better matching than the 3-hourly data.

Meanwhile, rainfall fluctuations of preceding and following the flood events show widely differs from event to event due to magnitude underestimation or overestimation by the GSMaP_MVK satellite estimates with respect to the rain gauge data. The GSMaP_MVK underestimated the rainfall intensity over Medan City, Pekanbaru City & Indragiri Hulu Regency and Manado City, but overestimated over Samarinda City. The GSMaP_MVK are generally overestimated to light rainfall and less sensitive to heavy rainfall.

Short-term period rainfall pattern is the most frequent occurred preceding flood events in Medan City, Pekanbaru City & Indragiri Hulu Regency, Samarinda City and Manado City accounted for about 63.6%, 60%, 66.7% and 66.7%, respectively. These areas are also known as urban regions with some rivers flows nearby, which likely indicate the regions are more susceptible to flash floods and river overflows.

Overall, the GSMaP_MVK product provides promising potentiality for the application of monitoring rainfall conditions preceding flood events over the research locations. Statistical verifications reveal that on average, correlation coefficients are (0.22-0.54) and (0.65-0.83) for 3-hourly and daily scale, respectively. While, probability of rain detections (PODs) are (0.57-0.75) and (0.93-0.99), accordingly.

In this study, the rain gauge density for Medan City, Pekanbaru City, Indragiri Hulu Regency, Samarinda City and Manado City are 265.1, 632.26, 8198, 718, 159.02 km^2 per station, respectively. These figures are much larger than the minimum requirement by the WMO (1994), which is about 10 to 20 km^2 per station for urban areas. Hence, the accuracy of the GSMaP_MVK product is roughly represented due to the scarcity of the rain gauge measurements or coarser rain gauge spatial resolution which results in unavoidable rain gauge sampling error.

As recommendations, more extents data, such as number of rain gauge station, flood locations and events are required for detail study on the accuracy of rainfall monitoring by the GSMaP_MVK product. This is in order to assess representativeness of Indonesia region and the applicability of the GSMaP_MVK product over the region with few or even non-existence rain gauges. Presently, however, availability of the rain gauge stations providing continuous rainfall data are very limited and low distributed over Indonesia, which considers as a challenge. For a comprehensive study on the prediction of flood events in Indonesia, the GSMaP_MVK product as well as the rain gauge data could be utilised in conjunction with other satellite data (e.g. MODIS, ALOS, etc.) and hydrological model.

TABLE OF CONTENTS

LIST OF FIGURES

LIST OF TABLES

LIST OF ABBREVIATIONS

ADEOS-II	:	Advanced Earth Observation Satellite-II
ALOS	:	Advanced Land Observing Satellite
AMSR	:	Advanced Microwave Scanning Radiometer
AMSR-E	:	Advanced Microwave Scanning Radiometer-Earth Observing System
AMW	:	Active Microwave
AVHRR	:	Advanced Very High Resolution Radiometer
BMKG	:	Badan Meteorologi, Klimatologi dan Geofisika
BNPB	:	Badan Nasional Penanggulangan Bencana
CMORPH	:	CPC MORPHing technique
CPC	:	Climate Prediction center
CPR	:	Cloud Profiling Radar
CPU	:	Central Processing Unit
CReSOS	:	Center for Remote Sensing and Ocean Sciences
CREST	:	Core Research for Evolutionary Science and Technology
CTT	:	Cloud Top Temperatures
DCM	:	Double Correlation Method
DFO	:	Dartmouth Flood Observatory
DMSP	:	Defense Meteorological Satellite Program
EORC	:	Earth Observation Research Center
FAR	:	False Alarm Ratio
GB	:	Gigabyte
GEO	:	Geostationary Earth Orbit
GFAS	:	Global Flood Alert System
GOES	:	Geostationary Operational Environmental Satellites
GPM	:	Global Precipitation Mission
GSMaP	:	Global Satellite Mapping of Precipitation
HDD	:	Hard Disk Drive
HRPP	:	High-Resolution satellite-based Precipitation Product
IFNet	:	International Flood Network
IR	:	Infrared
ITCZ	:	Inter-tropical Convergence Zone
JAXA	:	Japan Aerospace Exploration Agency
JJ	:	June-July
JST	:	Japan Science and Technology Agency
LEO	:	Low Earth Orbit
MAM	:	March-April-May
ME	:	Mean Error
MHS	:	Microwave Humidity Sounder
MJJAS	:	May-June-July-August-September
MLIT	:	Ministry of Land, Infrastructure, Transport and Tourism
MODIS	:	Moderate Resolution Imaging Spectroradiometer
MSG	:	Meteosat Second Generation

MV	:	Moving Vector
MVK	:	Moving Vector and Kalman filter
MW	:	Microwave
MWR	:	Microwave Radiometer
NDJFM	:	November-December-January-February-March
NOAA	:	National Oceanic and Atmospheric Administration
NW	:	Northwest
ON	:	October-November
PERSIANN	:	Precipitation Estimation from Remotely Sensed Information using Artificial Neural Networks
PMM	:	Precipitation Measuring Mission
PMW	:	Passive Microwave
POD	:	Probability of Detection
PR	:	Precipitation Radar
RAM	:	Random Access Memory
RMSE	:	Root Mean Square Error
SE	:	Southeast
SEVIRI	:	Spinning Enhanced Visible and InfraRed Imager
SSM/I	:	Special Sensor Microwave/Imager
SSMIS	:	Special Sensor Microwave Imager and Sounder
TB	:	Terrabyte
TMI	:	TRMM Microwave Imager
TMPA	:	TRMM Multi-satellite Precipitation Analysis
TRMM	:	Tropical rainfall Measuring Mission
TS	:	Threat Score
UTC	:	Coordinated Universal Time
VIS	:	Visible
WMO	:	World Meteorological Organization

CHAPTER I

INTRODUCTION

1.1   Background

Flood is a prevalent threatening natural disaster in Indonesia and spreading in many places throughout the country. Recurrence of the flood is usually during rainy season. Owing to the geographical location in the Tropical region, large rainfall amount is potential over the most area. Many rivers provide great advantages for rain water distribution from upstream to downstream. However, they may also contribute to the flood potential, especially at urban areas nearby the rivers as their upstream paths are artificially changed by intense human activities, such as deforestation.

Rainfall is commonly known as one of major factors triggering flood. Amount of rain falls during certain period of time over the area could determine how fast the flood starts to occur. Flash flood happens when a great amount of rain storm falls over a relatively small area in a very short period of time. This kind of storm causes the drainage systems to be out of capacity to flow the excess water, in which could quickly inundate the low land of the area. The study of rainfall is thus of fundamental importance for understanding flood mechanism and detection.

Monitoring and measurement of the rainfall is crucial to our well-being and critical to the application in hydrological and water resources management (Kidd and Huffman, 2011). The information on rainfall variations preceding flood

events in conjunction with the application of hydrological model is essential for establishing a reliable flood early warning system. Subsequently, providing real time or very near real time rainfall data are mandatory to support such a system. In general, there are two sources to collect the rainfall data, i.e. conventional rain gauge networks and remote sensing systems, such as ground-based weather radar and satellites.

The rain gauge is a relatively simple instrument which directly samples the rain by accumulating rain drops continuously over a fixed time interval at individual locations. With a good rain gauges network, it is possible to map rainfall over small areas but this approach is not practical for large areas, remote land areas of the globe or for oceans (Strangeways, 2007; Mustafa, 2007). The rain gauge observations are usually considered as a reference or ground truth due to a fairly accurate and reliable measurement with a very low error but its spatial coverage is limited (Sinclair and Pegram, 2005; Ciach and Krajewski, 1999).

Ground-based weather radar system is also an alternative to provide real time data of rainfall event. The use of weather radar addresses some of the issues of rain gauge coverage, at least where radar exists. In particular, it provides a spatial measurement of the rainfall (areal averages) rather than point measurements provided by the rain gauges. However, this system actually is still rare to be applied in Indonesia due to relatively high investment and maintenance costs. Instead of well arranged of the rain gauges network, many of watershed in Indonesia are in un-gauged condition, especially on the outside of Java Island (Suseno, 2009; Kidd and Huffman, 2011).

The other resource of real time rainfall data is provided by satellite observation based on areal-average estimates. Satellite-based rainfall data add valuable information to climate databases due to their wide geographical coverage, especially over areas with few or completely missing in situ data (WMO, 2011). The satellite-based rainfall data has the potential to become a cost effective source of input for flood predictions under a variety of circumstances in comparison with the in situ network measurements. This is due to their increasingly available on a global basis from the internet and uninterrupted during catastrophic situations (Harris *et al*., 2007).

There are several sources of global high-resolution satellite-based precipitation product (HRPP) that are freely accessible via internet, e.g. the GSMaP (GSMaP_MVK, GSMaP NRT), the TMPA (TRMM 3B42, 3B41RT), the CMORPH, the PERSIANN, etc. All of them are currently available on gridded datasets in both real time and post-real time. The GSMaP provides rainfall product with one hour temporal resolution and 0.1 degree of latitude by 0.1 degree of longitude spatial resolution (Okamoto *et al*., 2007). Presently, the GSMaP incorporates extensive satellite input data streams from both passive microwave and infrared sensors, and its global precipitation maps are appealing for a wide range of hydrological applications, such as flood monitoring and forecasting (Tian *et al*., 2010).

Previous study by Aryastana (2012) noted that the GSMaP_MVK product detected irregular rainfall pattern with no heavy rain before floods occur in the regency of Medan City (2 events), Indragiri Hulu (2 events), Samarinda City (2

events), Manado City (1 event) and Jambi City (2 events). Hence, further investigations are needed to verify that the rainfall events were correctly captured by the GSMaP_MVK algorithm.

In this study, rain gauge data are then used for comparison with the GSMaP_MVK estimates for those areas, except Jambi City due to no continuous rain gauge data available. This study addresses evaluation of the potentiality of the GSMaP_MVK application through preliminary verification of its performance in terms of rain/no-rain detection of the flood events compared with the rain gauge data. It is not to predict when and where the floods will start to occur. The verification is constraint by very limited number of rain gauge stations providing continuous data (i.e. only one rain gauge station is available for each regency). Subsequently, it is expected that applicability of the GSMaP_MVK product could be extended over other areas with few or even non-existence rain gauges data.

1.2 Problems Formulation

The research questions addressed in this study are as follows:

a. What are variations of rainfall intensity of flood events as monitored by the GSMaP_MVK product compared with the rain gauge measurements?

b. What are rainfall patterns of preceding flood events monitored by the GSMaP_MVK product and the rain gauge measurements?

c. What is the accuracy of the GSMaP_MVK product compared with the rain gauge measurements for monitoring rainfall condition of flood events?

1.3   Research Objectives

The main objective of the study is to evaluate potentiality of the GSMaP_MVK product for the application of monitoring rainfall condition of flood events in Indonesia, especially in Medan City, Indragiri Hulu Regency, Pekanbaru City, Samarinda City and Manado City.

The specific objectives include:

a. To compare variations of rainfall intensity of the flood events as observed by the GSMaP_MVK product with that measured by rain gauge station.

b. To identify pattern of rainfall preceding flood events based on the GSMaP_MVK product estimates and the rain gauge measurements.

c. To verify accuracy of the GSMaP_MVK product estimates versus the rain gauge measurements using continuous and categorical verification statistic scores (i.e. ME, MAE, RMSE, correlation coefficient, POD, FAR and TS).

1.4   Research Benefits

The research benefits expected to be achieved are as follows:

a. To deliver information on the variations of rainfall intensity based on the satellite and rain gauge data, in which could be used in conjunction with hydrological models to evaluate flood response of the areas.

b. To provide information on the pattern of rainfall condition preceding flood events, which can be useful for flood identification, monitoring and early warning of the areas.

c. To provide preliminary information on the accuracy of the GSMaP_MVK product estimates and its applicability to support implementation of a reliable flood detection system over un-gauged areas.

CHAPTER II

LITERATURE REVIEW

2.1   Climate of Indonesia

Indonesia consists of a large number of islands spanning the Equator from 6°N to 11°S and 95 °E to 141 °E. The equatorial situation means that temperatures remain high throughout the year with little variation from month to month. The main variable of Indonesia's climate is not temperature or air pressure, but rainfall. Winds are moderate and generally predictable, with monsoons usually blowing in from the south and east in June through September and from the northwest in December through March (Met Office, 2011; Frederick and Worden, 2011).

Extreme variations in rainfall are linked with the monsoons. There is a dry season (June to September), influenced by the Australian continental air masses, and a rainy season (December to March) that is influenced by air masses from mainland Asia and the Pacific Ocean. Local conditions in Indonesia, however, can greatly modify these patterns, especially in the central islands of the Maluku group. This oscillating seasonal pattern of wind and rain is related to Indonesia's geographic location as an archipelago between two continents and astride the equator (Frederick and Worden, 2011).

Prevailing wind patterns interact with local topographic conditions to produce significant variations in rainfall throughout the archipelago. In general, the western and northern parts of Indonesia experience the most precipitation because the northward- and westward-moving monsoon clouds are heavy with

moisture by the time they reach these more distant regions. The average annual rainfall for Indonesia is around 3,175 millimeters. Western Sumatra, Java, Bali, and the interiors of Kalimantan, Sulawesi, and Papua are the most consistently damp regions of Indonesia, with rainfall measuring more than 2,000 millimeters per year (Frederick and Worden, 2011).

2.1.1 Rainfall regions

Aldrian and Susanto (2003) divided Indonesia into three dominant rainfall regions with distinct characteristics based on the annual rainfall cycle or the annual mean variability using double correlation method (DCM) as can be seen in Figures 2.1 and 2.2.
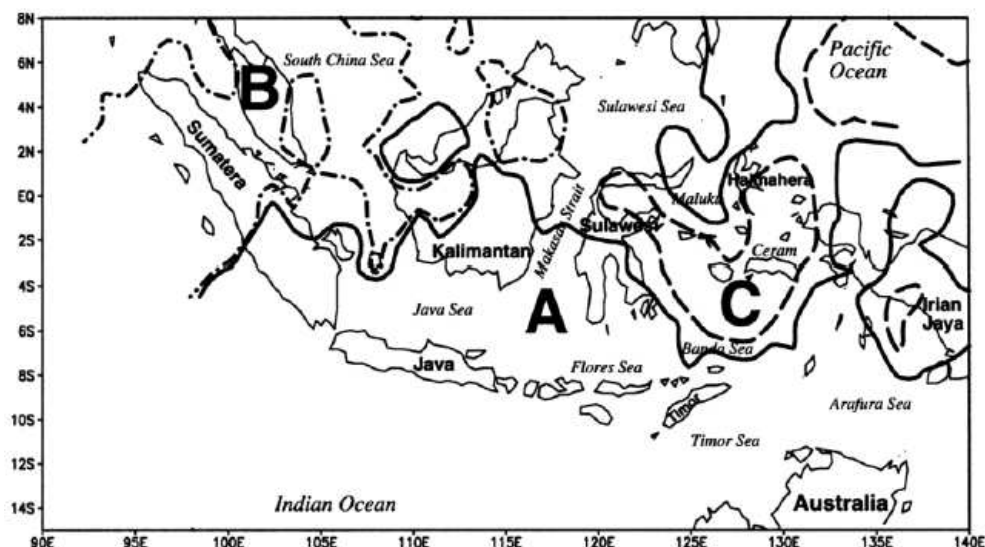
Figure 2.1 The three climatic regions of Indonesia based on DCM. Region A in solid line, Region B in short dashed line and Region C in long dashed line
(Aldrian and Susanto, 2003)

Region A is located in southern Indonesia from south Sumatera to Timor Island, southern Kalimantan, Sulawesi and part of Irian Jaya. Region B is located in northwest Indonesia from northern Sumatra to northwestern Kalimantan. Region C encompasses Maluku and northern Sulawesi (Aldrian and Susanto, 2003).
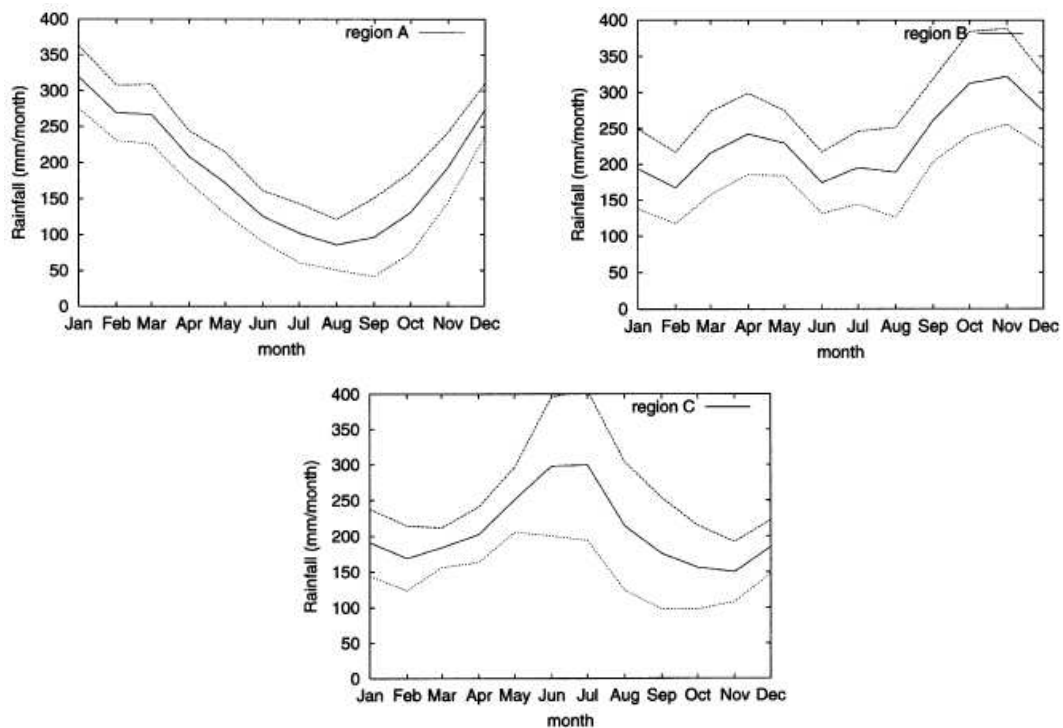
Figure 2.2 The annual cycles of the three climate regions (solid lines) using the DCM. Dashed lines indicate one standard deviation (σ) above and below average (Aldrian and Susanto, 2003)

Region A has one peak and one trough and experiences strong influences of two monsoons, namely the wet northwest (NW) monsoon from November to March (NDJFM) and the dry southeast (SE) monsoon from May to September (MJJAS). Region B has two peaks, in October–November (ON) and in March to May (MAM). Those two peaks are associated with the southward and northward

movement of the inter-tropical convergence zone (ITCZ). Region C has one peak in June to July (JJ) and one trough (November–February). The JJ peak in Region C is about 300 mm/month, whereas the peaks in Regions A and B are 320 mm/month and 310 mm/month respectively (Aldrian and Susanto, 2003).

The minimum in region A is the lowest and reaches a mean below 100 mm/month. Thus, Region A is the driest region during the dry season in July–September and the wettest region in December. Region C has one peak in the middle of year (JJ), whereas the other two regions have their peaks near the end or beginning of the year. There is a strong evidence of the possibility of ocean influence in Region C. Region C, or Maluku, is along the eastern route of the Indonesian Through Flow (Aldrian and Susanto, 2003).

2.1.2   Flood events

Flood has great impacts to many communities and economics in Indonesia. Recurrence of the flood in the country is increasing considerably with heavy losses to life and property. Within the period of 2003-2010, there were about 5,186 flood disaster incidences (Figure 2.3), which accounted for 45.5% of the total natural disasters (BNPB, 2013; Brakenridge, 2013). During that course of period, there were about 648 flood events occurred annually. Java Island experienced the most frequent flood occurrence accounted for 44.3 % of the total events, followed by Sumatera, Sulawesi and Kalimantan with 23.4%, 14.7% and 11.9%, respectively. In total about 2,388 people died and more than 4.5 million people were evacuated. The impacts on infrastructures included more than 3.1

million units houses, 1.69 million ha crop fields and 100,196 km roads were inundated or damage.
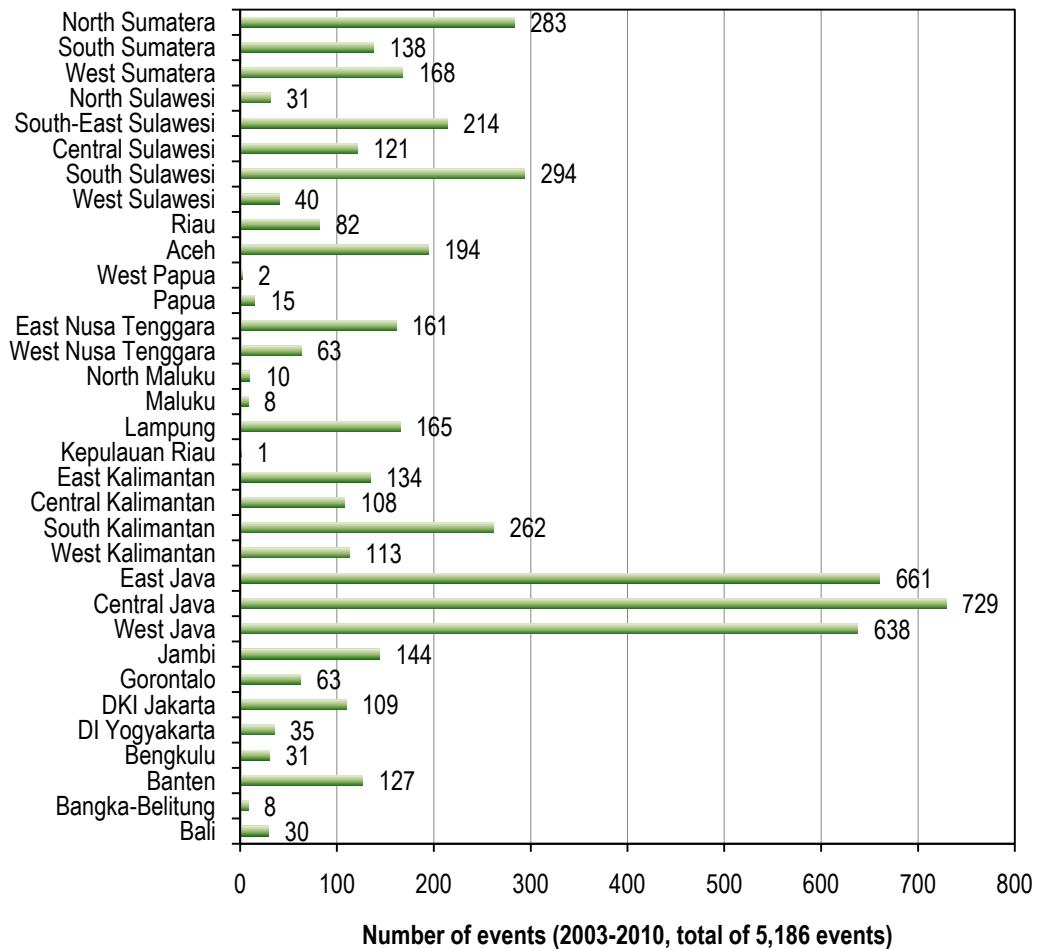
Figure 2.3 Statistic of flood events in Indonesia by province (2003-2010)
(BNPB, 2013; Brakenridge, 2013)

Based on Sutardi (2006) the conversion of upland forests and coastal wetlands to agricultural use in Java, Sumatra, Kalimantan and Sulawesi has led to soil erosion, watershed degradation and the loss of valuable marine resources. Because of the high rainfall intensities and watershed erosion, most river carry large quantities of sediment which result in river regime problems as well as river

mouth clogging. Due to the flat slopes and inadequate carrying capacity in lower reaches, many rivers experience flooding in the lower reaches.

There are several factors contributing to the increased number of flood casualties, such as economic development on floodplains, urbanisation to the area at risk from floods forced by increased population and poor drainage networks as well as their management and control. According to WMO (1994), urban flooding can be of two distinct kinds. First, urban areas can be inundated by rivers overflowing their banks. Second, the urban flooding can occur as a special case of flash flooding. In this case, intense rainfall over the urban area may cause flooding of streets and property in low-lying areas or in built-up areas in old waterways, underpasses, depressions in highways, etc.

Table 2.1

Examples of flooding mechanisms, reproduced from Sene (2008)

Type	Example	Typical types of flooding
Atmospheric	Frontal depressions	Extensive river flooding, coastal surge and wave overtopping, estuary and delta flooding, urban and pluvial (surface water) flooding
	Thunderstorms	Fast response/flash flooding and urban and pluvial (surface water) flooding
	Monsoon	Extreme prolonged rainfall causing a range of river and urban flooding issues
	Tropical cyclones	Coastal surge and wave overtopping, inland flooding, estuary and delta flooding
	Snowmelt	Extensive river flooding
	Ice jams	Rapid rises in river levels
	Glacial lake outburst flows	Fast moving, deep river flows
Geotechnical	Dam break	Fast moving, deep river flows
	Defence breach	Extensive inundation of coastal or inland areas
	Tsunami	Extensive inundation of coastal margins
	Debris flow	Destructive flows with high mud and rock content

Sene (2008) described that the causes of flooding are either atmospheric or geotechnical as can be seen in Table 2.1. Atmospheric hazards include heavy rainfall causing rivers to flood, coastal and estuarine flooding due to surge, wave and wind effects. Geotechnical factors (e.g. landslides, debris flows and earthquakes) can also lead to raised river levels causing inland flooding and tsunami waves resulting in coastal flooding.

2.2   Satellite-based Rainfall Monitoring

Meteorological satellites have been at the forefront of Earth observation with improvements in satellite and sensor technology to provide the current range of operational meteorological observations and quantitative information on precipitation from the satellite observations. There are two broad categories of meteorological satellites, i.e. geostationary (GEO) satellites and low orbiting (LEO) satellites, which include polar-orbiting satellites (Kidd and Huffman, 2011, Ceccato and Dinku, 2010) and they are complementary each other (Kelkar, 2007). Figure 2.4 shows global meteorological satellites orbit and Table 2.2 summarises the main instrumentation used for the estimation of precipitation, covering both visible (VIS) and infrared (IR) sensors and those in the microwave (MW) region of the spectrum.

GEO satellites orbit the Earth about 35,800 km above the equator. At this distance, the orbital period of the satellite is equal to the rotational period of the Earth, exactly one sidereal day. The result is that the satellite is at a fixed position relative to the Earth. Each GEO satellite is able to view about one third of the

Earth's surface. From their position they are able to provide imagery on a frequent and regular basis (Kidd and Huffman, 2011; Tempfli *et al*., 2009).
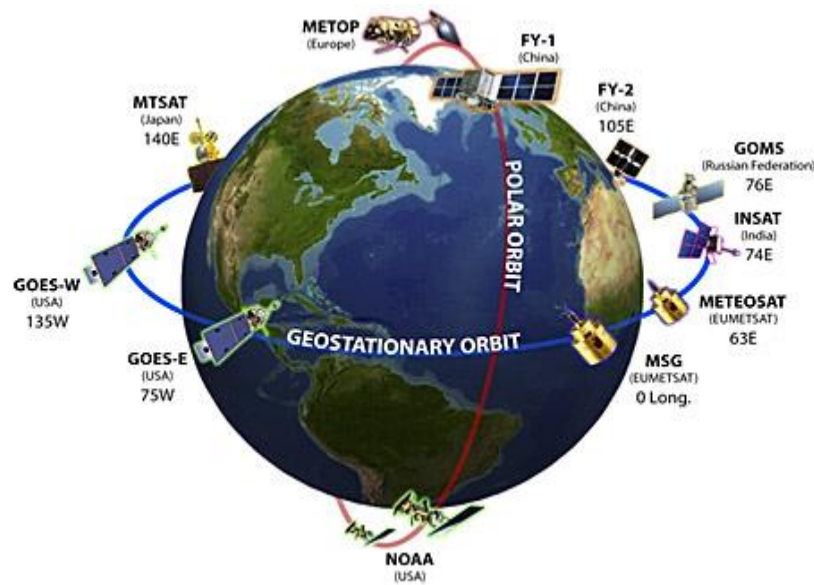
**Figure 2.4 Illustration of global meteorological satellites orbit
(http://www.eumetsat.int)**

LEO satellites can be subdivided into sun-synchronous and non-sun-synchronous missions. Operational meteorological satellites fall into the former category, with orbital characteristics such that they cross the Equator at the same local time on each orbit, providing up to two overpasses daily. Most sun-synchronous orbits cross the equator at mid-morning at around 10:30 hour local solar time. In addition to day-time images, a sun-synchronous orbit also allows the satellite to record night-time images (thermal or radar) during the ascending phase of the orbit at the dark side of the Earth (Kidd and Huffman, 2011; Tempfli *et al*., 2009).

Table 2.2

Summary of commonly-used satellite instrumentation for precipitation estimation, reproduced from Kidd and Huffman (2011)

Instrument	Satellite	Channels	Bands	Resolution (km)	Sampling
AVHRR	NOAA/MetOp	5	VIS-IR	1	Twice daily
SEVIRI	MSG	11	VIS-IR	1-3	15 min
GOES Imager	GOES	5	VIS-IR	1-4	30 min
MODIS	Aqua/Terra	36	VIS-IR	0.25-1	Twice daily
SSM/I	DMSP	7	19-85 GHz	12.5-25	Twice daily
SSMIS	DMSP	11	19-183 GHz	13-45	Twice daily
TMI	TRMM	9	10-85 GHz	5-25	Twice 2-days
AMSU	NOAA/MetOp	5	23.8-183 GHz	20-50	Twice daily
MHS	NOAA/MetOp	5	89-190 GHz	17-50	Twice daily
AMSR	Aqua	12	6-85 GHz	5-25	Twice daily
PR	TRMM	1	13.6 GHz	5	Twice 3-days
CPR	CloudSat	1	94 GHz	1.4	Once 16-days

The choice of polar-orbiting versus geostationary platforms for rainfall estimation entails several tradeoffs with regard to temporal and spatial sampling and geographical coverage: a geostationary satellite positioned over the equator can provide high frequency (hourly or better) images of a portion of the tropics and middle latitudes, while a polar orbiter provides roughly twice-daily coverage of the entire globe (Petty and Krajewski, 1996).

The primary scope of satellite rainfall monitoring is to provide information on rainfall occurrence, amount and distribution over the globe for meteorology at all scales, climatology, hydrology, and environmental sciences. The accuracy of hydro-meteorological predictions significantly relies on the quality of observed rainfall intensity, pattern, duration, and aerial extent. The uneven distribution of rain gauges and weather radars and the relative lack of rainfall measurements over the oceans have significantly limited the use of global and local data, thus

highlighting the importance of satellite-based global rainfall data (Levizzani *et al*., 2002; Sorooshian *et al*., 2011).
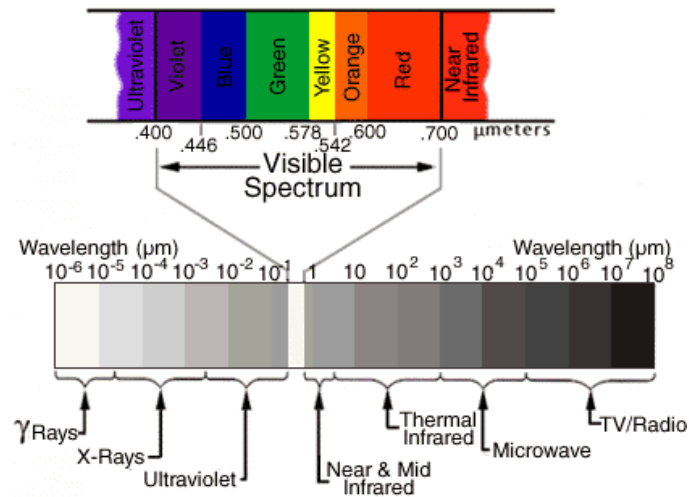
Figure 2.5 Electromagnetic spectrum of particular wavelength
(http://www.astro.virginia.edu/class/oconnell/astr130/dev2.html)

The rainfall measurements from space are based on the interpretation of the electromagnetic radiation that is scattered and emitted from clouds, precipitation and the underlying surface, and is monitored by the satellite instruments at the various wavebands (Rosenfeld, 2007). Satellite estimates of rainfall can be derived from a range of observations from many different sensors. The retrieval methodologies fall primarily into three main categories based upon type of observation, primarily VIS/IR techniques, MW (passive and active) techniques, and multi-sensor techniques (Kidd and Levizzani, 2011; Kelkar, 2007). Figure 2.5 shows electromagnetic spectrum of particular wavelengths.

2.2.1   VIS/IR-based techniques

Observations made in the VIS and IR parts of the spectrum remain the mainstay of operational meteorological Earth observations. Rainfall can be inferred from VIS images since bright clouds tend to be thick, and thick clouds are more likely to be associated with rainfall. However, the relationship between brightness and the rainfall is poor and consequently VIS imagery is usually only available during daylight and used in conjunction with other observations (Kidd and Levizzani, 2011; Kidd and Huffman, 2011; Ceccato and Dinku, 2010).

IR imagery at wavelengths between 8.0 and 15.0 µm that measures the thermal emissions from objects is potentially more useful, and is available night and day. Heavier rainfall tends to be associated with larger, taller clouds with colder cloud tops. By observing cloud top temperatures (CTT) a simple rainfall estimate can be derived. However, the CTT to rainfall relationship is indirect, with significant variations in the relationship during the lifetime of a rainfall event, between rain systems, and between climatological regimes (Kidd and Levizzani, 2011; Kidd and Huffman, 2011; Ceccato and Dinku, 2010).

The main drawback of VIS/IR techniques, despite the frequency of their observations, is that the relationship between the cloud top temperature and the surface rainfall is indirect. This is often manifested in thin and high-cloud (i.e. cirrus) appearing as rain bearing cloud, while warm and low-level rain cloud (i.e. stratus) is omitted (Kidd *et al*., 2009) Although the high spatial and temporal resolution of VIS/IR data from geostationary satellites make them ideally suited for satellite precipitation estimates, the relationship between rainfall rate and the

characteristics is best suited for convective precipitation, for which the cloud-top height and cloud depth are somewhat related (Scofield and Kuligowsky, 2003).

2.2.2 Passive microwave techniques

Radiation emitted at microwave wavelengths (between 1.0 and 300 mm) is influenced strongly by the nature of emitting surface (whether rough or smooth, wet or dry) and the size of particles through which it passes. Microwaves (MW) are strongly affected by water drops and ice crystals in cloud. MW can actually distinguish between clouds with drops big enough to produce rain and other clouds. MW frequencies can also penetrate cirrus clouds. However, though rainy areas show up very well over the oceans as bright against a dark background, it more complicated over the land because the background emission from the surface is very variable (Ceccato and Dinku, 2010; Kelkar, 2007).

Passive MW (PMW) rainfall retrieval algorithms can be generally classified into (1) emission type algorithms (e.g. Wilheit *et al*., 1991), (2) scattering type algorithms (e.g. Spencer *et al*., 1989), and (3) multichannel inversion algorithms (e.g., Bauer, 2001). These can in turn be divided into empirical techniques which are calibrated against surface data sets (and incorporate beam-filling/inhomogeneous field-of-view, absolute calibration issues, resolution differences), and physical techniques that minimise the difference between modelled and the observed radiation (Kidd and Levizzani, 2011; Kidd and Huffman, 2011).

The main drawback of PMW-based techniques is that observations are currently only available from low-Earth orbiting satellites, typically resulting in

two observations per day per satellite. The retrieval of precipitation using PMW observations has always represented a problem over coastal areas; often techniques omit retrievals over the coastline, or use a less optimum technique (Kidd and Levizzani, 2011; Kidd and Huffman, 2011; Kelkar, 2007). PMW rainfall retrieval is subject to errors caused by various factors ranging from instrument issues (e.g. calibration and measurement noise) to the high complexity and variability in the relationship of brightness temperatures to precipitation parameters (Hossain *et al*., 2004).

2.2.3   Active microwave techniques

Active MW (AMW) techniques offer the most direct of all satellite quantitative estimation methods. Despite this, radar technology for spaceborne precipitation estimation has been limited primarily to the TRMM PR. As with all radar systems, the PR relies upon the interpretation of the backscatter of radiation from the precipitation, the amount being broadly proportional to the number of precipitation-sized particles and therefore intensity. However, the precipitation intensity to backscatter relationship is not constant. Nevertheless, the PR has been extensively used as a primary source of high-quality rainfall estimates for evaluating the differences of rainfall regimes over land and over the ocean (Kidd and Huffman, 2011; Kelkar, 2007).

2.2.4   Multi sensor techniques

Single-sensor retrievals have the relative advantage of processing simplicity, but the VIS/IR lack the directness of the PMW and the PMW lack the frequency sampling of the VIS/IR. Therefore, to overcome the deficiencies of

individual satellite systems a number of techniques have been developed to exploit the combination of different satellite observations. Techniques developed to exploit VIS/IR and PMW observations essentially fall into those that use the PMW to calibrate the IR observations, and those that derive cloud motion from the IR data to move PMW precipitation estimates (Kidd *et al.*, 2009; Kidd and Levizzani, 2011; Kidd and Huffman, 2011).

IR data can be usefully employed to measure cloud movement, which can be used to advect, or morph the more direct PMW-retrieved precipitation between the successive LEO PMW satellite overpasses. Examples of current state-of-the-art methodologies are the Climate Prediction Center Morphing technique (CMORPH; Joyce *et al.*, 2004) and the Global Satellite Mapping of Precipitation (GSMaP; Kubota *et al.*, 2007). The main drawback of this methodology is that the retrieved cloud motion might not necessarily represent the true motion of the precipitation at the surface, particularly if changes in the surface precipitation pattern occur between the infrequent PMW overpasses (Kidd and Huffman, 2011).

2.3 Rainfall Measurement by Rain Gauges

Historically, rain gauges have been the main source of rainfall data. However, in many parts of the world the rain gauge network is too sparse to produce reliable areal estimates, and radar is not feasible either on the grounds because of cost, technological infrastructure or topography. The rain gauges that measure rainfall at a point remain the most common approach to ground-based measurement (Kidd, 2001; New *et al.*, 2001; Grimes *et al.*, 1999).

The rain gauge networks provide rainfall measurements with a high degree of accuracy at specific locations but, in most cases, the instruments are too sparsely distributed to accurately capture the high spatial and temporal variability of precipitation systems (Villarini *et al.*, 2008). The optimum density of a rainfall gauge network depends on the purpose for which data are to be used. For example, accurate measurements of rainfall for flood forecasting require denser networks as compared to rainfall-runoff modelling (Jain and Singh, 2003). WMO (1994) recommended minimum network densities for precipitation stations as depicted in Table 2.3. At least 10% are automatic recording gauges.

Table 2.3

Recommended minimum densities for precipitation stations, reproduced from WMO (1994)

Physiographic Unit	Minimum densities per station (area in km^2 per station)	
	Non-recording	Recording
Coastal	900	9,000
Mountainous	250	2,500
Interior plains	575	5,750
Hilly/undulating	575	5,750
Small islands	25	250
Urban areas		10-20
Polar/arid	10,000	100,000

The rain gauge rainfall data are subject to errors, biases and inhomogeneities arising from several sources. Inaccurate measurements for individual days and months most often arise through observer errors, either during measurement or transcription to paper or digital records. Comprehensive checking of suspect measurements is time consuming, usually requiring comparison with

nearby station data, station metadata and documentary records and possibly, original registers (New *et al*., 2001).

For analysis of climate change and trends at regional and larger scales, the effects of errors and inhomogeneities at individual stations are reduced in the averaging of multiple station series that occurs in the calculation of regional time series (New *et al*., 2001). In general, the rain gauge observations yield relatively accurate point measurements of rainfall but also suffer from sampling error in representing areal average (Adeyewa and Nakamura, 2003).

2.4   Comparison between Satellite-based and Rain Gauge Estimates

Measured data from rain gauge networks are still conventionally the most reliable source of area-averaged precipitation for the land surface of the Earth. Satellite-based rainfall products are subject to larger biases and stochastic errors and need to be adjusted to in situ observations (Barrett *et al*. 1994; Rudolf *et al*. 1996). Satellites have biases and random errors that are caused by factors such as the sampling frequency, the diurnal cycle of rainfall, the non-uniform field of view of sensors, and the uncertainties in the rain retrieval algorithms (Adeyewa and Nakamura, 2003).

The rain gauges have quite high accuracy compared to remote sensing systems, and for this reason the rain gauges are relatively indispensable (Testik, 2011). Comparison of the satellite products against ground measurements from the rain gauges is required to determine their operational viability and to improve their accuracy and applicability (Duo *et al*., 2011). A thorough verification of the

satellite-based rainfall products should quantify their accuracy in a wide range of weather and climate regimes (Bajracharya *et al*., 2010).

However, there is a difficulty in comparing data from the gauges with those from the satellites in that they provide two different kinds of information. The satellite estimates are essentially averages over the area of the satellite pixel, whereas the gauges provide measurements made at a point. Thus, averages of the rain gauge data are prone to spatial sampling error and averages of the satellite data suffer from temporal sampling error. For a meaningful comparison between the two data sets, one must either derive point values from the satellite pixels or compute pixel areal averages from the rain gauge data. The verification process requires accurate samples of surface-measures rainfall over the same time and space scales as the satellite estimates (Grimes *et al.*, 1999; Morrissey and Janowiak, 1996).

2.5   The Global Satellite Mapping of Precipitation (GSMaP) Project

The GSMaP project was established by the Japan Science and Technology Agency (JST) in 2002 to produce global precipitation products with high resolution and high precision (Ushio *et al*., 2009). The GSMaP's goal is at developing an advanced microwave radiometer algorithm compatible with the TRMM precipitation radar (PR) algorithm based on the deterministic rain-retrieval algorithm of Aonashi *et al.* (2000), and providing hourly rain rate estimates with a resolution of 0.1 degrees longitude by 0.1 degrees latitude for the entire world, excluding polar areas outside 60 degrees north and south by

comprehensively analysing satellite microwave radiometer data including IR data (Okamoto *et al*., 2007; Kubota *et al*., 2007; Seto *et al*., 2012).

2.5.1   The GSMaP microwave radiometer algorithm

Spaceborne multi-frequency microwave radiometers observe the microwave brightness temperatures, which are the integration of radiation from rain drops and scattering power by the ice and snow particles above the rain. The algorithm used TRMM precipitation radar database, ground-based radar database and produce precipitation physical models (Okamoto *et al*., 2011).

The precipitation physical model is composed of rain type, rain profile, rain drop size distribution, melting layer, snow and so on. The precipitation physical model is built onto the radiation transfer equation and the relation between rain rate and brightness temperature is tabulated in the look-up table. By referring to the look-up table, rain rate retrieval algorithm tries to find the optimum surface rain rate which gives calculated bright temperatures which best fit with the observed brightness temperatures by the weighted least square methods (Okamoto *et al*., 2011; Kubota *et al*., 2007). Figure 2.6 shows the basis of rain rate retrieval by the developed GSMaP algorithm.

The GSMaP microwave radiometer algorithm is developed based on the physical models of precipitation including melting layers and particle-size distribution. The information obtained by the PR is introduced in order to share a common precipitation model between the microwave radiometers and the PR algorithms (Kubota *et al*., 2007).
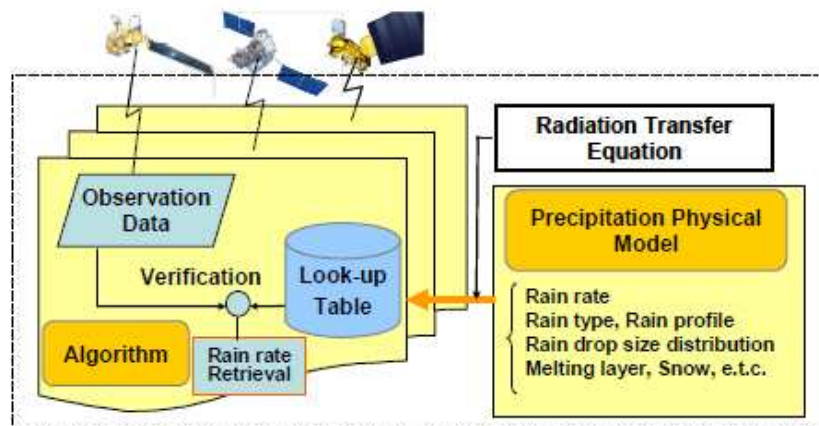
Figure 2.6 Outline of the developed GSMaP algorithm

(Okamoto *et al*., 2011)

2.5.2   The GSMaP products

In the original GSMaP project, surface rain rates have been retrieved by the microwave radiometer algorithm from brightness temperature data of TRMM TMI for eight years (1998 to 2005), Aqua AMSR-E for three years (2003 to 2005), ADEOS-II AMSR for seven months (April to October 2003), and DMSP F13, F14, F15 SSM/I for three years (2003 to 2005). The product of the TMI-only retrievals is referred to as the GSMaP_TMI. The product combined with these six microwave radiometer-derived rain rate estimates is referred to as the GSMaP_MWR. The spatial resolution of these microwave products is 0.25 degs by 0.25 degs, and typical temporal resolution is six hours (Okamoto *et al*. 2007; Okamoto *et al*., 2011).

The GSMaP project is also developing algorithms which combine microwave radiometer data with GEO infrared (IR) radiometer data. High temporal interpolation (1 hour) of the GSMaP_MWR is obtained by the morphing technique using IR cloud moving vector and Kalman filter technique. These

products are referred to as the GSMaP_MV or the GSMaP_MVK (Ushio *et al.*, 2009). The spatial resolution of these microwave-IR combined products is 0.1 degs by 0.1 degs. Figure 2.7 shows the composition of the GSMaP products. Figure 2.8 shows an example of the GSMaP_MVK product (Okamoto *et al.*, 2011).
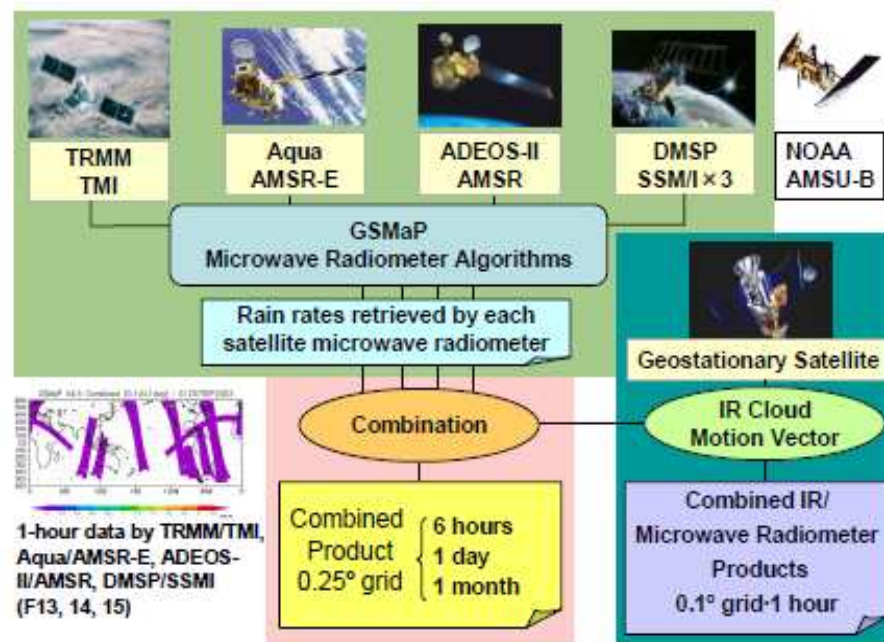
Figure 2.7 Composition of the GSMaP products
(Okamoto *et al.*, 2011)

Near real-time version of the GSMaP (i.e. GSMaP_NRT) is published with a latency of less than four hours (Kachi *et al.*, 2011). The reanalysis version of the GSMaP_MVK is processed with additional measurements and by using the latest algorithm (version 5.222.1) and is available for nearly 11 years, from March 2000 to November 2010 (Seto *et al.*, 2012).
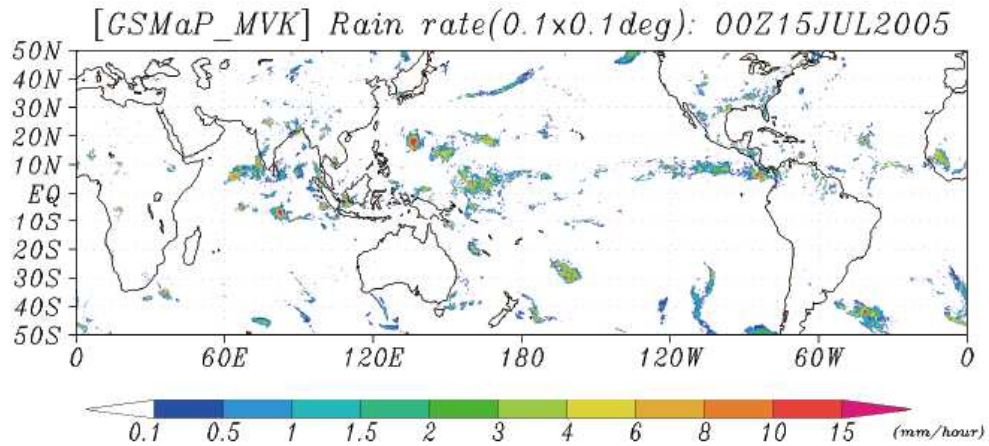
Figure 2.8 Example of the GSMaP_MVK product
(Aonashi *et al*., 2009)

2.5.3   Applications of the GSMaP

The GSMaP algorithm was improved by JAXA/EORC. JAXA/EORC has started to release global rainfall data once every hour in the near-real-time (about four hours after data acquisitions) by using TRMM/TMI, Aqua/AMSR-E, DMSP/SSMIS, and GEO IR data on the Internet. Figure 2.9 shows near-real-time quick report of global rainfall maps by the GSMaP algorithms (Okamoto *et al*., 2011).

Global Flood Alert System (GFAS) is promoted by MLIT (Ministry of Land, Infrastructure, Transport and Tourism) of Japan and JAXA and is developed by International Flood Network (IFNet). GFAS is an attempt to make the best use of global satellite precipitation estimates by the GSMaP and other data in flood forecasting and warning with Global Precipitation Mission (GPM) in mind. GFAS provides through internet useful information for flood forecasting

and warning to disaster prevention agency of every country which may have the

probability to encounter the rainfall disaster (Okamoto *et al*., 2011).
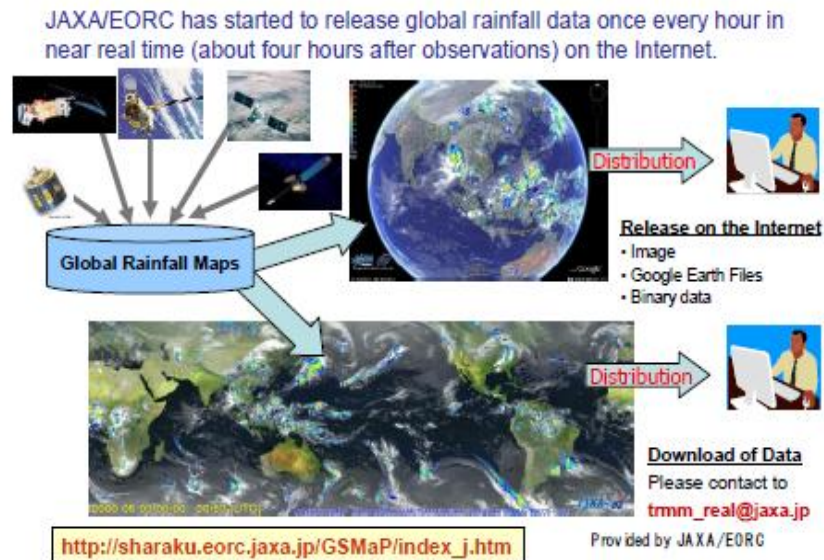
Figure 2.9 Near-real-time quick report of global rainfall maps by the GSMaP algorithms (Okamoto *et al*., 2011)

CHAPTER III

FRAMEWORK OF RESEARCH

Indonesia as an archipelago country, which lies in equatorial region, is recognised having potential of large rainfall amount during rainy season. As a consequence, the rainfall related natural disasters are profound. Flood is the most frequent natural disaster occurred in Indonesia. Urban areas are noticeably vulnerable due to flooding in terms of both infrastructure damage and life loss. Accurate monitoring of the rainfall is thus one of fundamental importance for designing reliable flood disaster mitigation and early warning.

Ground-based rain gauge is a conventional device to measure rainfall amount and considered as a point measurement. While, satellite-based rainfall estimates provides complement measurement over wide coverage area having few or even no in situ data. The combination of the two measurement systems is necessary for monitoring rainfall condition of the flood events, especially for the purpose of understanding accuracy of the satellite data.

The framework of research is designed based on the objectives of the research as previously mentioned in Chapter 1. The research is generally outlined into three main processes, i.e. collecting, processing and analysing data. Schematic diagram of the research framework can be seen in Figure 3.1.

This study evaluates rainfall condition of flood events (in the period of 2003-2010) using the GSMaP_MVK product with high temporal and spatial resolution (hourly, 0.1^0 x 0.1^0 latitude/longitude) and rain gauge station data as a

benchmark. The study area of urban city such as Medan City, Indragiri Hulu Regency, Pekanbaru City, Samarinda City and Manado City were chosen based on the previous study by Aryastana (2012).
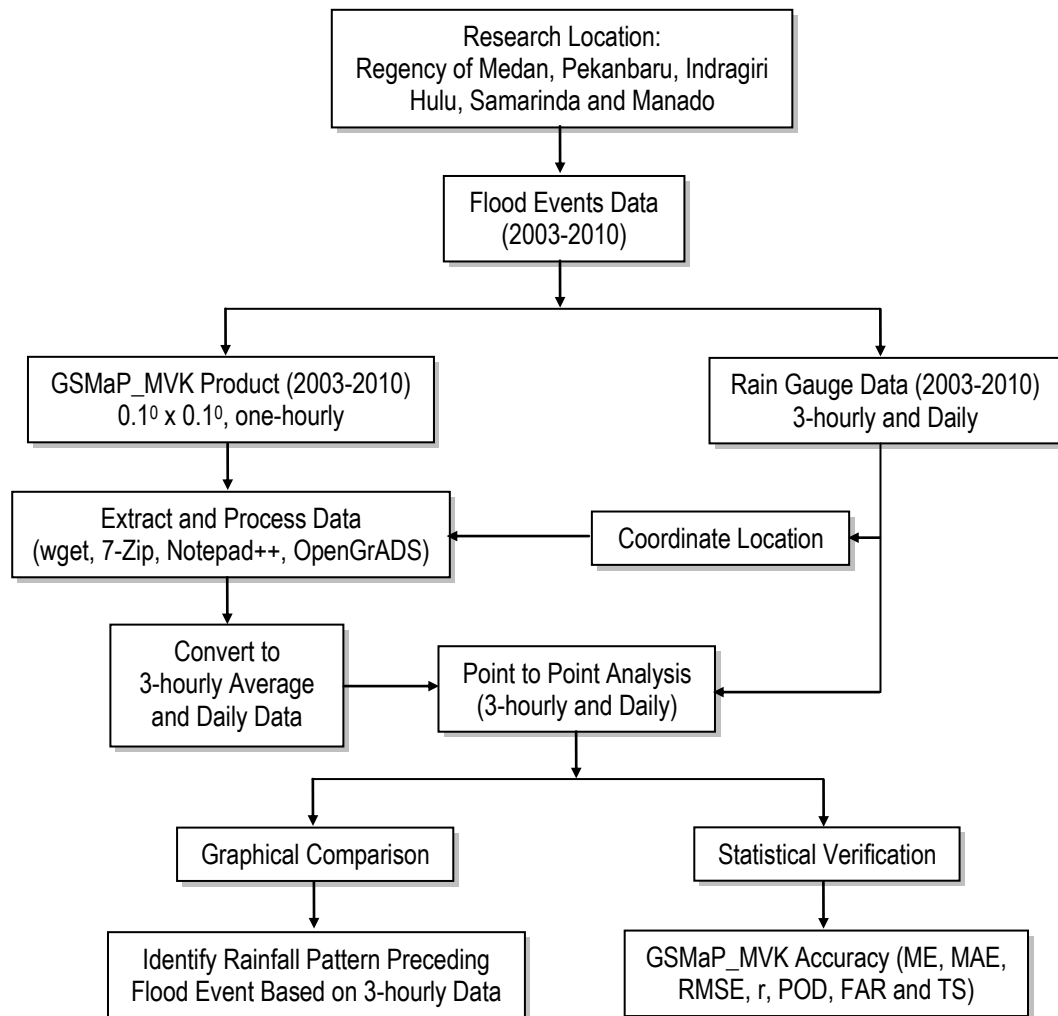
Figure 3.1 Schematic diagram of the research framework

Comparison of the GSMaP_MVK with rain gauge data is made in an attempt to understand the difference of the two measurements in capturing rainfall event fluctuations before and after the flood occur. The rainfall pattern before flooding can be identified based on graphical visualisation of the rainfall intensity

variations. Meanwhile, in purpose of evaluating the GSMaP_MVK applicability for the study area, accuracy assessment is conducted with respect to the rain gauge data using statistical verification indices, such as ME, MAE, RMSE, correlation coefficient (r), POD, FAR and TS.

CHAPTER IV

RESEARCH METHODOLOGY

4.1   Research Location

Research location was focused in Indonesia region, especially in the regency of Medan City, Pekanbaru City, Indragiri Hulu, Samarinda City and Manado City. These locations were chosen based on the previous study by Aryastana (2012) and the availability of rain gauge station providing continuous rainfall data in those areas.

Figure 4.1 Research location

(http://en.wikipedia.org/wiki/File:Indonesia_2002_CIA_map.png)

4.1.1 Medan city

Medan City is the capital city of North Sumatera Province in Indonesia. Its geographical location is from 2^0 27' N to 2^0 47'N latitude and from 98^0 35'E to 98^0 44'E longitude. Medan is located on the northern part and the topography is sloped northwards with elevation between 2.5 m and 37.5 m above sea level. The area is 265.1 km^2. There are seven rivers flowing through Medan City, i.e. Belawan River, Badra River, Sikambing River, Putih River, Babura River, Deli River and Sei Kera River

(http://www.sumutprov.go.id/ongkam.php?me=potensi_medan).

4.1.2 Pekanbaru city and Indragiri Hulu regency

Pekanbaru is the capital city of Riau Province on the island of Sumatera. Its geographical location is from 0^0 25' N to 0^0 45'N latitude and from 101^0 14'E to 101^0 34'E longitude. The area is 632.26 km² with elevation between 5 m and 50 m above sea level. Siak River flows through the city eastward. There are 11 rivers connected to the Siak River, i.e. Umban Sari River, Air Hitam River, Siban River, Setukul River, Pengambang River, Ukui River, Sago River, Senapelan River, Limau River, Tampan River and Sail River (http://www.pekanbaru.go.id/wilayah-geografis/).

Indragiri Hulu is a regency of Riau Province. It has an area of 8.198.26 km² with elevation from 50 m to 100 m above sea level. Its geographical location is from 0^0 15'N to 1^0 5'S latitude and from 101^0 10'E to 102^0 48'E longitude (http://www.riau.go.id/index.php?/detail/17).

4.1.3   Samarinda city

Samarinda is the capital city of East Kalimantan Province. Its geographical location is from 0^0 19'02" S to 0^0 42'34" S latitude and from 117^0 03'00" E to 117^0 18'14" E longitude. It has an area of 718 km² with elevation between 0 m and 200 m above sea level. Mahakam River is the main river flowing through the city (http://bappeda.samarindakota.go.id/profil.php).

4.1.4   Manado city

Manado is the capital city of North Sulawesi Province. Its geographical location is from 1^0 25'88" N to 1^0 39'50" N latitude and from 124^0 47'00" E to 124^0 56'00" E longitude. There are 5 rivers flowing through the city, i.e. Tondano River, Tikala River, Bailang River, Sario River and Malalayang River. It has an area of 159.02 km² with elevation between 0 m and 240 m above sea level (http://www.manadokota.go.id/page-101-geografis.html).

4.2   Research Materials and Data Source

The materials used in this study and the corresponding sources of data are as follows:

a. Flood events data from 2003 to 2010 in Medan, Pekanbaru, Samarinda and Manado were obtained from National Agency for Disaster Management/Badan Nasional Penanggulangan Bencana (BNPB) website and Brakenridge (2013).

BNPB homepage: http://www.bnpb.go.id/

b. One hourly satellite rainfall data of the GSMaP_MVK product (version 5.222.1) from 2003 to 2010. The data can be downloaded from Earth

Observation Research Center (EORC)/Japan Aerospace Exploration Agency (JAXA) website. The data is in the Coordinated Universal Time (UTC) format.

Homepage: ftp://rainmap:amechi-zu@hokusai.eorc.jaxa.jp/standard/v5

c. Three hourly and daily rain gauge data from 2003 to 2010 were obtained from Indonesian Agency for Meteorology, Climatology and Geophysics/ Badan Meteorologi, Klimatologi dan Geofisika (BMKG). The rain gauge stations are Polonia, Sutan Syarif Kasim II, Temindung, Sam Ratulangi for the regency of Medan, Pekanbaru, Samarinda and Manado, respectively. The data is in the Coordinated Universal Time (UTC) format.

Homepage: http://202.90.199.103 and www.ogimet.com.

4.3   Research Instruments

The instruments used in this study include hardware and software as follows:

a. Personal computer (PC), Intel Core Duo CPU E7500 @2.93 GHz, 2GB RAM, 120 GB HDD, 1.2 TB External HDD.

b. Wget version 1.11.4-1. This software was used to download large volume of the GSMaP_MVK data automatically.

Homepage: ftp://ftp.gnu.org/gnu/wget/

c. 7-Zip version 9.20. This software was used to extract the GSMaP_MVK data.

Homepage: http://www.7-zip.org/

d. OpenGrADS Bundle 2.0.1.oga.1. This software was used for processing the GSMaP_MVK data.

Homepage: http://opengrads.org/

e. Notepad++ version 6.3.2. This software was used to edit OpenGrADS control file and make script for processing the GSMaP_MVK data.

Homepage: http://notepad-plus-plus.org/

f. Microsoft Excel 2007. This software was utilised for analysing data, e.g. plotting time series and scatter graphs of rainfall intensity and statistical calculation.

4.4 Research Procedure

The research is conducted through three main stages in terms of data treatment, i.e. collecting, processing and analysing and presenting data.

4.4.1 Collecting data

The first stage of this study is to collect relevant data. The data include flood events and rainfall intensity (i.e. from the GSMaP_MVK product and rain gauge stations). Coordinate position of the rain gauge station are also gathered. The data can be downloaded from data sources via internet connection. The data refer to flood event data (i.e. the day of the flood starts to occur). This study utilises the data for 10 days preceding and 2 days following flood events for analysis.

4.4.2 Processing data

The steps in processing data for each flood event are as follows:

a. Modify control file that are provided by the GSMaP website to read the GSMaP_MVK data according to the time span of data considered for analysis

(i.e. 10 days preceding and 2 days following flood events) using Notepad++ software.

b. Create OpenGrADS script for calculating areal average of rain intensity of the GSMaP_MVK satellite pixel using Notepad++.

c. Calculate rainfall intensity of the GSMaP_MVK on hourly basis using OpenGrADS by area averaging of the satellite pixel (0.1^0 x 0.1^0) in which rain gauge station is located (Figure 4.2). The rain intensity value on a pixel is a single value of satellite rainfall estimates.
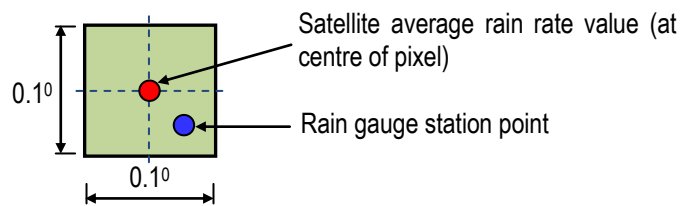
Figure 4.2 Example of the GSMaP_MVK single pixel and rain gauge station location

Table 4.1 shows the available rain gauge stations, for which data are analysed in this study and the corresponding GSMaP_MVK pixel or grid box that are chosen for comparisons. Table 4.2 denotes density of the rain gauge stations according to the data shown on Table 4.1.

d. Convert the GSMaP_MVK rainfall intensity from hourly to 3-hourly and daily time steps. The most popular way to make 3-hourly average from hourly data is for instance, by averaging hourly files of 02Z, 03Z, and 04Z to produce 3-hourly data of 03Z. That means 03Z is centre of 3 hour time period.

The daily data are derived by summing hourly data from 00Z to 23Z on the day.

Table 4.1

Available rain gauge stations and the corresponding GSMaP_MVK pixel used in this study

Province	Regency	Rain Gauge Station	Coordinate Position	Elevation (m)	GSMaP_MVK Pixel
North Sumatera	Medan City	Polonia	3.56^0 N, 98.67^0 E	25	3.50^0 N-3.50^0 N 98.60^0 E-98.70^0 E
Riau	Pekanbaru City	Sutan Syarif Kasim II	0.46^0 N, 101.44^0 E	31	0.40^0 N-0.50^0 N 101.40^0 E-101.50^0 E
Riau	Indragiri Hulu	Sutan Syarif Kasim II	0.46^0 N, 101.44^0 E	31	0.40^0 N-0.50^0 N 101.40^0 E-101.50^0 E
East Kalimantan	Samarinda City	Temindung	0.48^0 S, 117.16^0 E	3	0.40^0 S-0.50^0 S 117.10^0 E-117.20^0 E
North Sulawesi	Manado City	Sam Ratulangi	1.55^0 N, 124.93^0 E	80	1.50^0 N-1.60^0 N 124.90^0 E-125.00^0 E

Table 4.2

Density of the rain gauge station in this study

Regency	Area (km²)	Number of Station	Rain Gauge Density (area in km² per station)
Medan City	265.1	1	265.1
Pekanbaru City	632.26	1	632.26
Indragiri Hulu	8,198	1	8,198
Samarinda City	718	1	718
Manado City	159.02	1	159.02

e. Save the GSMaP_MVK data of 3-hourly and daily time steps as well as rain gauge data derived from rain gauge station on MS Excel file.

4.4.3 Analysing and presenting data

The third stage is to compare rainfall data of the GSMaP_MVK with the rain gauge station by firstly arranging a spreadsheet table. Point to point analysis

method was used in this study. Comparison of the GSMaP_MVK, which is represented by single value of pixel average were performed head to head with the rain gauge point value within satellite pixel. This is due to very limited rain gauge station available in the study area (i.e. only one station for each study area).

Time series of rainfall intensity from the GSMaP_MVK and rain gauge data are presented and graphical comparison are performed for 3-hourly and daily time steps. Rainfall pattern classification is done thereafter for each of the flood events. Subsequently, accuracy of the GSMaP_MVK is evaluated using statistical approach. The following Section 4.5 describes classification of rainfall pattern before the floods occur and the statistical indices used for analysing the data.

4.5   Data Analysis

Aryastana (2012) developed classification of the rainfall pattern before floods occur in Indonesia based on hourly data of the GSMaP_MVK product as can be seen in Figure 4.3. In this study, his classification is adopted. However, both the GSMaP_MVK and the rain gauge data on the basis of 3-hourly average time steps are used for determining the rainfall pattern.

There are three types of the rainfall pattern as follows (Aryastana, 2012):

a. Long term rainfall period, which is an accumulative rainfall several days or more than one day before flood starts to occur.

b. Short term rainfall period, which is an accumulative rainfall with high intensity for several hours until one day.

c. Irregular pattern, which is a condition when before floods occur, rainfall is not so heavy, but high intensity of rainfall occur several days before flooding.
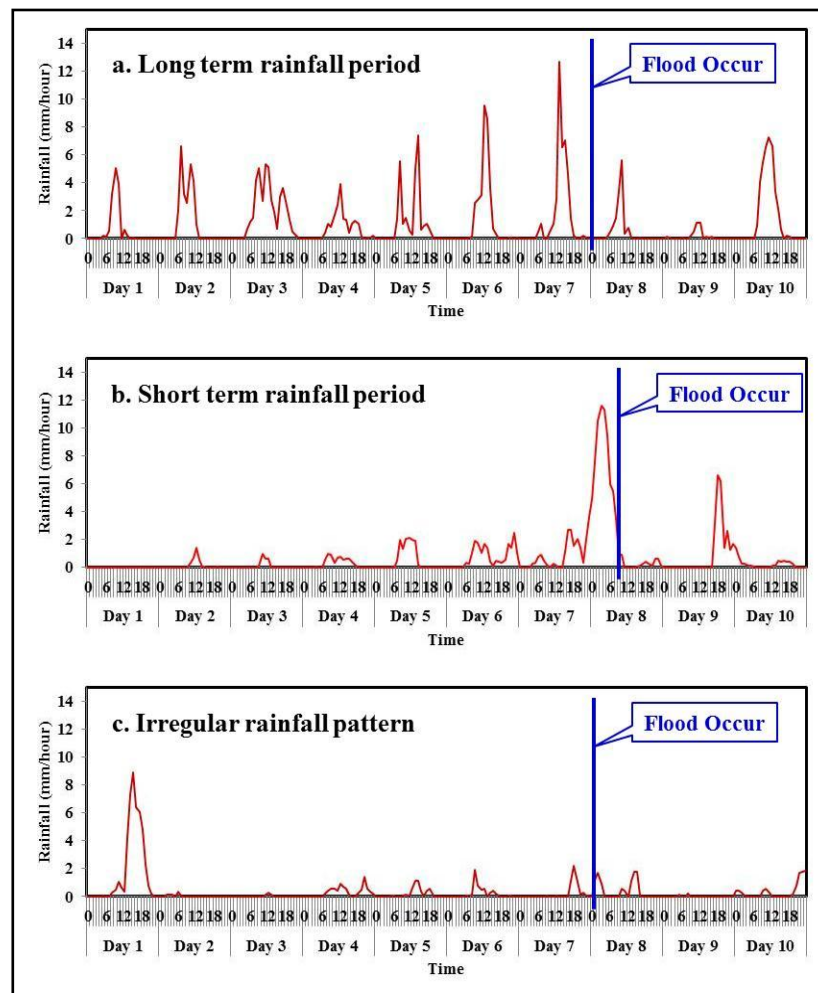
Figure 4.3 Rainfall patterns before floods occur

(Aryastana, 2012)

According to Ebert (2007), statistical scores used to verify accuracy of satellite rainfall estimate compared with the observed rain gauge values include continuous verification statistics and categorical verification statistics. The standard continuous and categorical verification statistics give quantitative measures of the accuracy of the satellite-estimated rain amount and occurrence.

4.5.1   Continuous verification statistics

Continuous verification statistics measure the accuracy of a continuous variable such as rain amount or intensity. These are the most commonly used statistics in the validation of satellite estimates (Ebert, 2007).

In this study, the statistics measures used include mean error, mean absolute error, root mean square error, and correlation coefficient. In the equations to follow, Y_i indicates the estimated value at point or grid box i, O_i indicates the observed value, and N is the number of samples (Ebert, 2007).

a. Mean Error (ME)

The mean error (ME) or bias measures the average difference between the estimated and observed values. The mean bias error indicates the average direction of the deviation from observed values, but may not reflect the magnitude of error. It measures the average error of a number of observations found by taking the mean value of the positive and negative errors without regard to sign (Ebert, 2007; Gomez, 2007).

$$ME = \frac{1}{N} \sum_{i=1}^{N} (Y_i - O_i) \qquad\qquad (4.1)$$

A positive ME indicates that the estimated value exceeds the observed value on the average, while the negative ME corresponds to underestimation the observed value on the average. Do not measure the correspondence between estimations and observations, i.e., it is possible to get a perfect score for a bad estimation if there are compensating errors (Murphy, 1995 in Gomez, 2007).

b. Mean Absolute Error (MAE)

The mean absolute error (MAE) measures the average magnitude of the errors in a set of estimated values, without considering their direction. It measures accuracy for continuous variables. The MAE is a linier score which means that all the individual differences are weighted equally in the average (Murphy, 1995 in Gomez, 2007; Ebert, 2007).

$$MAE = \frac{1}{N} \sum_{i=1}^{N} |(Y_i - O_i)| \qquad (4.2)$$

c. Root Mean Square Error (RMSE)

The root mean square error (RMSE) is a quadratic scoring rule which measures the average magnitude of the error. Compared to the MAE, the RMSE gives better weight to large errors than to small errors in the average. Since the errors are squared before they are averaged, the RMSE gives a relatively high weight to large errors. This means the RMSE is most useful when large errors are particularly undesirable (Murphy, 1995 in Gomez, 2007; Ebert, 2007).

$$RMSE = \sqrt{\frac{1}{N} \sum_{i=1}^{N} (Y_i - O_i)^2} \qquad (4.3)$$

d. Correlation Coefficient (r)

The correlation coefficient (r) measures the degree of linear association between the estimated and observed distributions. It is independent of absolute

or conditional bias, however, and therefore must be used along with other measures when verifying satellite estimates (Ebert, 2007).

$$r = \frac{\sum\limits_{i=1}^{N}(Y_i - \overline{Y})(O_i - \overline{O})}{\sqrt{\sum\limits_{i=1}^{N}(Y_i - \overline{Y})^2}\sqrt{\sum\limits_{i=1}^{N}(O_i - \overline{O})^2}} \qquad (4.4)$$

$$\overline{Y} = \frac{1}{N}\sum\limits_{i=1}^{N}Y_i \qquad (4.5)$$

$$\overline{O} = \frac{1}{N}\sum\limits_{i=1}^{N}O_i \qquad (4.6)$$

Visually, the correlation measures how close the points of a scatter plot are to a straight line. It is possible for a set of estimated values with large errors to still have a good correlation coefficient with the observations. It is sensitive to outliers and goes from -1 to 1 (Murphy, 1995 in Gomez, 2007).

4.5.2 Categorical verification statistics

Categorical verification statistics measure the correspondence between the estimated and observed occurrence of events. Most are based on a 2 × 2 contingency table of yes/no events, such as rain/no rain, shown in Table 4.1. The elements in the table (hits, misses, etc.) give the joint distribution of events, while the elements below and to the right (observed yes, observed no, etc.) are called the marginal distributions (Ebert, 2007).

To verify the frequency of the correct and incorrect estimated values, four combinations between the estimated and observed data can be done. These combinations are (Ebert 2007; Gomez, 2007):

- Hits - rain estimated to occur, and did occur

- Misses - rain estimated not to occur, but did occur

- False alarms - rain estimated to occur, but did not occur

- Correct negatives - rain estimated not to occur, and did not occur

Table 4.3

The off-diagonal elements characterise the errors (2 × 2 contingency table)

		Observed (Rain Gauge Data)		
		Yes	No	
Estimated (GSMaP_MVK)	Yes	**Hits**	**False alarms**	Estimated yes
	No	**Misses**	**Correct negatives**	Estimated no
		Observed yes	Observed no	N=total

Categorical statistics which can be computed from the "yes/no" contingency table (Table 4.1) are given below (Ebert 2007; Gomez, 2007):

a. Probability of Detection (POD)

$$POD = \frac{Hits}{Hits + Misses} \qquad (4.7)$$

The probability of detection (POD) measures the fraction of observed events that were correctly diagnosed, and is sometimes called the "hit rate". The POD is the number of correct estimations divided by the number

observed in each category. Range: 0 to 1. Perfect score: 1 (Ebert 2007; Gomez, 2007).

b. False Alarm Ratio (FAR)

$$FAR = \frac{False\ alarms}{Hits + False\ alarms} \qquad (4.8)$$

The false alarm ratio (FAR) gives the fraction of diagnosed events that were actually non-events. The FAR falls into the category of verification measures that imply stratification by estimations, and therefore, as the name implies, is sensitive only to false predictions of the severe event, not to missed event. Range: 0 to 1. Perfect score: 0 (Ebert 2007; Gomez, 2007).

c. Threat Score (TS)

The threat score (TS), also known as the critical success index, measures the fraction of all events estimated and/or observed that were correctly diagnosed. It is measure of relative accuracy (Ebert 2007; Gomez, 2007).

$$TS = \frac{Hits}{Hits + Misses + False\ alarms} \qquad (4.9)$$

The advantage of the threat score over the FAR and the POD is that is sensitive to both false alarms and missed events. Thus it gives more representative idea of accuracy both in situations where events are involved and in situations where the climatologically frequencies of the categories are nearly equal (Ebert 2007; Gomez, 2007).

CHAPTER V

RESULTS

5.1   Flood Events in Medan City

According to BNPB (2013) and Brakenridge (2013), there were 283 flood events recorded in North Sumatera Province from 2003 to 2010. Medan City experienced 21 flood events during that course of period. In this study, 11 flood events were analysed due to limited availability of data from the rain gauge station.

5.1.1   Rainfall condition

In this section, 2 flood events were presented according to the previous study by Aryastana (2012), i.e. on 22 September 2003 and 5 December 2003. The others can be seen in Appendix B.
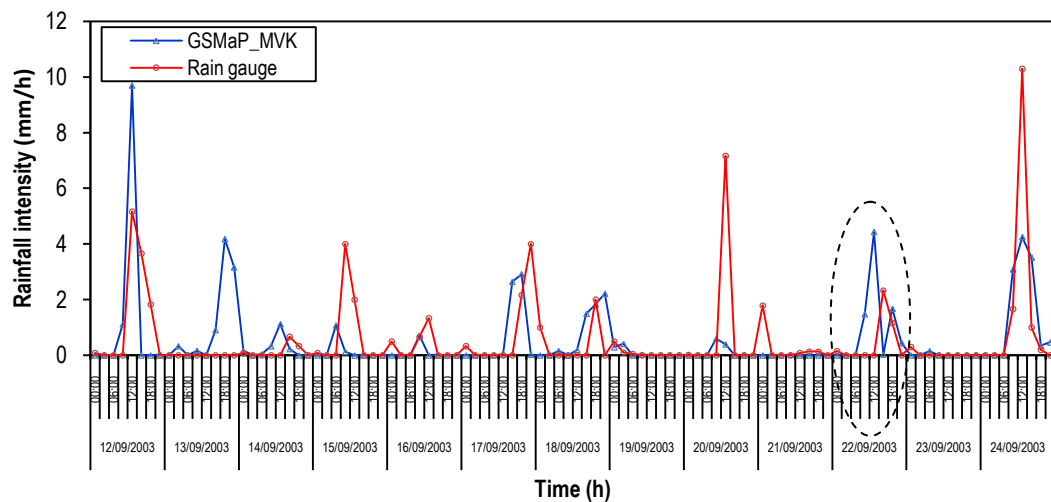
🌲   Flood event on 22 September 2003

Figure 5.1 Time-series of 3-hourly average rainfall intensity for the flood event on 22 September 2003

Figure 5.1 shows the time series of the 3-hourly average rainfall intensity for the flood event on 22 September 2003 obtained from the GSMaP_MVK and rain gauge data. The dash-line circle indicates the day of the flood began. The total number of data points is 104. The GSMaP_MVK estimated rainfall event on 13 September 2003 from 15:00 (UTC) to 21:00 (UTC) but rain gauge station did not observed it, which means false rainy detection by satellite data. The two data sources slightly match in capturing the peaks of the rainfall event.

The GSMaP_MVK shows underestimation of rain gauge data for rainfall intensity greater than 4 mm/h and also miss some small rainfall event. The rain gauge data showed rainfall intensity of 7.17 mm/h two days before flood began while the GSMaP_MVK data estimated much lower of about 0.4 mm/h. It represents approximately a 94% of underestimation.

$$y = 0.377x + 0.336$$
$$R^2 = 0.176$$
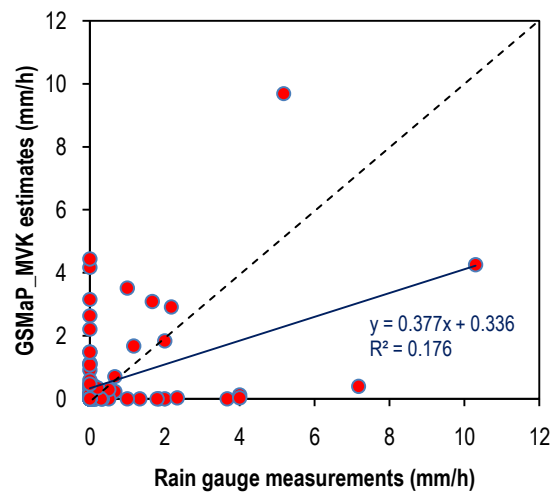
Figure 5.2 Scatter plot of the 3-hourly rainfall intensity for the flood event on 22 September 2003

The closeness of the 3-hourly rainfall intensity data pairs between the GSMaP_MVK and the rain gauge data is plotted in the form of scatter diagram in

Figure 5.2. Rainfall magnitude of the GSMaP_MVK estimation is seen to be on average slightly lower than that of the rain gauge observation. The data points are slightly concentrated below the 45^0 slope dash line indicates that the GSMaP_MVK underestimated of the rain gauge data.
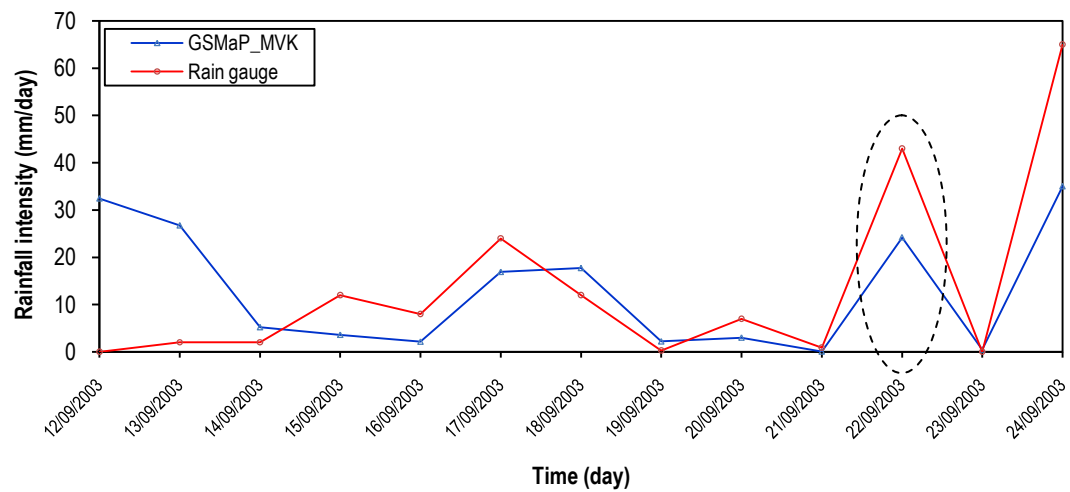
Figure 5.3 Same as Figure 5.1 but for daily data
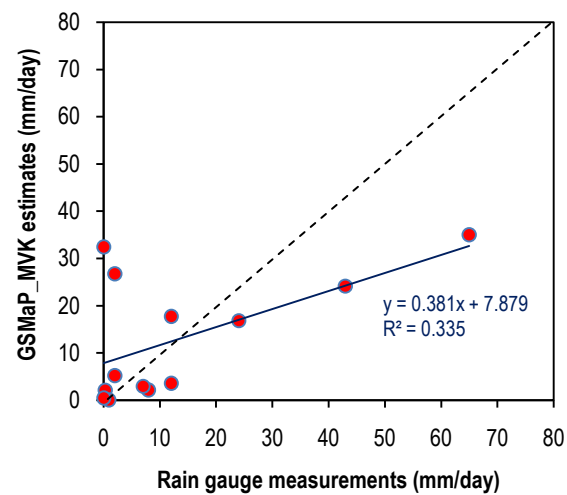
Figure 5.4 Same as Figure 5.2 but for daily data

Figure 5.3 shows the time-series of daily rainfall intensity from the GSMaP_MVK and rain gauge data for the flood event on 22 September 2003. The total number of data points is 13. On the day of flood began the GSMaP_MVK estimated about 56% lower than that of the rain gauge data, which were 24.2 mm/day and 43 mm/day respectively. The closeness of data pairs improves significantly for daily data as can be seen in Figure 5.4. On the average the GSMaP_MVK shows underestimation of the rain gauge data on daily scale.

🌐 Flood event on 5 December 2003
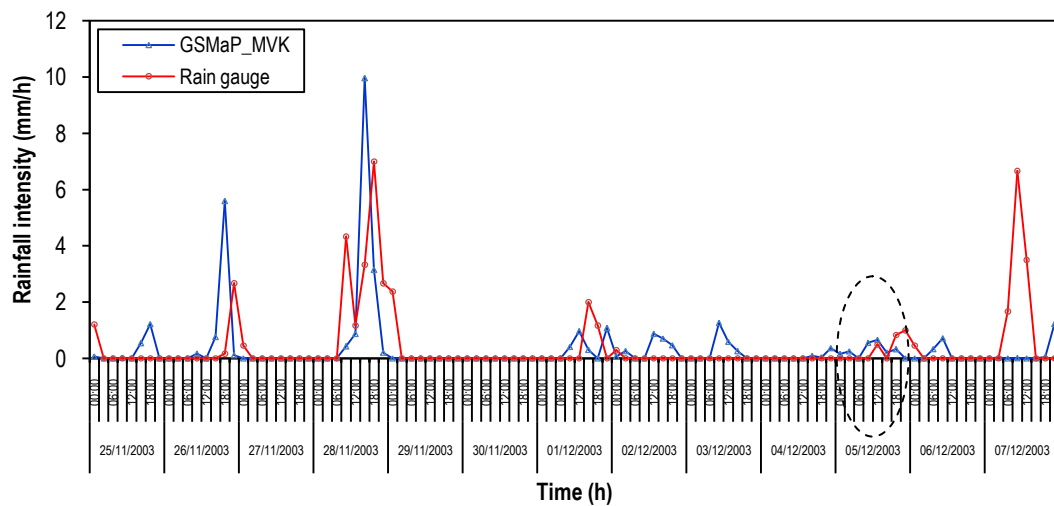
Figure 5.5 Time-series of 3-hourly average rainfall intensity for the flood event on 5 December 2003

Figure 5.5 presents the comparison of 3-hourly variations of rainfall intensity between the GSMaP_MVK and rain gauge data for the flood event on 5 December 2003. The GSMaP_MVK indicated overestimation about 3 mm/h of the rain gauge data for the two consecutive peaks starting 9 days preceding flood event. The GSMaP_MVK detected about 7 rainfall events up to 1.26 mm/h

intensity in which the rain gauge data did not observed them. Meanwhile, the GSMaP_MVK shows miss rainy detection of up to 6.67 mm/h rainfall intensity as captured by rain gauge data two days after flood began. Both the GSMaP_MVK and the rain gauge data show good agreement that no heavy rainfall observed 5 days before the day of flooding reported.
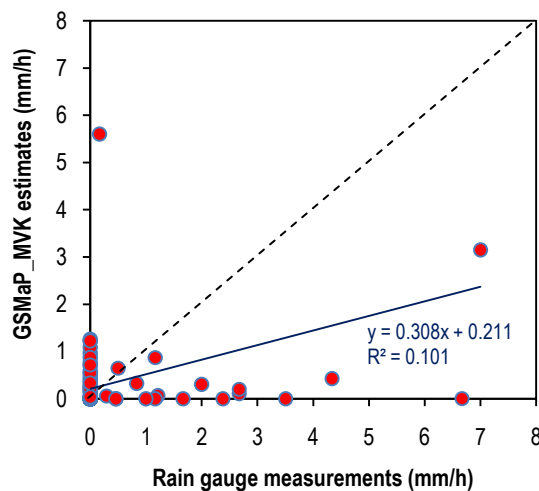

Figure 5.6 Scatter plot of the 3-hourly rainfall intensity for the flood event on 5 December 2003

Figure 5.6 illustrates the scatter plot of the GSMaP_MVK and the rain gauge data for 3-hourly average time steps. The total number of data points is 104. Rainfall magnitude of the GSMaP_MVK estimation is seen to be on average lower than that of the rain gauge observation. The data points are mostly concentrated below the 45^0 slope dash line indicates that the GSMaP_MVK underestimated of the rain gauge data.

Comparison between the GSMaP_MVK and the rain gauge data on daily basis is depicted in Figure 5.7. The total number of data points is 13. The GSMaP_MVK and the rain gauge observations shows better matching of

capturing peaks and rainfall intensity compared with the 3-hourly data. The highest rainfall peak 7 days preceding flood event was 43.90 mm/day and 57 mm/day as measured by the GSMaP_MVK and the rain gauge, respectively. Meanwhile, on the day of flood began the GSMaP_MVK estimated rainfall intensity about 50% lower than the rain gauge data, which were 5.94 mm/day and 11 mm/day, respectively.

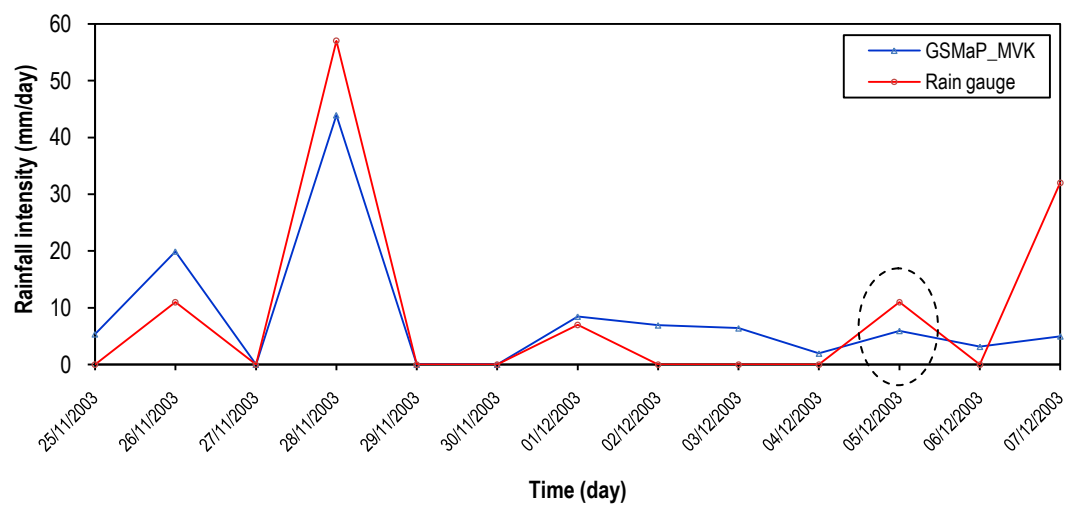

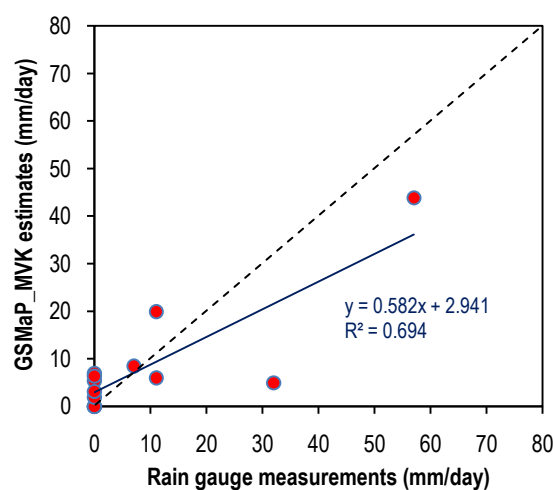**Figure 5.7 Same as Figure 5.5 but for daily data**

Figure 5.8 Same as Figure 5.6 but for daily data

Figure 5.8 illustrates the closeness of data pairs between the GSMaP_MVK and the rain gauge for daily data. On the average the GSMaP_MVK underestimated of the rain gauge data on daily time steps.

5.1.2 Rainfall patterns before floods occur

Classification of rainfall pattern before floods occur by Aryastana (2012) was adopted based on 3-hourly average rainfall data. Both the GSMaP_MVK and the rain gauge data are used to identify the pattern of rainfall preceding flood events. Table 5.1 shows the summary of the rainfall patterns before floods occur for the analysed flood events in Medan City.

Table 5.1

The rainfall patterns before floods occur in Medan City from 2003 to 2008

No.	Flood Event	Rainfall Patterns		
		Long-Term	Short-Term	Irregular
1	22/09/2003*	△		
2	19/10/2003		△	
3	02/11/2003		△	
4	05/12/2003*			△
5	12/01/2006			△
6	23/03/2006		△	
7	11/04/2006		△	
8	15/04/2006			△
9	10/05/2006		△	
10	31/10/2006		△	
11	02/11/2008		△	
	Total	**1**	**7**	**3**

* Data shown in Aryastana (2012) study

Variation of rainfall intensity of flood event on 22 September 2003 is illustrated in Figure 5.1, which can be identified as long-term period pattern, instead of irregular pattern classified by Aryastana (2012). Both the

GSMaP_MVK and the rain gauge data detected accumulative rainfall several days or more than one day before flood starts to occur.

Meanwhile, the flood event on 5 December 2003 (Figure 5.6) indicates irregular rainfall patterns due to the conditions that several hours before flood began, there was no heavy rainfall. However, the heavy rainfall occurred several days before flooding. This is good agreement with Aryastana study (2012).

Short-term period rainfall pattern is the most frequent occurred accounting for 63.6% of the total flood events analysed in Medan City.

5.1.3   Accuracy verification of the GSMaP_MVK

Table 5.2 denotes summary of the continuous statistical verification of the GSMaP_MVK product with respect to the rain gauge data for the 11 flood events analysed in Medan City. The comparison has also been made for 3-hourly average and daily data.

From Table 5.2, it can be seen that the GSMaP_MVK shows negative mean error (ME) for most of the flood events analysed based on 3-hourly and daily data, except on 23 March 2006 and 31 October 2006. The flood events on 22 September 2003 and 10 May 2006 show the lowest negative ME, while the highest positive ME is on 31 October 2006.

The MAE ranges from 0.42 mm/h to 0.96 mm/h and from 0.24 mm/h to 0.51 mm/h for 3-hourly and daily data, respectively. RMSE reached the highest value of 2.58 mm/h and 0.81 mm/h and the lowest value of 1.21 mm/h and 0.39 mm/h for 3-hourly and daily data, respectively. Flood events on 12 January 2006

and 5 December 2003 show the lowest RMSE for 3-hourly and daily data, respectively.

Table 5.2

The continuous statistical verification for the flood events analysed in Medan City from 2003 to 2008

Flood Event	3-hourly				Daily			
	ME (mm/h)	MAE (mm/h)	RMSE (mm/h)	r	ME (mm/h)	MAE (mm/h)	RMSE (mm/h)	r
22/09/2003	-0.005	0.72	1.54	0.42	-0.02	0.46	0.65	0.58
19/10/2003	-0.176	0.96	2.58	0.31	-0.12	0.51	0.84	0.65
02/11/2003	-0.056	0.96	2.16	0.32	0.03	0.47	0.72	0.83
05/12/2003	-0.078	0.57	1.38	0.32	-0.04	0.25	0.39	0.83
12/01/2006	-0.040	0.42	1.21	0.30	-0.05	0.24	0.44	0.84
23/03/2006	0.129	0.49	1.79	0.19	-0.05	0.38	0.81	0.50
11/04/2006	-0.186	0.54	1.68	0.13	-0.09	0.30	0.52	0.68
15/04/2006	-0.181	0.54	1.73	0.11	-0.08	0.29	0.51	0.70
10/05/2006	-0.014	0.48	1.32	0.20	-0.03	0.36	0.50	0.44
31/10/2006	0.271	0.59	1.54	0.53	0.22	0.39	0.58	0.80
02/11/2008	-0.136	0.86	2.45	0.55	-0.13	0.34	0.47	0.94
Average	**-0.043**	**0.65**	**1.76**	**0.31**	**-0.03**	**0.36**	**0.58**	**0.71**

The correlation coefficient is in the range from 0.11 to 0.55 and from 0.44 to 0.94 for 3-hourly and daily data, respectively. The lowest correlation of 0.11 is on 15 April 2006, while the highest is of 0.55 on 2 November 2008 for 3-hourly data. For daily data, the lowest correlation is on 10 May 2006, while the highest is on 2 November 2008.

On the average, the GSMaP_MVK underestimates of the rain gauge data for the entire flood events analysed in Medan City. The correlation coefficients are 0.31 and 0.71 for 3-hourly and daily data, respectively.

Subsequently, Table 5.3 shows summary of the categorical verification statistics for the flood events analysed in Medan City and for the 3-hourly average and daily time steps data.

The probability of rain detection (POD) of the GSMaP_MVK indicates more than 50% for the entire flood events studied. The range is from 0.55 to 0.94 and from 0.83 to 1 for 3-hourly and daily data, respectively. The lowest POD is on 23 March 2006 and 12 January 2006 for 3-hourly and daily data, respectively. On average, the POD performs moderate to high value of 0.73 and 0.97 for 3-hourly and daily data, respectively.

Table 5.3

The categorical verification statistics for the flood events analysed in Medan City from 2003 to 2008

Flood Event	3-hourly			Daily		
	POD	FAR	TS	POD	FAR	TS
22/09/2003	0.63	0.63	0.31	1.00	0.15	0.85
19/10/2003	0.66	0.66	0.29	1.00	0.31	0.69
02/11/2003	0.89	0.62	0.37	1.00	0.38	0.62
05/12/2003	0.70	0.74	0.23	1.00	0.58	0.42
12/01/2006	0.68	0.68	0.28	0.83	0.58	0.38
23/03/2006	0.58	0.63	0.29	1.00	0.38	0.63
11/04/2006	0.82	0.65	0.32	1.00	0.46	0.54
15/04/2006	0.94	0.69	0.30	1.00	0.58	0.42
10/05/2006	0.55	0.60	0.30	0.89	0.33	0.62
31/10/2006	0.71	0.61	0.34	1.00	0.46	0.54
02/11/2008	0.86	0.56	0.41	1.00	0.36	0.64
Average	**0.73**	**0.64**	**0.31**	**0.97**	**0.42**	**0.58**

The false alarm ratio (FAR) means probability of the GSMaP_MVK data to estimate rain event in which did not observed by the rain gauge measurements. From Table 5.3, the FAR score shows more than 50% and 15% with its lowest

reached nearly 0.56 on 2 November 2008 and 0.15 on 22 September 2003 for 3-hourly and daily time steps, respectively.

The threat score (TS) spans from 0.23 to 0.41 and from 0.38 to 0.85 for 3-hourly and daily data, respectively. The highest TS reached on 2 November 2008 and 22 September 2003 for 3-hourly and daily data, respectively.

5.2 Flood Events in Pekanbaru City and Indragiri Hulu Regency

There were 82 flood events recorded in Riau Province from 2003 to 2010 (BNPB, 2013; Brakenridge, 2013). Pekanbaru City and Indragiri Hulu Regency experienced flood events of 7 and 13, respectively during that period. Ten flood events were analysed over the two regencies due to limited availability of data from the rain gauge station.

5.2.1 Rainfall condition

This section presents results of 2 flood events in Indragiri Hulu Regency according to the previous study by Aryastana (2012), i.e. on 25 January 2003 and 21 February 2003. The others can be seen in Appendix C.

● Flood event on 25 January 2003

Figure 5.9 shows the time series of the 3-hourly average rainfall intensity for the flood event on 25 January 2003 derived from the GSMaP_MVK and rain gauge data. The dash-line circle indicates the day of the flood began. The total number of data points is 104. The GSMaP_MVK missed detection for rainfall events on 17 January 2003 (at 09:00 UTC) and 19 January 2003 (at 12:00 UTC) whereas the rain gauge station captured them. On the contrary, the GSMaP_MVK

estimated that the rainfall event occurred at 03:00 (UTC) on 24 January 2003 but rain gauge station did not observed it, which means false rainy detection by satellite data.
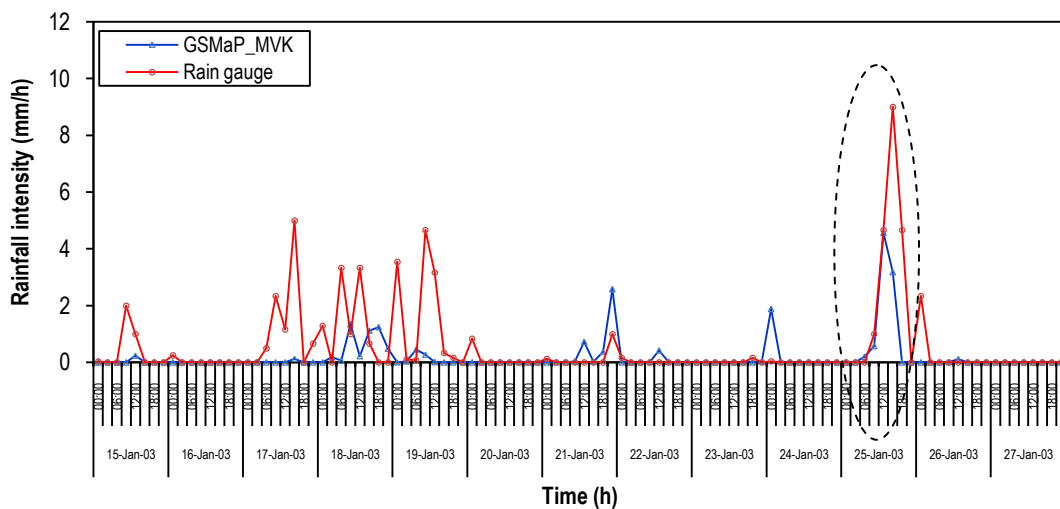

Figure 5.9 Time-series of 3-hourly average rainfall intensity for the flood event on 25 January 2003

The two data sources slightly match in capturing the peaks of the rainfall events but the rainfall intensity is to be lower by the GSMaP_MVK estimation. The GSMaP_MVK shows underestimation of the rain gauge data for rainfall intensity greater than 2 mm/h during 3 days of consecutive rainfall before flood began. Meanwhile, on the day of flood occurred at 15:00 (UTC), the rain gauge observed 9 mm/h of rainfall intensity, while the GSMaP_MVK underestimated about 48%.

Figure 5.10 shows the scatter plot of the GSMaP_MVK and the rain gauge data on 3-hourly average scale for the flood event on 25 January 2003. Rainfall magnitude of the GSMaP_MVK estimation is seen to be on average lower than

that of the rain gauge observation. The data points are mostly concentrated below

the 45^0 slope dash line indicates that the GSMaP_MVK underestimated of the rain
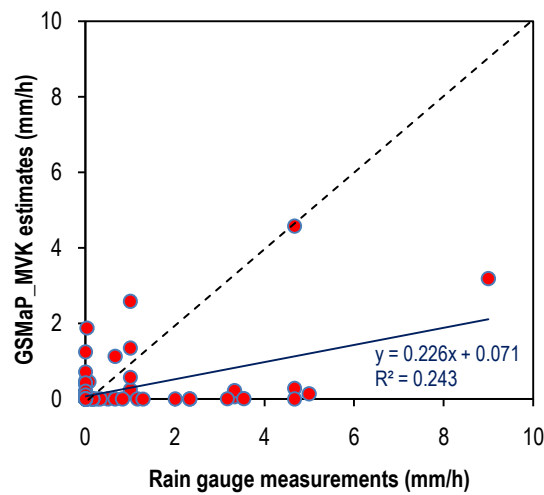
gauge data.

Figure 5.10 Scatter plot of the 3-hourly rainfall intensity for the flood event on 25 January 2003
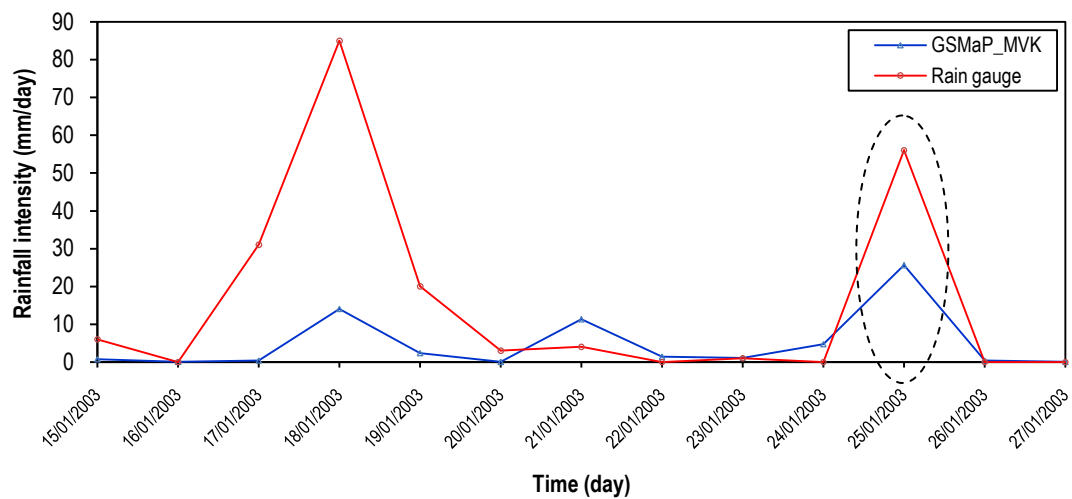

Figure 5.11 Same as Figure 5.9 but for daily data

Figure 5.11 shows the time-series of daily rainfall intensity from the

GSMaP_MVK and rain gauge data for the flood event on 25 January 2003. The

total number of data points is 13. Comparing with 3-hourly data, the daily observations show better matching of capturing peaks and rainfall intensity. On the day of flood began the GSMaP_MVK estimated about 46% lower than that of the rain gauge data, which were 25.6 mm/day and 56 mm/day, respectively. The closeness of data pairs between the GSMaP_MVK and rain gauge improves significantly for daily data as can be seen in Figure 5.12. On the average the GSMaP_MVK underestimated of the rain gauge data on daily scale.
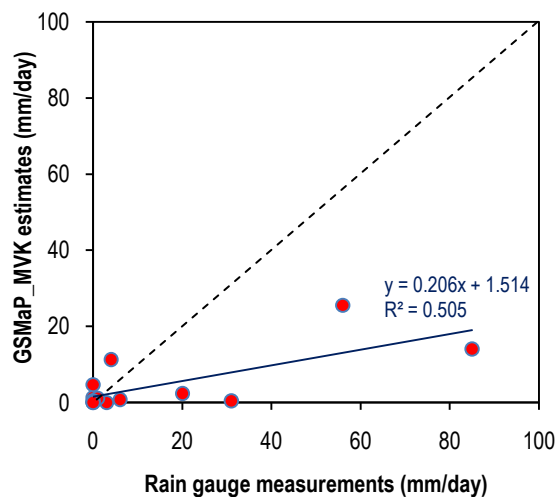

Figure 5.12 Same as Figure 5.10 but for daily data

🌐 Flood event on 21 February 2003

Figure 5.13 presents comparison of 3-hourly variations of rainfall intensity between the GSMaP_MVK and rain gauge data for the flood event on 21 February 2003. The two observations show quite match to capture the peaks of the rainfall event. However, the GSMaP_MVK indicated underestimation about 80% of the rain gauge data on 18 February 2003 at 15:00 (UTC). The GSMaP_MVK estimated rainfall intensity about 1.64 mm/h compared with 19.33 mm/h by the rain gauge measurement for 3 hours before the flood began. It represents

approximately a 91.5% of underestimation. This is the highest rainfall intensity observed by the rain gauge data within less than 6 hours before flood began that might be as main cause of triggering the flood.
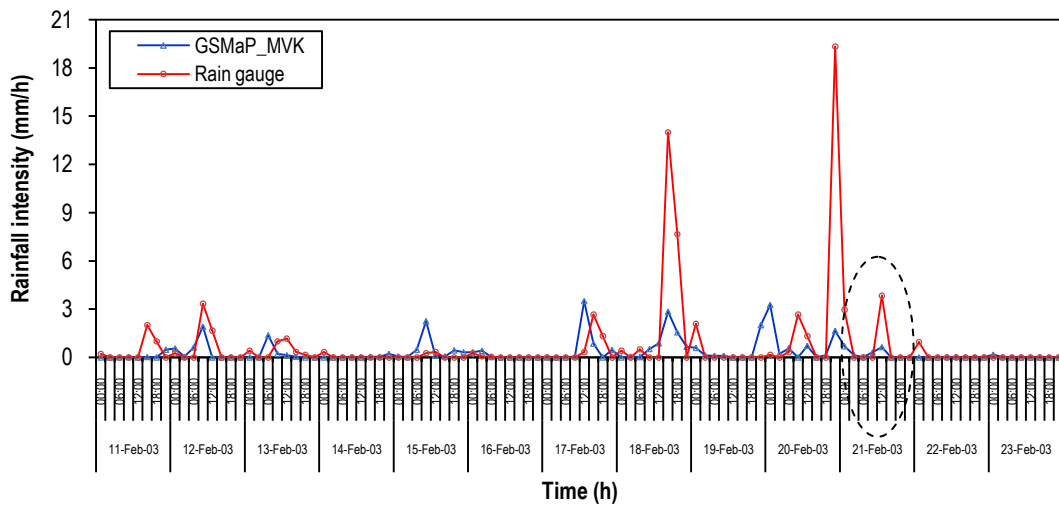

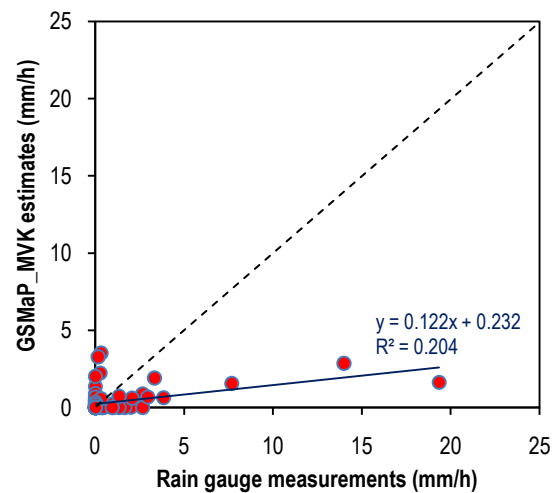**Figure 5.13 Time-series of 3-hourly rainfall intensity for the flood event on 21 February 2003**

Figure 5.14 Scatter plot of the 3-hourly rainfall intensity for the flood event on 21 February 2003

From the scatter plot (Figure 5.14), rainfall magnitude of the GSMaP_MVK estimation is seen to be on average lower than that of the rain

gauge data. The data points are mostly concentrated below the 45^0 slope dash line indicates that the GSMaP_MVK underestimated of the rain gauge data.
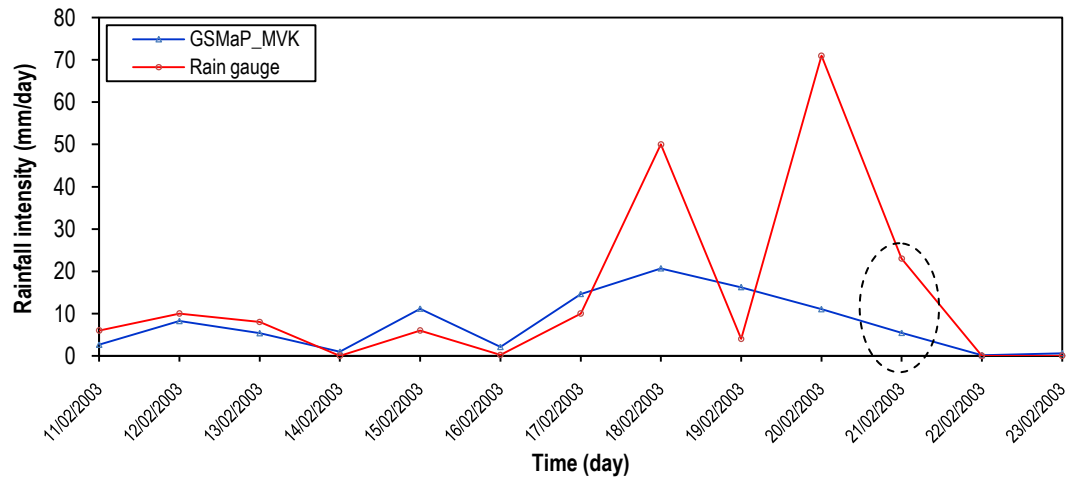

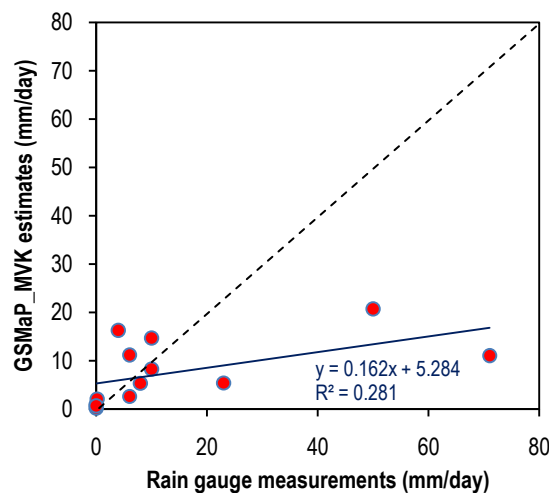**Figure 5.15 Same as Figure 5.13 but for daily data**

Figure 5.16 Same as Figure 5.14 but for daily data

The daily observations (Figure 5.15) show better matching of capturing peaks and rainfall intensity than the 3-hourly data. One day before flood began the GSMaP_MVK estimated about 85% lower than that of the rain gauge data, which were 11 mm/day and 71 mm/day, respectively. Consecutive rainfall was captured

by the two measurements from 4 days preceding the flood event. The closeness of observation between the GSMaP_MVK and rain gauge improves significantly for daily data as can be seen in Figure 5.16. On the average the GSMaP_MVK underestimated of the rain gauge data on daily scale.

5.2.2   Rainfall patterns before floods occur

Table 5.4 denotes summary of the rainfall patterns before floods occur for the analysed flood events in Pekanbaru City and Indragiri Hulu Regency.

Table 5.4

The rainfall patterns before floods occur in Pekanbaru City and Indragiri Hulu Regency from 2003 to 2009

No.	Flood Event	Rainfall Patterns		
		Long-Term	Short-Term	Irregular
1	25/01/2003*		△	
2	21/02/2003*		△	
3	30/11/2003		△	
4	10/12/2003*	△		
5	22/12/2006		△	
6	30/10/2007		△	
7	24/03/2008			△
8	17/09/2008			△
9	05/12/2009		△	
10	09/12/2009	△		
	Total	**2**	**6**	**2**

* Data shown in Aryastana (2012) study

From Figure 5.9, variation of rainfall intensity of flood event on 25 January 2003 can be identified as short-term period pattern, instead of irregular pattern classified by Aryastana (2012). Both the GSMaP_MVK and the rain gauge detected accumulative rainfall with high intensity one day or several hours before flood starts to occur. The flood event on 21 February 2003 (Figure 5.13) also

indicates short-term period pattern, instead of irregular pattern classified by Aryastana (2012). Short-term period rainfall pattern is the most frequent occurred accounting for 60% of the total flood events analysed in Pekanbaru City and Indragiri Hulu Regency.

5.2.3   Accuracy verification of the GSMaP_MVK

Table 5.5 shows summary of the continuous statistical verification of the GSMaP_MVK product with respect to the rain gauge data for the 10 flood events analysed in Pekanbaru City and Indragiri Hulu Regency. The comparison has also been made for 3-hourly average and daily data.

Table 5.5

The continuous statistical verification for the flood events analysed in Pekanbaru City and Indragiri Hulu Regency from 2003 to 2009

Flood Event	3-hourly				Daily			
	ME (mm/h)	MAE (mm/h)	RMSE (mm/h)	r	ME (mm/h)	MAE (mm/h)	RMSE (mm/h)	r
25/01/2003	-0.36	0.53	1.28	0.49	-0.46	0.55	0.99	0.71
21/02/2003	-0.39	0.76	2.30	0.45	-0.29	0.45	0.82	0.53
30/11/2003	-0.30	0.58	2.00	0.57	-0.35	0.45	0.74	0.79
10/12/2003	-0.02	1.06	2.39	0.23	-0.38	0.77	0.98	0.46
22/12/2006	-0.16	0.92	3.31	0.23	-0.11	0.72	1.15	0.30
30/10/2007	0.09	0.97	2.18	0.33	0.22	0.61	0.82	0.56
24/03/2008	-0.23	0.71	1.71	0.53	-0.33	0.48	1.05	0.71
17/09/2008	0.14	0.24	0.75	0.39	-0.03	0.21	0.36	0.61
05/12/2009	-0.29	0.58	1.67	0.69	-0.29	0.46	0.80	0.87
09/12/2009	-0.37	0.59	1.67	0.71	-0.43	0.48	0.81	0.91
Average	**-0.19**	**0.69**	**1.93**	**0.46**	**-0.21**	**0.47**	**0.78**	**0.65**

The GSMaP_MVK shows negative mean error (ME) for 3-hourly and daily data for most of the flood events, except on 30 October 2007 and 17

September 2008. The flood events on 10 December 2003 and 17 September 2008 show the lowest negative ME, while the highest positive ME is on 30 October 2007.

The MAE ranges from 0.24 mm/h to 1.06 mm/h and from 0.21 mm/h to 0.77 mm/h for 3-hourly and daily data, respectively. RMSE reached the highest value of 3.31 mm/h and 1.15 mm/h and the lowest value of 0.75 mm/h and 0.36 mm/h for 3-hourly and daily data, respectively. Flood event on 17 September 2008 shows the lowest RMSE for 3-hourly and daily data.

The correlation coefficient is in the range from 0.23 to 0.71 and from 0.30 to 0.91 for 3-hourly and daily data, respectively. The lowest correlation is on 22 December 2006, while the highest is on 9 December 2009 for 3-hourly and daily data.

On the average, the GSMaP_MVK underestimates of the rain gauge data for the entire flood events analysed in Pekanbaru City and Indragiri Hulu Regency. The correlation coefficients are 0.46 and 0.65 for 3-hourly and daily data, respectively.

Table 5.6 shows summary of the categorical verification statistics for the flood events analysed in Pekanbaru City and Indragiri Hulu Regency for the 3-hourly average and daily time steps data.

The probability of rain detection (POD) of the GSMaP_MVK indicates more than 60% for the entire flood events studied. The range is from 0.63 to 0.96 and from 0.88 to 1 for 3-hourly and daily data, respectively. The lowest POD is on 25 January 2003 and 9 December 2009 for 3-hourly and daily data, respectively.

On the average, the POD performs moderate to high value of 0.75 and 0.99 for 3-hourly and daily data, respectively.

Table 5.6

The categorical verification statistics for the flood events analysed in Pekanbaru City and Indragiri Hulu Regency from 2003 to 2009

Flood Event	3-hourly			Daily		
	POD	FAR	TS	POD	FAR	TS
25/01/2003	0.63	0.53	0.36	1.00	0.38	0.62
21/02/2003	0.74	0.61	0.34	1.00	0.23	0.77
30/11/2003	0.67	0.72	0.24	1.00	0.31	0.69
10/12/2003	0.71	0.68	0.28	1.00	0.15	0.85
22/12/2006	0.68	0.67	0.28	1.00	0.38	0.62
30/10/2007	0.81	0.63	0.34	1.00	0.38	0.62
24/03/2008	0.67	0.54	0.38	1.00	0.25	0.75
17/09/2008	0.77	0.59	0.37	1.00	0.45	0.55
05/12/2009	0.96	0.54	0.45	1.00	0.40	0.60
09/12/2009	0.83	0.52	0.44	0.88	0.30	0.64
Average	**0.75**	**0.60**	**0.35**	**0.99**	**0.33**	**0.67**

The FAR score shows more than 50% and 15% with its lowest reached nearly 0.52 on 9 December 2009 and 0.15 on 10 December 2003 for 3-hourly and daily time steps, respectively. The TS ranges from 0.24 to 0.45 and from 0.55 to 0.85 for 3-hourly and daily data, respectively. The highest TS are on 5 December 2009 and 10 December 2003 for 3-hourly and daily data, respectively.

5.3 Flood Events in Samarinda City

There were 134 flood events reported in East Kalimantan Province from 2003 to 2010 and Samarinda City accounted for 21 (BNPB, 2013; Brakenridge, 2013). Nine flood events were analysed for Samarinda City due to limited availability of data from the rain gauge station.

5.3.1   Rainfall condition

This section presents results of 2 flood events in Samarinda City according to the previous study by Aryastana (2012), i.e. on 25 January 2004 and 7 May 2004. The others can be seen in Appendix D.
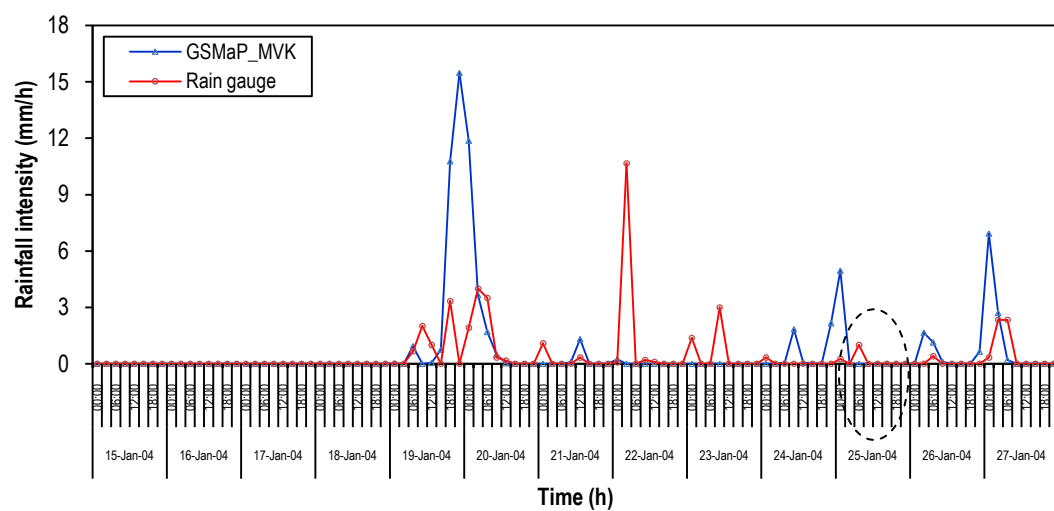
🌳   Flood event on 25 January 2004

Figure 5.17 Time-series of 3-hourly average rainfall intensity for the flood event on 25 January 2004

Figure 5.17 shows time series of the 3-hourly average rainfall intensity for the flood event on 25 January 2004 obtained from the GSMaP_MVK and rain gauge data. The dash-line circle indicates the day of the flood began. The total number of data points is 104. The GSMaP_MVK estimation shows discrepancies in capturing rainfall events and intensity with respect to the rain gauge data. The GSMaP_MVK missed detection for rainfall event on 22 January 2004 at 03:00 (UTC) while the rain gauge station observed it. On the contrary, the GSMaP_MVK estimated that the rainfall occurred on 19 January 2004 (at 21:00

UTC) and on 24 January 2004 (at 09:00 UTC) but rain gauge station did not observed them, which means false rainy detection by satellite data.

The two data sources slightly match in capturing the peaks of the rainfall events but the rainfall intensity is to be higher by the GSMaP_MVK estimation. The GSMaP_MVK overestimated rainfall intensity of 15.48 mm/h when the rain gauge did not capture the event as seen on 19 January 2004 (at 21:00 UTC). This is the highest peak detected by the GSMaP_MVK before flood occurred. Meanwhile, the rain gauge observed the highest peak of 10.67 mm/h 3 days before the flood began when the GSMaP_MVK missed it. The two observations agree that no consecutive high intensity rainfall observed up to 3 days before the flood began.
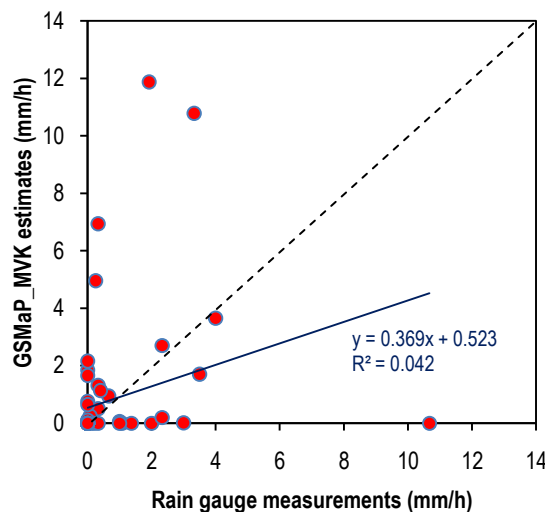
Figure 5.18 Scatter plot of the 3-hourly rainfall intensity for the flood event on 25 January 2004

From the scatter plot (Figure 5.18), rainfall magnitude of the GSMaP_MVK estimation is seen to be on average higher than that of the rain

gauge data. The data points are concentrated above the 45^0 slope dash line indicates that the GSMaP_MVK overestimated of the rain gauge data.
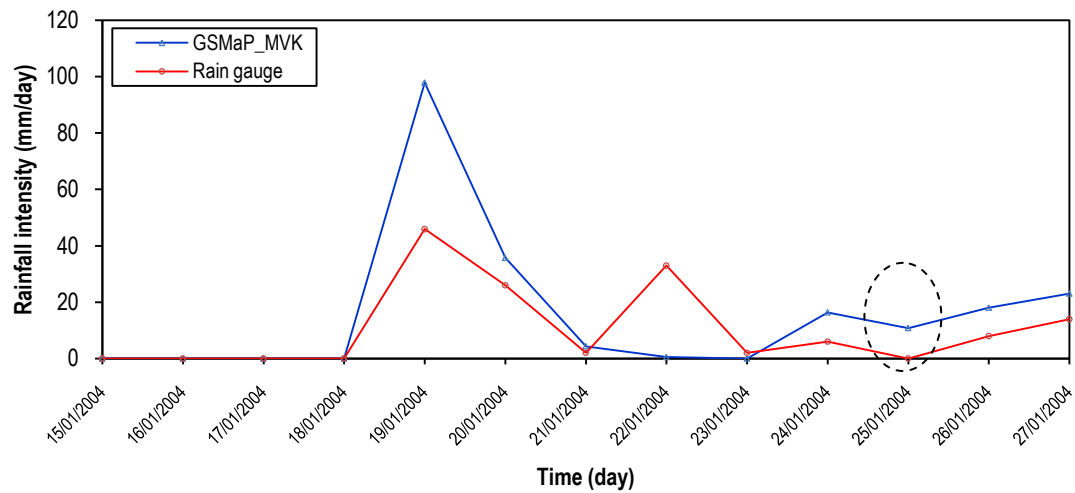

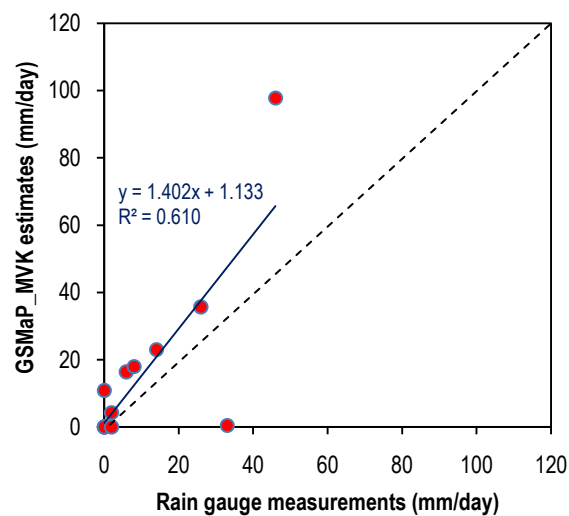**Figure 5.19 Same as Figure 5.17 but for daily data**

Figure 5.20 Same as Figure 5.18 but for daily data

Figure 5.19 denotes time-series of daily rainfall intensity from the GSMaP_MVK and rain gauge data for the flood event on 25 January 2004. The total number of data points is 13. On the day of flood began the GSMaP_MVK

estimated 10.84 mm/day of rainfall intensity, while the rain gauge data did not report it. The closeness of data pairs between the GSMaP_MVK and rain gauge improves significantly for daily data as can be seen in Figure 5.20. On the average the GSMaP_MVK overestimated of the rain gauge data on daily scale.

🌍 Flood event on 7 May 2004
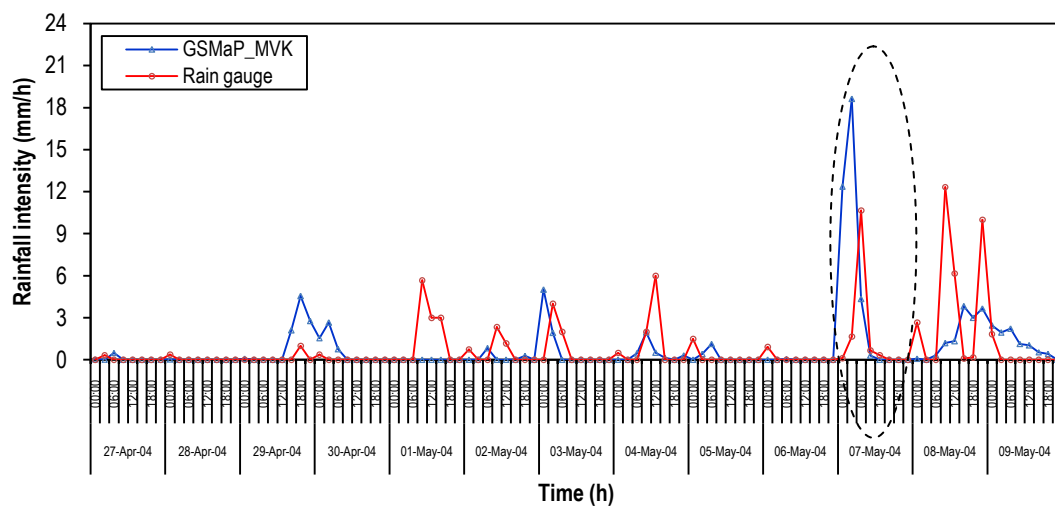
Figure 5.21 Time-series of 3-hourly average rainfall intensity for the flood event on 7 May 2004

Figure 5.21 presents the comparison of 3-hourly variations of rainfall intensity between the GSMaP_MVK and rain gauge data for the flood even t on 7 May 2004. The two observations show quite match to capture the peaks of the rainfall event but differ for the rainfall intensity. The GSMaP_MVK missed detection for rainfall event on 1 May 2004 from 09:00 (UTC) to 15:00 (UTC) while the rain gauge station observed it. On the contrary, the GSMaP_MVK estimated the rainfall occurred on the day of the flood began at 00:00 (UTC) but the rain gauge data did not observed it. The GSMaP_MVK overestimated of the

rain gauge data about 91% on the day of the flood began at 03:00 (UTC), which was the highest peak (18.63 mm/h) estimated by the GSMaP_MVK. The rain gauge data observed consecutive rainfall with high intensity after the flood began, which underestimated by the GSMaP_MVK.
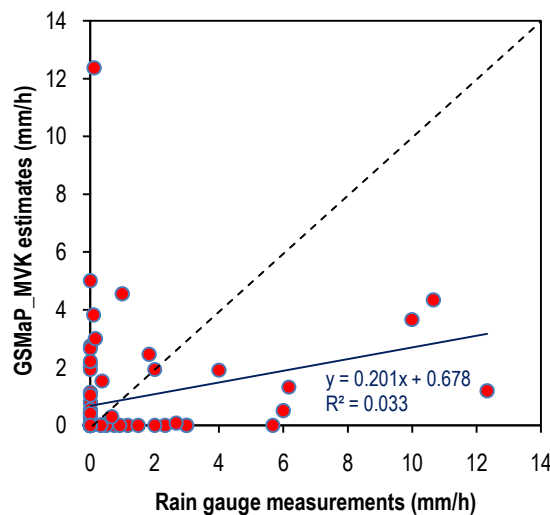

Figure 5.22 Scatter plot of the 3-hourly rainfall intensity for the flood event on 7 May 2004

From the scatter plot (Figure 5.22), rainfall magnitude of the GSMaP_MVK estimation is seen to be on average slightly higher than that of the rain gauge data. The data points are concentrated below the 45^0 slope dash line indicates that the GSMaP_MVK overestimated of the rain gauge data.

Figure 5.23 denotes time-series of daily rainfall intensity from the GSMaP_MVK and rain gauge data for the flood event on 7 May 2004. The total number of data points is 13. The GSMaP_MVK estimated rainfall intensity of 106.4 mm/day on the day of the flood began compared with the rain gauge data of 64 mm/day. It represents approximately a 44.7% of overestimation. This figure is

the highest peak reported by the two observations. The closeness of data pairs between the GSMaP_MVK and rain gauge improves significantly for daily data as can be seen in Figure 5.24. On the average the GSMaP_MVK overestimated of the rain gauge data on daily scale.
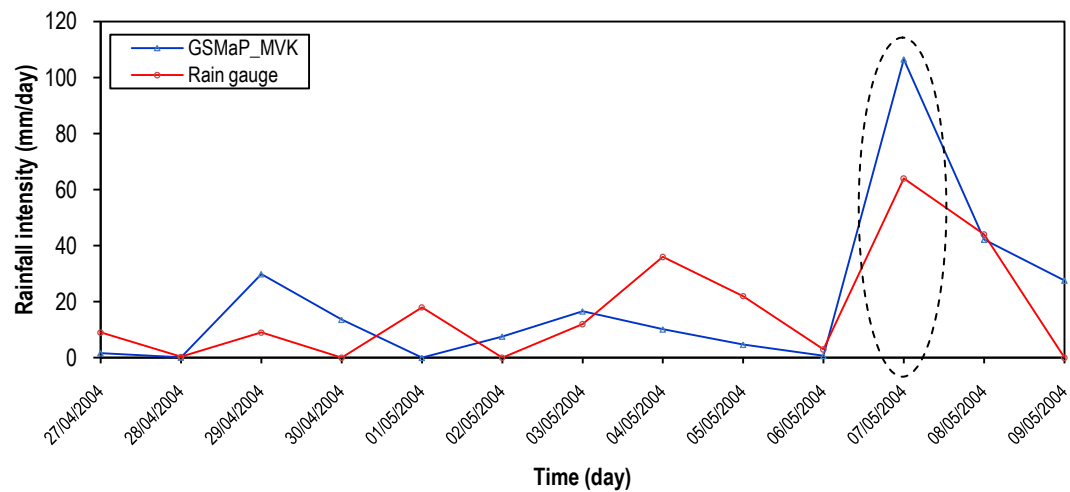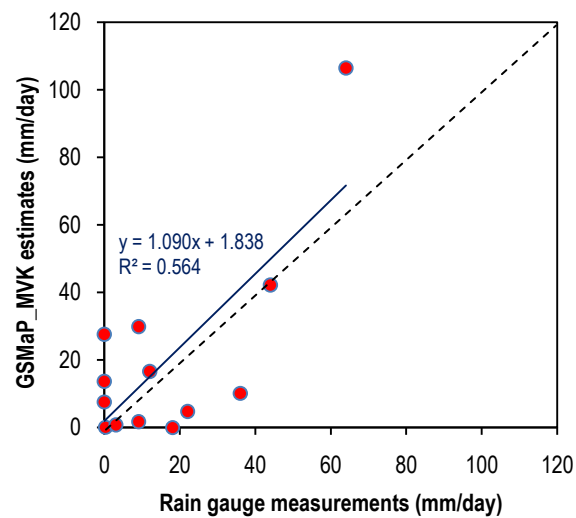

Figure 5.23 Same as Figure 5.21 but for daily data

Figure 5.24 Same as Figure 5.22 but for daily data

5.3.2   Rainfall patterns before floods occur

Table 5.7 denotes summary of the rainfall patterns before floods occur for the analysed flood events in Samarinda City.

Table 5.7

The rainfall patterns before floods occur for Samarinda City from 2004 to 2010

No.	Flood Event	Rainfall Patterns		
		Long-Term	Short-Term	Irregular
1	25/01/2004*			△
2	20/04/2004		△	
3	07/05/2004*		△	
4	02/02/2007		△	
5	20/06/2007	△		
6	04/11/2008		△	
7	01/12/2008	△		
8	19/04/2009		△	
9	01/11/2010		△	
Total		**2**	**6**	**1**

* Data shown in Aryastana (2012) study

Variation of rainfall intensity of flood event on 25 January 2004 as seen in Figure 5.17 can be identified as irregular pattern, which shows good agreement with Aryastana (2012) study. This is due to the condition that several hours before flood began, there was no heavy rainfall. However, the heavy rainfall occurred several days before flooding. Meanwhile, the flood event on 7 May 2004 (Figure 5.21) indicates short-term period pattern, instead of irregular pattern classified by Aryastana (2012). Both the GSMaP_MVK and the rain gauge detected accumulative rainfall with high intensity one day or several hours before flood starts to occur.

Short-term period rainfall pattern is the most frequent occurred accounting for about 66.7% of the total flood events analysed in Samarinda City.

5.3.3   Accuracy verification of the GSMaP_MVK

Table 5.8 shows summary of the continuous statistical verification of the GSMaP_MVK product with respect to the rain gauge data for the 9 flood events analysed in Samarinda City.

The GSMaP_MVK shows positive mean error (ME) of more than 67% of the total flood events for 3-hourly and daily data. The flood events on 7 May 2004 and 20 June 2007 show the lowest positive ME for 3-hourly and daily data, respectively. While the highest positive ME are on 19 April 2009 for both 3-hourly and daily data.

Table 5.8

The continuous statistical verification for the flood events analysed in Samarinda City from 2004 to 2010

Flood Event	3-hourly				Daily			
	ME	MAE	RMSE	r	ME	MAE	RMSE	r
25-Jan-04	0.28	0.76	2.43	0.21	0.22	0.44	0.75	0.78
20-Apr-04	-0.23	0.77	2.18	0.18	-0.34	0.39	0.72	0.93
07-May-04	0.05	1.22	2.89	0.18	0.14	0.61	0.78	0.75
02-Feb-07	-0.06	0.87	2.72	0.10	0.13	0.28	0.45	0.75
20-Jun-07	0.23	0.62	1.75	0.20	0.12	0.44	0.75	0.57
04-Nov-08	0.12	0.79	2.09	0.33	0.14	0.45	0.58	0.65
01-Dec-08	-0.18	0.55	1.27	0.63	-0.19	0.33	0.47	0.83
19-Apr-09	0.40	1.14	3.47	0.05	0.40	0.87	1.36	0.33
01-Nov-10	0.26	0.70	1.50	0.13	0.14	0.43	0.68	0.33
Average	**0.10**	**0.83**	**2.26**	**0.22**	**0.09**	**0.47**	**0.73**	**0.66**

The MAE ranges from 0.55 mm/h to 1.22 mm/h and from 0.28 mm/h to 0.87 mm/h for 3-hourly and daily data, respectively. RMSE reached the highest value of 3.47 mm/h and 1.36 mm/h and the lowest value of 1.27 mm/h and 0.45 mm/h for 3-hourly and daily data, respectively. Flood events on 1 December 2008 and on 2 February 2007 show the lowest RMSE for 3-hourly and daily data, respectively.

The correlation coefficient is in the range from 0.05 to 0.63 and from 0.33 to 0.93 for 3-hourly and daily data, respectively. The lowest correlation is on 19 April 2009, while the highest is on 1 December 2008 for 3-hourly data.

On the average, the GSMaP_MVK overestimates of the rain gauge data for the entire flood events analysed in Samarinda City. The correlation coefficients are 0.22 and 0.66 for 3-hourly and daily data, respectively.

Table 5.9 shows summary of the categorical verification statistics for the flood events analysed in Samarinda City and for the 3-hourly average and daily time steps data.

The POD of the GSMaP_MVK indicates more than 50% for the entire flood events studied. The range is from 0.5 to 0.81 and from 0.9 to 1 for 3-hourly and daily data, respectively. The lowest POD is on 20 April 2004 for 3-hourly data, while on 7 May 2004 and 1 November 2010 are the lowest POD for daily data. On the average, the POD performs moderate to high value of 0.68 and 0.97 for 3-hourly and daily data, respectively.

The FAR score shows more than 48% and 10% with its lowest reached nearly 0.49 on 2 February 2007 and 0.11 on 25 January 2004 for 3-hourly and

daily time steps, respectively. The TS ranges from 0.3 to 0.42 and from 0.5 to 0.89 for 3-hourly and daily data, respectively. The highest TS are on 19 April 2009 and 25 January 2004 for 3-hourly and daily data, respectively.

Table 5.9

The categorical verification statistics for the flood events analysed in Samarinda City from 2004 to 2010

Flood Event	3-hourly			Daily		
	POD	FAR	TS	POD	FAR	TS
25-Jan-04	0.67	0.53	0.38	1.00	0.11	0.89
20-Apr-04	0.50	0.56	0.31	1.00	0.23	0.77
07-May-04	0.63	0.60	0.32	0.90	0.25	0.69
02-Feb-07	0.63	0.49	0.39	0.91	0.09	0.83
20-Jun-07	0.75	0.56	0.38	1.00	0.50	0.50
04-Nov-08	0.81	0.60	0.36	1.00	0.31	0.69
01-Dec-08	0.65	0.64	0.30	1.00	0.33	0.67
19-Apr-09	0.79	0.53	0.42	1.00	0.33	0.67
01-Nov-10	0.68	0.63	0.31	0.90	0.25	0.69
Average	**0.68**	**0.57**	**0.35**	**0.97**	**0.27**	**0.71**

5.4   Flood Events in Manado City

There were 31 flood events recorded in North Sulawesi Province from 2003 to 2010 and Manado City accounted for 9 (BNPB, 2013; Brakenridge, 2013). Six flood events were analysed for Manado City due to limited availability of data from rain

5.4.1   Rainfall condition

This section presents results of 1 flood event in Manado City according to the previous study by Aryastana (2012), i.e. on 26 December 2003. The others can be seen in Appendix E.

🌑 Flood event on 26 December 2003

Figure 5.25 shows the time series of the 3-hourly average rainfall intensity for the flood event on 26 December 2003 derived from the GSMaP_MVK and rain gauge data. The dash-line circle indicates the day of the flood began. The total number of data points is 104. The GSMaP_MVK estimation shows discrepancies in capturing rainfall events and intensity with respect to the rain gauge data. The GSMaP_MVK missed detection for rainfall events on 17 December 2003 from 15:00 (UTC) to 00:00 (UTC), on 19 December 2003 from 12:00 (UTC) to 21:00 (UTC) and on 24 December 2003 at 00:00 (UTC) while the rain gauge station observed them. On the contrary, the GSMaP_MVK estimated that the rainfall occurred on 16 December 2003 at 12:00 (UTC) but rain gauge station did not observed it, which means false rainy detection by satellite data.
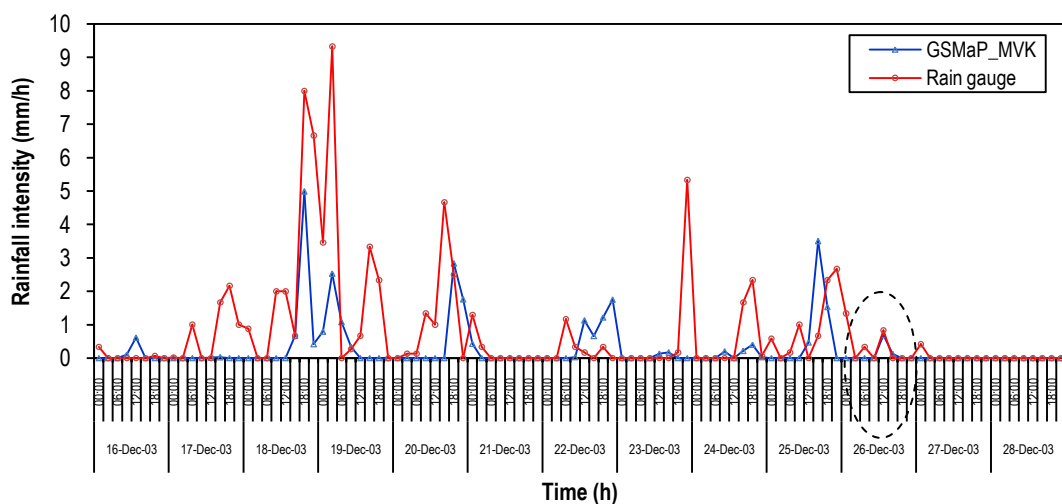
Figure 5.25 Time-series of 3-hourly average rainfall intensity for the flood event on 26 December 2003

Consecutive high intensity rainfall occurred from 18 December 2003 to 19 December 2003 has been observed by the rain gauge and the GSMaP_MVK data.

The two data sources slightly match in capturing the peaks of the rainfall events but the rainfall intensity is to be lower by the GSMaP_MVK estimation. The GSMaP_MVK underestimated rainfall intensity of about up to 72% during the highest peak observed by the rain gauge from 18 December 2003 to 19 December 2003. Accumulative rainfall mostly observed by the rain gauge with the highest peak is 5.33 mm/h three days before the flood began, while the GSMaP_MVK detected the highest peak of 3.5 mm/h one day before flooding.
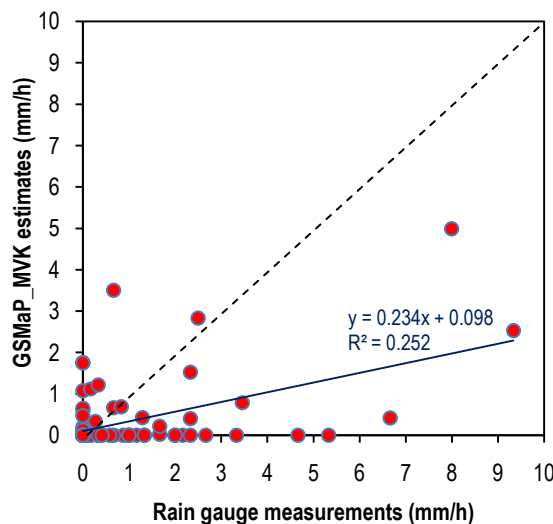
Figure 5.26 Scatter plot of the 3-hourly rainfall intensity for the flood event on 26 December 2003

Figure 5.26 shows rainfall magnitude of the GSMaP_MVK estimation is seen to be on average lower than that of the rain gauge observation. The data points are mostly concentrated below the 45^0 slope dash line indicates that the GSMaP_MVK underestimated of the rain gauge data.

Figure 5.27 shows the time-series of daily rainfall intensity from the GSMaP_MVK and rain gauge data for the flood event on 26 December 2003. The

total number of data points is 13. The GSMaP_MVK estimated rainfall intensity of 16.5 mm/day one day before flood began compared with the rain gauge data of 32 mm/day. It represents approximately a 48% of underestimation. The closeness of data pairs between the GSMaP_MVK and rain gauge improves significantly for daily data as can be seen in Figure 5.28. On the average the GSMaP_MVK underestimated of the rain gauge data on daily scale
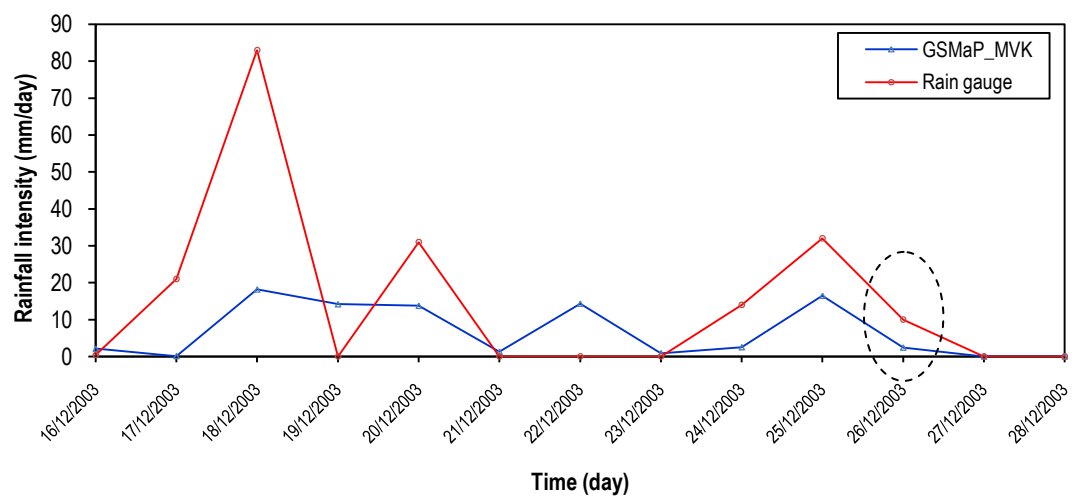
Figure 5.27 Same as Figure 5.25 but for daily data
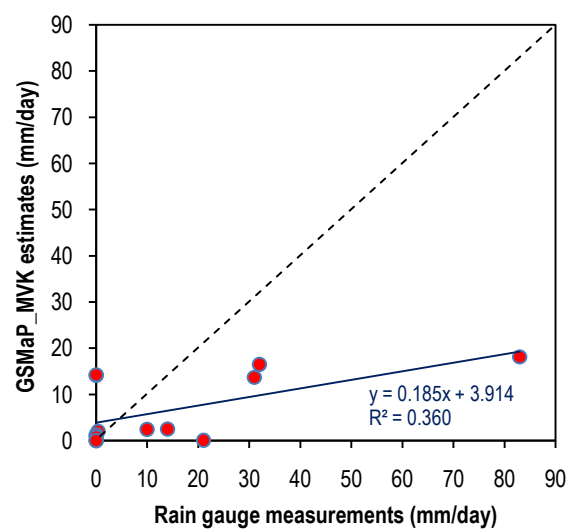
Figure 5.28 Same as Figure 5.26 but for daily data

5.4.2   Rainfall patterns before floods occur

Table 5.10 denotes summary of the rainfall patterns before floods occur for the analysed flood events in Manado City. Variation of rainfall intensity of flood event on 26 December 2003 as seen in Figure 5.25 can be identified as long-term period pattern, instead of irregular pattern classified by Aryastana (2012). Both the GSMaP_MVK and the rain gauge data detected accumulative rainfall several days or more than one day before flood starts to occur.

Table 5.10

The rainfall patterns before floods occur for Manado City from 2003 to 2010

No.	Flood Event	Rainfall Patterns		
		Long-Term	Short-Term	Irregular
1	10/01/2003		△	
2	26/12/2003*	△		
3	01/02/2006			△
4	13/02/2006		△	
5	13/01/2009		△	
6	22/05/2010		△	
Total		**1**	**4**	**1**

* Data shown in Aryastana (2012) study

Short-term period rainfall pattern is the most frequent occurred accounting for about 66.7% of the total flood events analysed in Manado City.

5.4.3   Accuracy verification of the GSMaP_MVK

Table 5.11 shows summary of the continuous statistical verification of the GSMaP_MVK product with respect to the rain gauge data for the 6 flood events analysed in Manado City.

The GSMaP_MVK shows negative mean error (ME) for the entire flood events analysed based on 3-hourly and daily data. The flood event on 1 February 2006 shows the lowest negative ME for both 3-hourly and daily scale. While the highest negative ME is on 13 January 2009 for both 3-hourly and daily data.

Table 5.11

The continuous statistical verification for the flood events analysed in Manado City from 2003 to 2010

Flood Event	3-hourly				Daily			
	ME	MAE	RMSE	r	ME	MAE	RMSE	r
10-Jan-03	-0.46	0.83	2.33	0.58	-0.46	0.46	0.79	0.96
26-Dec-03	-0.48	0.72	1.48	0.50	-0.34	0.54	0.88	0.60
01-Feb-06	-0.39	0.65	1.69	0.47	-0.32	0.37	0.64	0.96
13-Feb-06	-0.72	1.11	2.26	0.63	-0.75	0.78	0.99	0.89
13-Jan-09	-0.75	0.88	2.64	0.71	-0.89	0.89	1.28	0.93
22-May-10	-0.40	0.86	1.99	0.38	-0.34	0.59	0.75	0.64
Average	**-0.53**	**0.84**	**2.07**	**0.54**	**-0.52**	**0.61**	**0.89**	**0.83**

The MAE ranges from 0.65 mm/h to 1.11 mm/h and from 0.37 mm/h to 0.89 mm/h for 3-hourly and daily data, respectively. RMSE reached the highest value of 2.64 mm/h and 1.28 mm/h and the lowest value of 1.48 mm/h and 0.64 mm/h for 3-hourly and daily data, respectively. Flood events on 26 December 2003 and on 1 February 2006 show the lowest RMSE for 3-hourly and daily data, respectively.

The correlation coefficient is in the range from 0.38 to 0.71 and from 0.60 to 0.96 for 3-hourly and daily data, respectively. The lowest correlation is on 22 May 2010, while the highest is on 13 January 2009 for 3-hourly data.

On the average, the GSMaP_MVK underestimates of the rain gauge data for the entire flood events analysed in Manado City. The correlation coefficients are 0.54 and 0.83 for 3-hourly and daily data, respectively.

Table 5.12 shows summary of the categorical verification statistics for the flood events analysed in Manado City and for the 3-hourly average and daily time steps data.

Table 5.12

The categorical verification statistics for the flood events analysed in Manado City from 2003 to 2010

Flood Event	3-hourly			Daily		
	POD	FAR	TS	POD	FAR	TS
10-Jan-03	0.41	0.38	0.33	0.78	0.00	0.78
26-Dec-03	0.50	0.42	0.37	1.00	0.41	0.58
01-Feb-06	0.72	0.28	0.56	1.00	0.11	0.89
13-Feb-06	0.75	0.34	0.54	0.90	0.10	0.82
13-Jan-09	0.53	0.30	0.43	0.92	0.00	0.92
22-May-10	0.52	0.45	0.37	1.00	0.00	1.00
Average	**0.57**	**0.36**	**0.43**	**0.93**	**0.10**	**0.83**

The POD of the GSMaP_MVK indicates more than 40% for the entire flood events studied. The range is from 0.41 to 0.72 and from 0.78 to 1 for 3-hourly and daily data, respectively. The lowest POD is on 10 January 2003 for both 3-hourly and daily data. On average, the POD performs moderate to high value of 0.57 and 0.93 for 3-hourly and daily data, respectively.

The lowest FAR score of 0.28 shows on 1 February 2006 for 3-hourly data. While, the perfect FAR score of 0 is shown on 10 January 2003, 13 January 2009 and 22 May 2010 for daily data. The TS ranges from 0.33 to 0.56 and from 0.58

to 1 for 3-hourly and daily data, respectively. The highest TS are on 1 February 2006 and 22 May 2010 for 3-hourly and daily data, respectively.

CHAPTER VI

DISCUSSION

6.1 Rainfall Condition of Flood Events

Visual comparisons between the GSMaP_MVK and rain gauge data show discrepancies in capturing rainfall events and intensity of preceding and following the flood events over Medan City, Pekanbaru City & Indragiri Hulu Regency, Samarinda City and Manado City for 3-hourly average and daily time steps data. According to Sorooshian *et al*. (2011), it is well known that the discrepancy between satellite estimates and ground-rain gauge observations is not limited to the magnitude of rain rates but also includes rainfall patterns and geometrical features. This is also complicated by the nature of the rain gauge, which conventionally measures the rainfall as an integral of time at a point in space, whereas satellites measure an integral of space at a point in time (Kidd *et al*., 2003).

Subsequently, Krajewski (1993) in Petty and Krajewski (1996) pointed out that the observed differences between satellite-based estimates and a reference estimate such as rain gauge station can be attributed to errors in both compared measurements. The errors can be classified as: (1) sampling; (2) measurement; and (3) estimation. Satellite data suffer from some inherent shortcomings and have biases and random errors that are caused by various factors like sampling frequency, non-uniform field of view of the sensors, and uncertainties in the rainfall retrieval algorithms (Nair *et al*. 2009 in Li *et al.*, 2013). Meanwhile, the

amount of rainfall measured in a rain gauge is less than the actual rainfall reaching the ground. This is mainly due to systematic errors (Huey and Ibrahim, 2012). The systematic errors include losses due to wind, wetting, evaporation, and splashing (Habib *et al.*, 2008).

Comparing with 3-hourly average scale, the daily observations show better matching of capturing the peaks and rainfall intensity. This is due to the longer time accumulation results in minimising detection of rainfall fluctuations, while the shorter time accumulation captures higher rainfall variability. In addition, Petty and Krajewski (1996) noted that rainfall rate and short term rain accumulation display high degrees of zero-rain intermittence as seen for 3-hourly average data. As the time scale increases, the zero-rain intermittence becomes less of a problem and rainfall fields are more continuous.

Meanwhile, rainfall fluctuations of preceding and following the flood events show widely differs from event to event due to magnitude underestimation or overestimation by the GSMaP_MVK satellite estimates with respect to the rain gauge data. The GSMaP_MVK underestimated the rainfall intensity over Medan City, Pekanbaru City & Indragiri Hulu Regency and Manado City, but overestimated over Samarinda City. The GSMaP_MVK are generally overestimated to light rainfall and less sensitive to heavy rainfall. According to Barrett (1997), it is intrinsically difficult to establish rain/no-rain boundary with precision because the gradients of rainfall intensity may instead be very shallow, which lead to underestimation/overestimation.

6.2   Rainfall Patterns before Floods Occur

Based on the regional rainfall classification by Aldrian and Susanto (2003) Medan City, Pekanbaru City and Indragiri Hulu are located in Region B, which has two rainfall peaks, i.e. in October to November (ON) and in March to May (MAM). The peaks are associated with the southward and northward movement of the inter-tropical convergence zone (ITCZ). Most of the flood events analysed for Medan City occurred during that peak period, while, in Pekanbaru City and Indragiri Hulu Regency occurred mostly during the trough period.

On the other hand, Samarinda City and Manado City are located in Region A, which has one peak and one trough and experiences strong influences of two monsoons, namely the wet northwest (NW) monsoon from November to March (NDJFM) and the dry southeast (SE) monsoon from May to September (MJJAS). Most of the flood events analysed for Samarinda City and Manado City coincided with the wet northwest (NW) monsoon period.

Overall, short-term period rainfall pattern is the most frequent occurred preceding flood events in Medan City, Pekanbaru City & Indragiri Hulu Regency, Samarinda City and Manado City accounted for about 63.6%, 60%, 66.7% and 66.7%, respectively. These areas are also known as urban regions with some rivers flows nearby, which likely indicate the regions are more susceptible to flash floods and river overflows. According to Marchi *et al.* (2010) flash floods are associated with short, high-intensity rainfalls, mainly of convective origin that occur locally. As noted by Hapuarachchi and Wang (2008) urbanisation can significantly increase the risk of flash floods. As land is converted from fields or

woodlands to roads and parking lots, the land loses its ability to absorb rainfall. On average, urbanisation increases runoff two to six times over what would occur on natural terrain.

For the flood events on 5 December 2003 and 12 January 2006 (Appendix B), in Medan City, which indicated irregular rainfall pattern, the GSMaP_MVK and rain gauge observations show quite good agreement to capture rainfall events. However, both of them detected no heavy rainfall about 4 to 5 days before the day of flooding reported. Similarly, the two observations show quite good agreement to capture the peaks for the flood events on 24 March 2008 and 17 September 2008 (Appendix C) in Pekanbaru City. Both the two observations agree that no heavy rainfall detected about 2 days before the flood began. These flood occurrences may be caused by other than rainfall simultaneously.

6.3   Accuracy Verification of the GSMaP_MVK

Verification of 3-hourly and daily rainfall intensity of the flood events at study areas using continuous statistic score, i.e. mean error (ME) shows that the GSMAP_MVK data on average underestimates for Medan City, Pekanbaru City & Indragiri Hulu Regency, and Manado City and overestimates for Samarinda City. From Table A.1, for 3-hourly (daily) data the lowest negative ME is -0.04 mm/h (-0.03 mm/h) for Medan City followed by Pekanbaru City & Indragiri Hulu Regency and Manado City with -0.19 mm/h (-0.21 mm/h) and -0.53 mm/h (-0.52 mm/h), respectively. The positive ME of 0.1 mm/h (0.09 mm/h) is shown for Samarinda City.

On the average, the highest MAE of 0.84 mm/h (0.61 mm/h) is for Manado City followed by Pekanbaru City & Indragiri Hulu Regency and Medan City with 0.69 mm/h (0.47 mm/h), 0.65 mm/h (0.36 mm/h), respectively. The similar trend is also shown in the same order for RMSE score with 2.07 mm/h (0.89 mm/h), 1.93 mm/h (0.78) mm/h, 1.76 mm/h (0.58 mm/h). While for Samarinda City shows the value of 0.83 mm/h (0.47 mm/h) and 2.26 mm/h (0.73 mm/h) for the MAE and the RMSE, respectively. Meanwhile, the highest correlation coefficient is for Manado City, which is 0.54 and 0.83 for 3-hourly and daily scale, respectively. While, the lowest is 0.22 for Samarinda City and 0.65 for Pekanbaru City & Indragiri Hulu Regency, that is respectively for 3-hourly and daily data.

Overall, the daily data reveal lower ME, MAE and RMSE than 3-hourly data. The trends of change of the RMSE are similar as the MAE. The daily data provide improvement of the correlation coefficient compared with the 3-hourly data. The MAE and RMSE decrease as the time step increases. This is because of the shorter the time steps the more errors are included (e.g. due to higher variability), while the longer time steps removes the representativeness of errors.

Verification on rainfall events of the flood events at study areas using categorical statistics scores shows that on average (Table A.2) the GSMaP_MVK provides moderate to high probability of rain detection (POD) in the range from 0.57 to 0.75 and from 0.93 to 0.99 for 3-hourly and daily data, respectively. The highest POD is found for Pekanbaru City & Indragiri Hulu Regency, while the lowest is shown for Manado City for both the two data. The false alarm ratio

(FAR) ranges from 0.36 to 0.64 and from 0.10 to 0.42 for 3-hourly and daily data, respectively. The lowest FAR is shown for Manado City, while the highest is found for Medan city for both the two data. Meanwhile, the threat score (TS) spans from 0.31 to 0.43 and from 0.58 to 0.83 for 3-hourly and daily data, respectively. The highest TS is observed for Manado City, while the lowest is found for Medan City for both the two data.

Overall, as the time steps increases, the POD increases accordingly. The trends of change of the FAR are on the contrary with the POD score. Similar to the POD, the TS increases as the time steps increases. These may be because of the intense rain fell that are in gauge proximity are missed by the satellites snapshot and picked by gauges for shorter period (Crosson *et al*., 1996 in Bangira, 2013). It is expected that for good accuracy of the satellite estimates with respect to the rain gauge measurements, the POD and the TS are as high as possible approaching value of 1, which represents higher probability of rainfall events is correctly observed or estimated. On the contrary, the lower the FAR score the higher the satellite accuracy. It means less possibility to falsely detected rainfall events in which did not measure by the rain gauge observation.

According to the statistics verification, performance of the GSMaP_MVK differs among the regencies and also from event to event. Local effects, such as terrain profile, near to coastal area with sea and land breeze circulations (e.g. Manado City, Medan City and Samarinda City) may contribute to the results deviation (Islam *et al.*, 2005). Furthermore, retrieval of precipitation using PMW observations has always represented a problem over coastal areas; often

techniques omit retrievals over the coastline, or use a less optimum technique (Kidd and Levizzani, 2011; Kidd and Huffman, 2011; Kelkar, 2007).

Kubota *et al.* (2009) reported that large errors of the GSMaP were found in areas with frequently heavy orographic rainfall over the Japanese Archipelago. They investigated performance of six satellite rainfall estimates using passive microwave (PMW) and infrared (IR) radiometers around Japan with reference to a ground-radar dataset calibrated by rain gauges provided by the Japan Meteorological Agency (JMA) from January through December 2004. Overall, validation results over the ocean were best, and results over mountainous regions were worst. Rainfall estimates were poor over coasts and small islands. One reason for the errors was the relatively low POD values due to the rain/no-rain identification problem over coasts.

Shrestha *et al.* (2011) investigated that the GSMaP_MVK tends to underestimate of daily rainfall over the Nepal Himalayas. They used daily rainfall data from 176 rain gauge stations over Nepal from 2003 to 2006. By applying the standard statistical verification technique, the ME is -0.11 mm/h (-2.6 mm/day), the RMSE is 0.4 mm/h (4.8 mm/day), the correlation coefficient is 0.79, the POD is 0.96 and the FAR is 0.07. In the case of Ethiopia, with a complex terrain similar to their study area, Dinku *et al*. (2010) investigated the performance of various satellite rainfall products and found that satellite-based estimates did well in detecting the occurrence of rainfall, but were not good in estimating the amount of daily rainfall.

Fu *et al.* (2011) evaluated the accuracy of GSMaP_MVK ver. 4.8.4 using in situ data from 45 rain gauge stations across Poyang Lake Basin in the period between 2003 and 2006 at daily, monthly and annual scales. Their results show that the GSMaP products generally underestimate rainfall amount. The monthly correlation coefficient is 0.85, which shows a significant linear relationship between product estimations and rain-gauged observations while the daily correlation coefficient is less than 0.50 on average. The performance of rainfall estimation based on satellite data is poorer in mountainous areas than that in flatlands. According to them, the possible cause of the satellite underestimation may be due to topographic factors, mechanism of precipitation, and the defects in GSMaP algorithm itself.

In this study, the rain gauge density for Medan City, Pekanbaru City, Indragiri Hulu Regency, Samarinda City and Manado City are 265.1, 632.26, 8198, 718, 159.02 km^2 per station, respectively. These figures are much larger than the minimum requirement by the WMO (1994), which is about 10 to 20 km^2 per station for urban areas. Hence, the accuracy of the GSMaP_MVK product is roughly represented due to the scarcity of the rain gauge measurements or coarser rain gauge spatial resolution which results in unavoidable rain gauge sampling error. However, for preliminary assessment, this study is expected to be slightly adequate and needed to be improved, if possible by using more extents of the rain gauge station number.

For comparison, Artabudi (2012) considered that the average density of rain gauge network is about 531.6 km^2 per station for the study area in Denpasar

City and the surrounding areas. Five rain gauge station data were utilised over 2,658 km^2 area. The study estimated groundwater recharge in that area based on rainfall data from the GSMaP and rain gauge station and reported that the GSMaP_MVK underestimated about 41% of the precipitation measured by the rain gauge for monthly average precipitation.

CHAPTER VII

CONCLUSION AND RECOMMENDATION

7.1 Conclusion

Based on the objectives of this study and the results obtained, some concluding remarks can be drawn as follows:

a. The GSMaP_MVK product provides promising potentiality for the application of monitoring rainfall conditions preceding flood events in Indonesia, especially in Medan City, Pekanbaru City, Indragiri Hulu Regency, Samarinda City and Manado City. The GSMaP_MVK performs underestimation for the most areas, except Samarinda City, which is overestimated.

b. Comparisons of the GSMaP_MVK with the rain gauge data show discrepancies in capturing rainfall events and intensity of preceding and following the flood events in Medan City, Pekanbaru City & Indragiri Hulu Regency, Samarinda City and Manado City. However, the GSMaP_MVK product quite matches in detecting rainfall occurrences. The three-hourly observations show less matching than the daily data. This is due to the shorter time accumulation captures higher rainfall variability. Thus, the reliability of the GSMaP_MVK with respect to the rain gauge observations reduces for the 3-hourly data as compared with the daily data.

c. Both the two observations agree that no heavy rainfall detected before the flood began for the flood events on 5 December 2003 and 12 January 2006

in Medan City and on 24 March 2008 and 17 September 2008 in Pekanbaru City. These flood occurrences may be caused by other than rainfall simultaneously.

d. Short-term period rainfall pattern is the most frequent occurred preceding flood events in Medan City, Pekanbaru City & Indragiri Hulu Regency, Samarinda City and Manado City accounted for about 63.6%, 60%, 66.7% and 66.7%, respectively, which indicate that these areas are more susceptible to flash floods and river overflows.

7.2 Recommendation

a. More extents data, such as number of rain gauge station, flood locations and events are required for detail study on the accuracy of rainfall monitoring by the GSMaP_MVK product. This is in order to assess representativeness of Indonesia region and the applicability of the GSMaP_MVK product over the region with few or even non-existence rain gauges. Presently, however, availability of the rain gauge stations providing continuous rainfall data are very limited and low distributed over Indonesia, which considers as a challenge.

b. This study is limited to monitoring rainfall conditions before floods began using the GSMaP_MVK and rain gauge data, but not to predicting when and where the flood will occur. For a comprehensive study on the prediction of flood events in Indonesia, the GSMaP_MVK product as well as the rain gauge data could be utilised in conjunction with other satellite data (e.g. MODIS, ALOS, etc.) and hydrological model.

REFERENCES

Adeyewa, Z.D., Nakamura, K. 2003. Validation of TRMM Radar Rainfall Data over Major Climatic Regions in Africa. *J. Appl. Meteor*, 42:331-347

Aldrian, E., Susanto, R.D. 2003. Identification of three dominant rainfall regions within Indonesia and their relationship to sea surface temperature. *Int. J. Climatol*, 23:1435-1452

Aonashi, K., Liu, G. 2000. Passive Microwave Precipitation Retrievals Using TMI during the Baiu Period of 1998. Part I: Algorithm Description and Validation. *J. Appl. Meteor,* 39:2024–2037.

Artabudi, I.N. 2012. "Remote Sensing Application to Estimate Groundwater Recharge in Denpasar and Surrounding Areas" (Master Thesis). Denpasar: Udayana University.

Aryastana, P. 2012. "Flood Assessment in Indonesia Based on Rainfall Data from GSMaP" (Master Thesis). Japan: Yamaguchi University

Badan Nasional Penanggulangan Bencana (BNPB), Data Informasi Bencana Indonesia. (Last access: March, 2013)
Available from: URL: http://www.bnpb.go.id/

Bajracharya, S.R., Shreatha, M.S., Mool, P.K., Thapa, R. 2010. Validation of Satellite Rainfall Estimation in the Summer Monsoon Dominated Area of the Hindu Kush Himalayan Region. *Grazer Schriften der Geographie und Raumforschung*. Band 45, pp. 281-290

Bangira, T. 2013. "Mapping of Flash Flood Potential Areas in the Western Cape (South Africa) Using Remote Sensing and In Situ Data" (Msc Thesis). The Netherlands: The University of Twente.

Barrett, E. C., Doodge, J., Goodman, M., Janowiak, J., Smith, E., Kidd, C. 1994. The First WetNet Precipitation Intercomparison Project (PIP-1). *Remote Sens. Rev.,* 11**:**49–60.

Barrett, E.C. 1997. Satellite rainfall monitoring: recent progress and remaining problems. *Remote Sensing and Geographic Information Systems for Design and Operation of Water Resources Systems (Proceedings of Rabat Symposium S3, April 1997).* IAHS Publ. No. 242, pp. 141-148

Bauer, P. 2001. Over-ocean rainfall retrieval from multisensory data or the Tropical Rainfall Measuring Mission, Part I: Design and evaluation of inversion databases. *J. Atmos. Ocean. Techn.,* 18:1315–1330

Brakenridge, G.R. 2013. Global Active Archive of Large Flood Events, Dartmouth Flood Observatory, University of Colorado. (Last access: February, 2013) Available from:
URL: http://floodobservatory.colorado.edu/Archives/index.html.

Ceccato, P., Dinku, T. 2010. Introduction to Remote Sensing for Monitoring Rainfall, Temperature, Vegetation and Water Bodies. IRI Technical Report 10-04, 15 p. Palisades, N.Y.: International Research Institute for Climate and Society. Available from: URL: http://hdl.handle.net/10022/AC:P:8914

Ciach, G.J., Krajewski, W.F. 1999. On the estimation of radar rainfall error variance. *Advances in Water Resources,* 22(6):585-595

Crosson, W. L., Duchon, C. E., Raghavan, R., Goodman, S. J. 1996. Assessment of rainfall estimates using a standard Z-R relationship and the probability matching method applied to composite radar data in central Florida. *Journal of Applied Meteorology, 35*(8):1203-1219.

Dinku, T., Ruiz, F., Connor, S.J., Ceccato, P. 2010. Validation and Intercomparison of Satellite Rainfall Estimates over Colombia. *J. Appl. Meteor. Climatol.*, 49:1004-1014

Duo, C., Tundrop, P., Ghancan, N., Bajracharya, S., Shrestha, M., Jianping, G. 2011. Validation of the Satellite-Derived Rainfall Estimates over the Tibet. *Acta Meteor. Sinica*, 25(6):734-741

Ebert, E.E. 2007. Methods for Verifying Satellite Precipitation Estimates. In: Levizzani, V., Bauer, P., Turk, F.J., editors. *Measuring Precipitation from Space: EURAINSAT and the Future*. The Netherlands: Springer. p 345-355.

Frederick, W.H., Worden, R.L. 2011. Indonesia: A Country Report- 6[th]ed. Library of Congress, Federal Research Division. Washington, 440 p. Available from: URL: http://lcweb2.loc.gov/frd/cs/pdf/CS_Indonesia.pdf

Fu, Q., Ruan, R., Liu, Y. 2011. Accuracy Assessment of Global Satellite Mapping of Precipitation (GSMaP) Product over Poyang Lake Basin, China. *Procedia Environmental Sciences*, 10:2265-2271

Gomez, M.R.S. 2007. "Spatial and Temporal Rainfall Gauge Data Analysis and Validation with TRMM Microwave Radiometer Surface Rainfall Retrievals" (MSc Thesis). The Netherlands: International Institute for Geo-Information Science and Earth Observation

Grimes, D. I. F., Pardo-Iguzquiza, E., Bonifacio, R. 1999. Optimal areal rainfall estimation using raingauges and satellite data. *Journal of Hydrology*, 222:93-108.

Habib, E. H., Meselhe, E. A., Aduvala, A. V. 2008. Effect of Local Errors of Tipping-Bucket Rain Gauges on Rainfall-Runoff Simulations. *Journal of Hydrologic Engineering*, 13(6):488-496

Hapuarachchi, H.A.P, Wang, Q.J. 2008. A review of methods and systems available for flash flood forecasting. CSIRO: Water for a Healthy Country National Research Flagship

Harris, A., Rahman, S., Hossain, F., Yarborough, L., Bagtzoglou, A.C., Easson, G. 2007. Satellite based Flood Modeling Using TRMM-based Rainfall Product. *Sensors*, 7:3416-3427

Hossain, F., Anagnostou, E.N., Dinku, T. 2004. Sensitivity Analyses of Satellite Rainfall Retrieval and Sampling Error on Flood Prediction Uncertainty. *IEEE Transactions on Geoscience and Remote Sensing*, 42(1):130-139

Huey, T.T., Ibrahim, A.L. 2012. Statistical Analysis of Annual Rainfall Patterns in Peninsular Malaysia Using TRMM Algorithms. *The 33rd Asian Conference on Remote Sensing*, November 26-30, 2012, Pattaya, Thailand

Islam, M.N., Terao, T., Uyeda, H., Hayashi, T., Kikuchi, K. 2005. Spatial and Temporal Variations of Precipitation in and around Bangladesh. *Journal of the Meteorological Society of Japan*, 83(1):21-39

Jain, S.K., Singh, V.P. 2003. Water Resources Systems Planning and Management. First Edition. The Netherlands: Elsevier Science B.V.

Joyce, R.J., Janowiak, J.E., Arkin, P.A., Xie, P. 2004. CMORPH: a method that produces global precipitation estimates from passive microwave and infrared data at high spatial and temporal resolutions. Journal of Hydrometeorology, 5: 487–503.

Kachi, M., Kubota, T., Ushio, T., Shige, S., Kida, S., Aonashi, K., Okamoto, K. 2011. Development and utilization of "JAXA Global Rainfall Watch" system. *IEEJ Transactions on Fundamentals and Materials*, 131:729–737 (In Japanese with English abstract).

Kelkar, R.R. 2007. Satellite Meteorology. Hyderabad, India: BS Publications

Kidd, C. 2001. Satellite rainfall climatology: a review. *Int. J. Climatol*, 21:1041-1066

Kidd, C., Kniveton, D.R., Todd, M.C., Bellerby, T.J. 2003. Satellite Rainfall Estimation Using Combined Passive Microwave and Infrared Algorithms. *J. Hydrometeor*, 4:1088-1104

Kidd, C., Levizzani, V., Turk, J., Ferraro, R. 2009. Satellite precipitation measurements for water resource monitoring. *Journal of the American Water Resources Association*, 45(3):567-579

Kidd, C., Huffman, G. 2011. Review. Global precipitation measurement. *Meteorol. Appl.*, 18:334-353

Kidd, C., Levizzani, V. 2011. Status of satellite precipitation retrievals. *Hydrol. Earth Syst. Sci.*, 15:1109-1116

Krajewski, W. F. 1993. Global estimation of rainfall: certain methodological issues. In: Bras, R., editor. *World at Risk: Global Climate Change and Natural Hazards*, Proc. Conf. American Institute of Physics 277:180-192.

Kubota, T., Shige, S., Hashizume, H., Aonashi, K., Takahashi, N., Seto, S., Hirose, M., Takayabu, Y.N., Ushio, T., Nakagawa, K., Iwanami, K., Kachi, M.,

Okamoto, K. 2007. Global Precipitation Map Using Satellite-Borne Microwave Radiometers by the GSMaP Project: Production and Validation. *IEEE Transactions on Geoscience and Remote Sensing*, 45(7):2259-2275

Kubota, T., Ushio, T., Shige, S., Kida, S., Kachi, M., Okamoto, K. 2009. Verification of High-Resolution Satellite-based Rainfall Estimates around Japan Using a Gauge-Calibrated Ground-Radar Dataset. *Journal of the Meteorological Society of Japan*, 87A:203-222

Levizzani, V., Amorati, R., Meneguzzo, F. 2002. A Review of Satellite-based Rainfall Estimation Methods. MUSIC-EVKI-CT-2000.00058 Deliverable 6.1, 66 p. Bologna. Italy. Available from: URL: http://satmet.isac.cnr.it/papers/MUSIC-Rep-Sat-Precip-6.1.pdf

Li, X., Zhang, Q., Xu, C.-Y. 2013. Assessing the performance of satellite-based precipitation products and its dependence on topography over Poyang Lake basin. *Theoretical and Applied Climatology*, DOI 10.1007/s00704-013-0917-x

Marchi, L., Borga, M., Preciso, E., Gaume, E. 2010. Characterisation of selected extreme flash floods in Europe and implications for flood risk management. *Journal of Hydrology*, 394:118-133

Met Office, 2011. Climate: Observations, projections and impacts-Indonesia. Crown. United Kingdom, 136 p. Available from: URL: http://www.metoffice.gov.uk/climate-change/policy-relevant/obs-projections-impacts

Morrissey, M.L., Janowiak, J.E. 1996. Sampling-Induced Conditional Biases in Satellite Climate-Scale Rainfall Estimates. *J. Appl. Meteor.*, 35:541–548.

Murphy, A.H. 1995. The Coefficients of Correlation and Determination as Measures of Performance in Forecast Verification. *Wea. Forecasting*, 10:681-688

Mustafa, M. 2007. "Validation of Satellite-based Rainfall Estimation over the Limpopo Basin" (MSc Thesis). Zimbabwe: University of Zimbabwe

Nair, S., Srinivasan, G., Nemani, R. 2009. Evaluation of multi-satellite TRMM derived rainfall estimates over a western state of India. *J. Meteorol. Soc. Jap.*, 87(6):927–939

New, M., Todd, M., Hulme, M., Jones, P. 2001. Review. Precipitation measurements and trends in the twentieth century. *Int. J. Climatol.*, 21:1899-1922

Okamoto, K., Iguchi, T., Takahashi, N., Ushio, T., Awaka, J., Kozu, T., Shige, S., Kubota, T. 2007. High Precision and High Resolution Global Precipitation Map from Satellite Data. *Proceedings of ISAP* (pp. 506-509). Niigata, Japan: IEICE.

Okamoto, K., Shige, S., Kachi, M., Kubota, T., Ushio, T. 2011. The Global Precipitation Map Produced by Spaceborn Microwave Radiometers and It's Application-Overview of the GSMaP (Global Satellite Mapping of Precipitation) Project. *IEEE*, p. 4.

Petty, G. W., Krajewski, W.F. 1996. Satellite estimation of precipitation over land. *Hydrol. Sci. J.,* 41: 433–451.

Rosenfeld, D. 2007. Is Man Actively Changing the Environment? In: Levizzani, V., Bauer, P., Turk, F.J., editors. *Measuring Precipitation from Space: EURAINSAT and the Future*. The Netherlands: Springer. p. 7-24.

Rudolf, B., Hauschild, H., Rueth, W., Schneider, U. 1994. Terrestrial precipitation analysis: Operational method and required density of point measurements. In: Desbois, M., Desalmand, F., editors. *Global Precipitations and Climate Change,* NATO ASI Series I, Vol. 26: Springer-Verlag, p. 173–186.

Scofield, R. A., Kuligowski, R. J. 2003. Status and outlook of operational satellite precipitation algorithms for extreme precipitation events. *Weather Forecast*, 18:1037–1051

Sene, K. 2008. Flood Warning, Forecasting and Emergency Response. United Kingdom: Springer Science+Business Media B.V.

Seto, S., Tsunekawa, T., Oki, T. 2012. A new rain detection method to complement high-resolution global precipitation products. *Hydrological Research Letters*, 6: 82-86

Shrestha, M.S., Takara, M.S., Kubota, T., Bajracharya, S.R. 2011. Verification of GSMaP Rainfall Estimates over the Central Himalayas. *Journal of Japan Society of Civil Engineers, ser. B1 (Hydraulic Engineering)*, 67(4):37-42

Sinclair, S., and Pegram, G. 2005. Combining radar dan rain gauge rainfall estimates using conditional merging. *Atmospheric Sciences Letters*, 6(1):19-22.

Sorooshian, S., Aghakouchak, A. Arkin, P., Eylander, J., Foufoula-Georgiou, E., Harmon, R., Hendrickx, J.M.H., Imam, B., Kuligowski, R., Skahill, B., Skofronick-Jackson, G. 2011. Advanced Concepts on Remote Sensing of Precipitation at Multiple Scales. *Bull. Amer. Meteor. Soc.*, 92:1353-1357

Spencer, R.W., Goodman, H. M., Hood, R. E. 1989. Precipitation retrieval over land and ocean with SSM/I, Part I: Identification and characteristics of the scattering signal. *J. Atmos. Ocean. Techn.*, 6:254–273

Strangeways, I. 2007. Precipitation Theory, Measurement and Distribution. Cambridge, Cambridge Univerisity Press.

Suseno, D.P.Y., 2009. "Geostationary Satellite Based Rainfall Estimation for Hazard Studies and Validation: A case study of Java Island, Indonesia" (MSc Thesis). Yogyakarta: Gadjah Mada University-International Institute for Geo-Information Science and Earth Observation.

Sutardi. 2006. Action Report toward Flood Disasters Reduction Indonesian Case. In IFNet Action Report 2006-Good Practices for Substantial Human Loss Reduction from Floods. Available from: URL: http://www.internationalfloodnetwork.org/AR2006/AR2006.html

Tempfli, K., Kerle, N., Huurneman, G.C., Janssen, L.L.F. 2009. Principles of Remote Sensing An introductory textbook, Fourth Edition. The Netherlands: The International Institute for Geo-Information Science and Earth Observation (ITC)

Testik, F., Gebremichael, M. 2011. Rainfall: State of the Science. *Eos*, 92(43):378-379

Tian, Y., Peters-Lidard, C.D., Adler, R.F., Kubota, T., Ushio, T. 2010. Evaluation of GSMaP Precipitation Estimates over the Contiguous United States. *Journal of Hydrometeorology*, 11:566-574

Ushio, T., Sasashige, K., Kubota, T., Shige, S., Okamoto, K., Aonashi, K., Inoue, T., Takahashi, N., Iguchi, T., Kachi, M., Oki, R., Morimoto, T., Kawasaki, Z-I. 2009. A Kalman Filter Approach to the Global Satellite Mapping of Precipitation (GSMaP) from Combined Passive Microwave and Infrared Radiometric Data. *Journal of the Meteorological Society of Japan,* 87A:137-151

Villarini, G., Mandapaka, P.V., Krajewski, W.F., Moore, R.J. 2008. Rainfall and sampling uncertainties: A rain gauge perspective. *Journal of Geophysical Research*, Vol. 113, D11102, doi:10.1029/2007JD009214

Wilheit, T. T., Chang, A. T. C., Chiu, L. S. 1991. Retrieval of monthly rainfall indices from microwave radiometric measurements using probability distribution functions. *J. Atmos. Oceanic. Technol.*, 8:118–136

World Meteorological Organization, 1994. Guide to Hydrological Practices: Data Acquisition and Processing, Analysis, Forecasting and other Applications. 5th edition. WMO-No 168. Geneva

World Meteorological Organization, 2011. Guide to Climatological Practices. WMO-No.100. Geneva

APPENDIX A   Summary of the Statistical Verification for the Research Locations

Table A.1

Summary of the continuous statistical verification for the research   locations

Regency	3-hourly				Daily			
	ME (mm/h)	MAE (mm/h)	RMSE (mm/h)	r	ME (mm/h)	MAE (mm/h)	RMSE (mm/h)	r
Medan	-0.04	0.65	1.76	0.31	-0.03	0.36	0.58	0.71
Pekanbaru & Indragiri Hulu	-0.19	0.69	1.93	0.46	-0.21	0.47	0.78	0.65
Samarinda	0.10	0.83	2.26	0.22	0.09	0.47	0.73	0.66
Manado	-0.53	0.84	2.07	0.54	-0.52	0.61	0.89	0.83

Table A.2

Summary of the categorical verification statistics for the research locations

Regency	3-hourly			Daily		
	POD	FAR	TS	POD	FAR	TS
Medan	0.73	0.64	0.31	0.97	0.42	0.58
Pekanbaru& Indragiri Hulu	0.75	0.60	0.35	0.99	0.33	0.67
Samarinda	0.68	0.57	0.35	0.97	0.27	0.71
Manado	0.57	0.36	0.43	0.93	0.10	0.83

APPENDIX B   Time Series of 3-Hourly and Daily Rainfall Intensity for Flood Events in Medan City
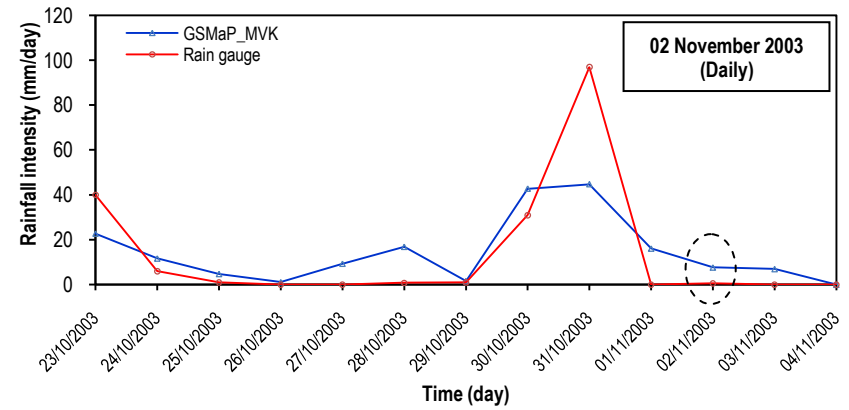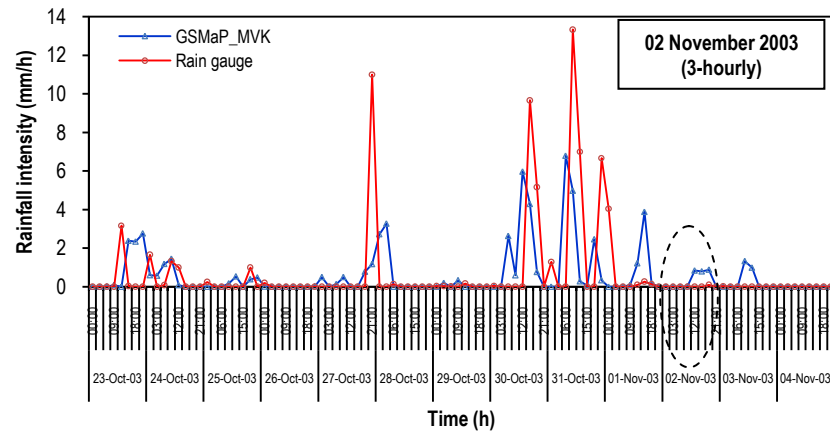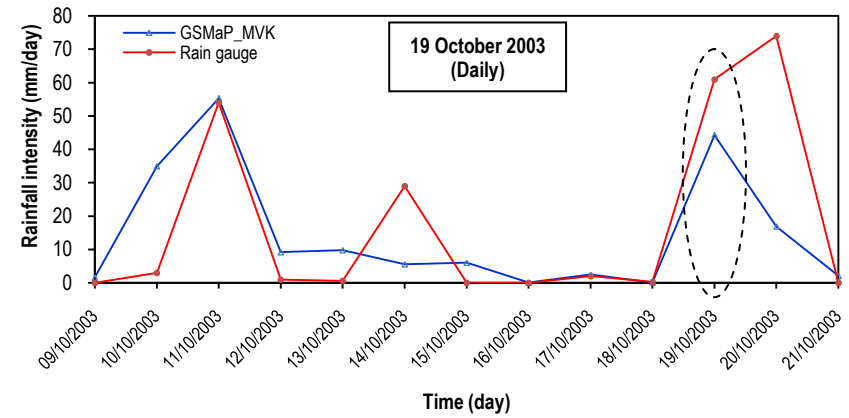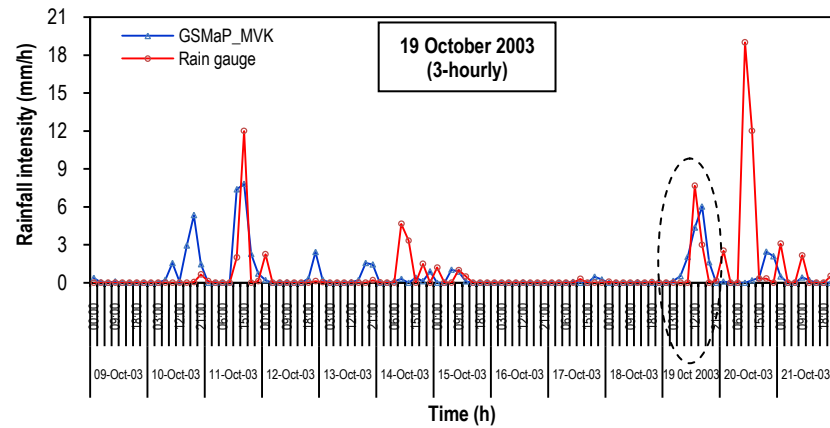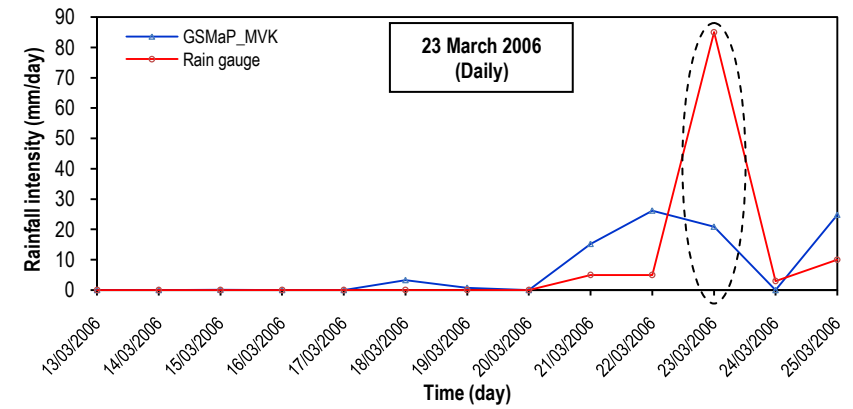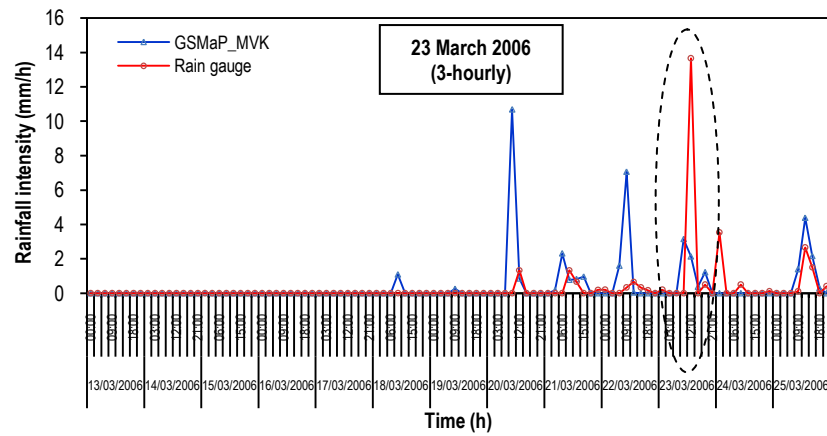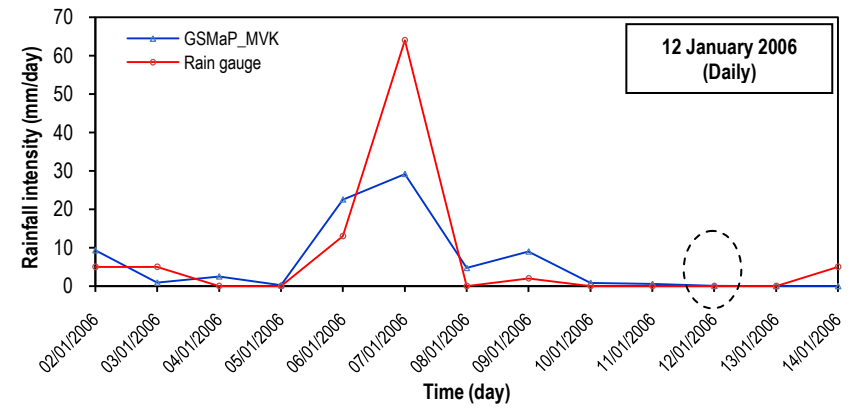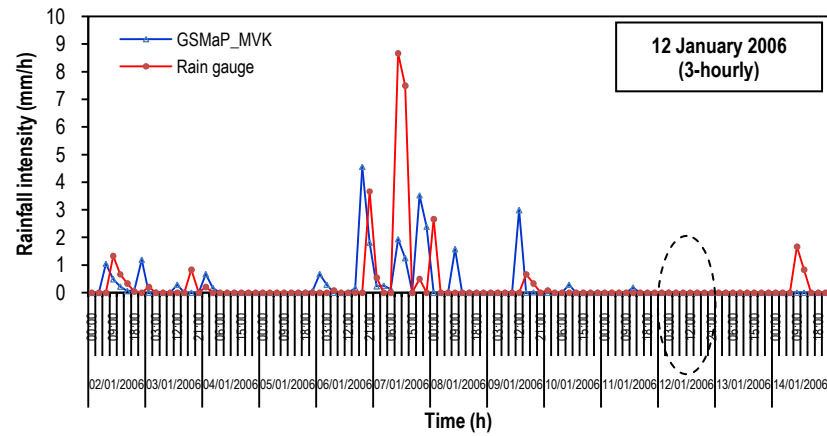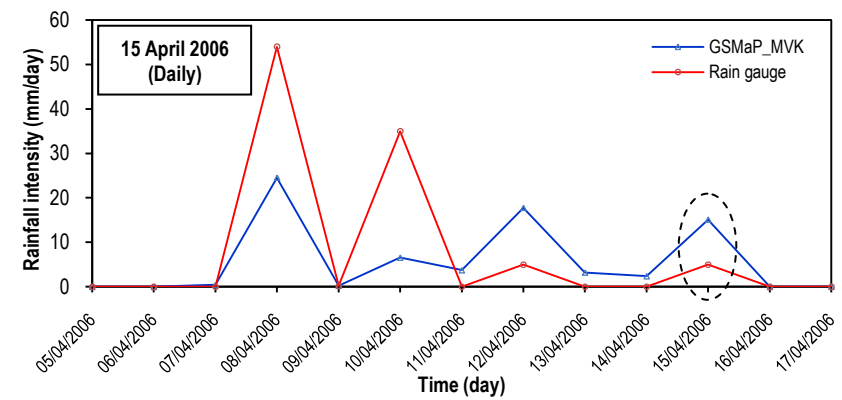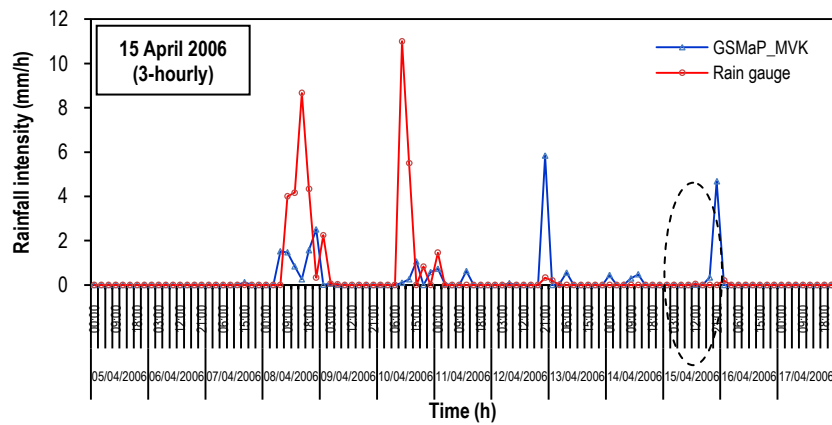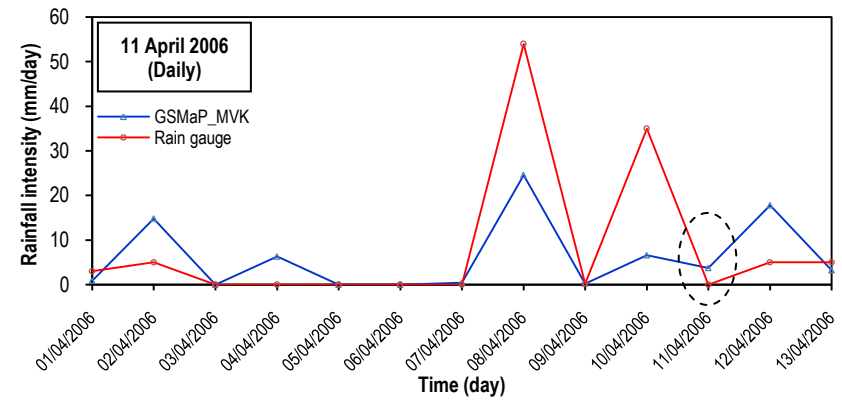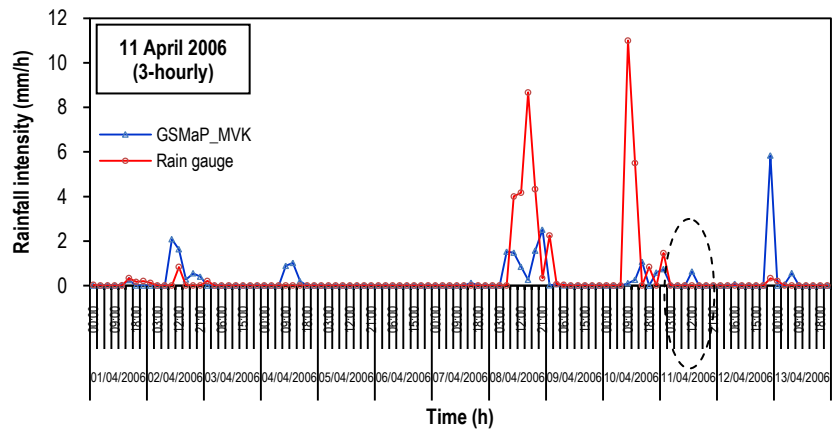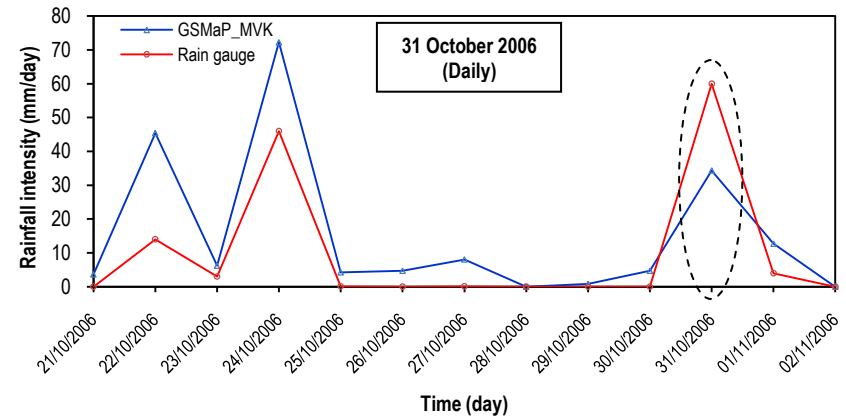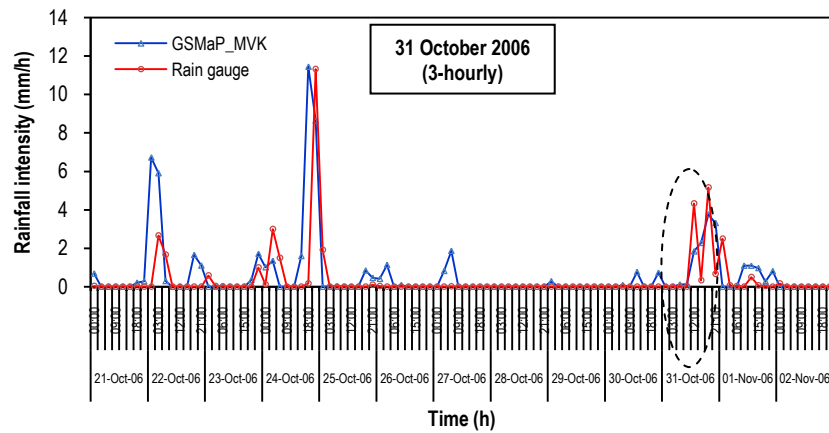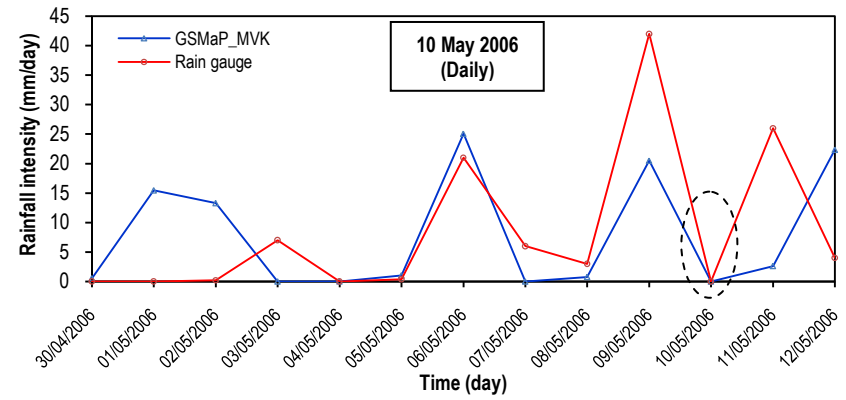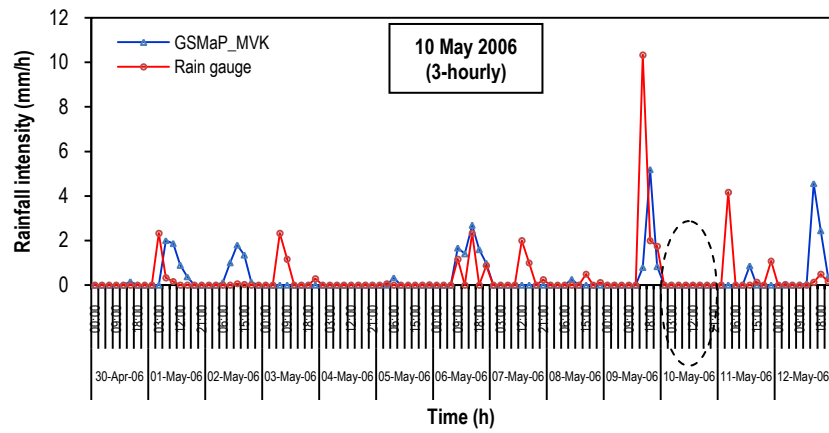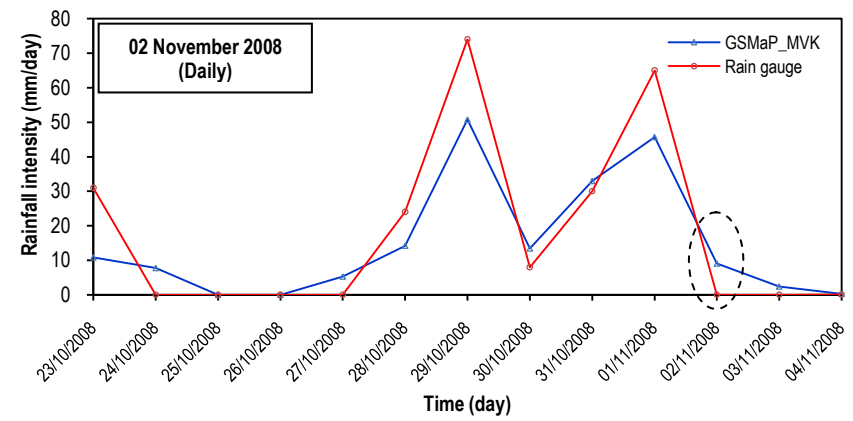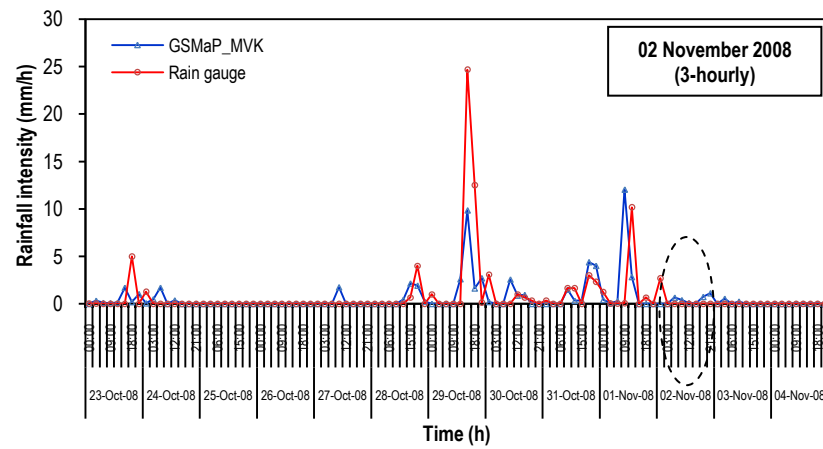
APPENDIX C **Time Series of 3-Hourly and Daily Rainfall Intensity for Flood Events in Pekanbaru City and Indragiri Hulu Regency**
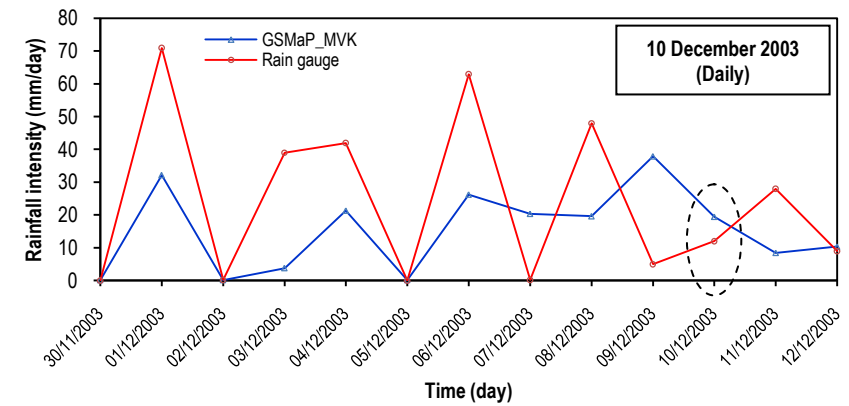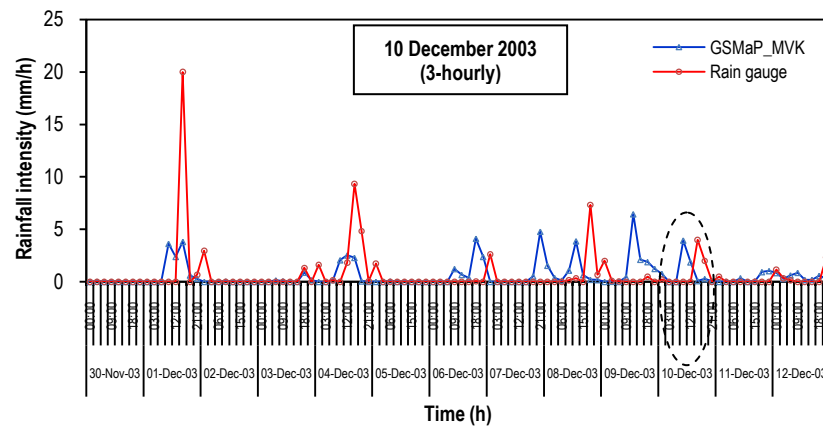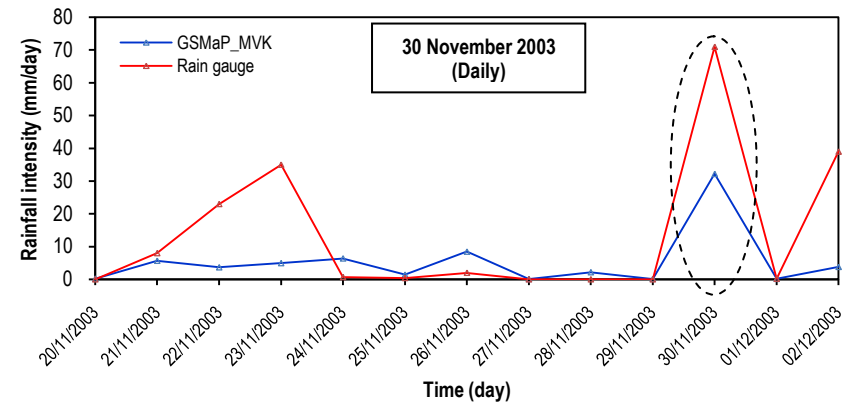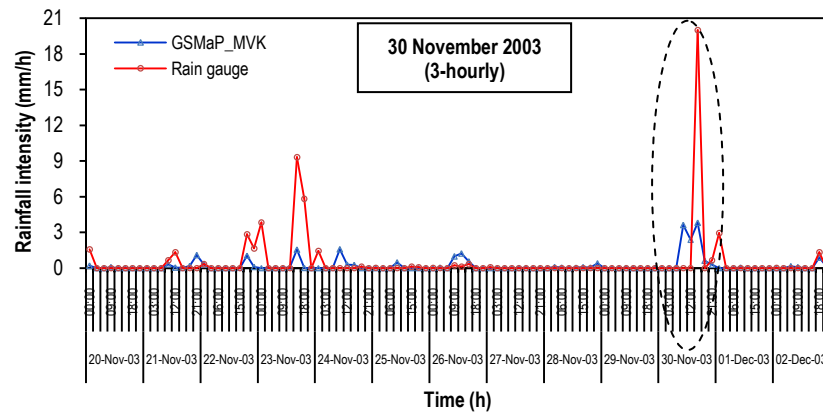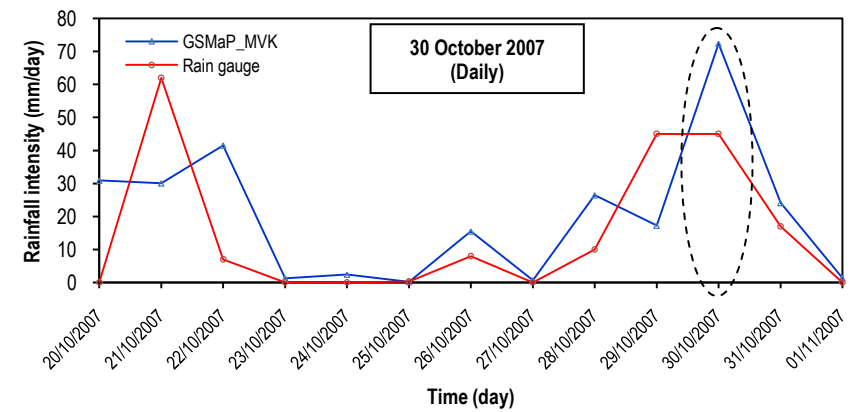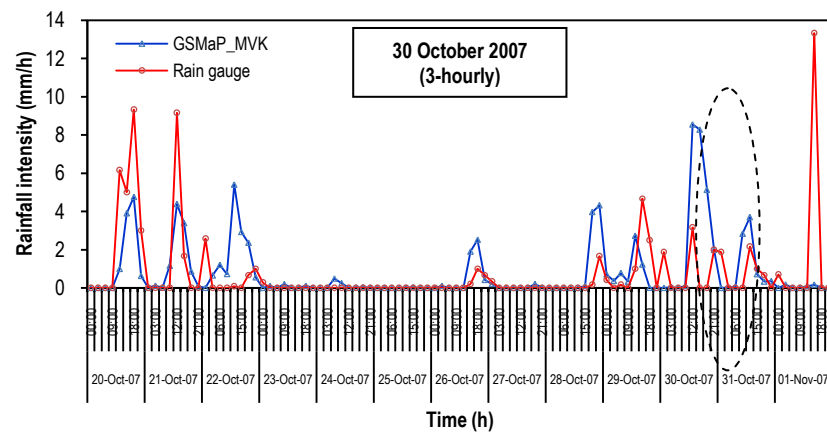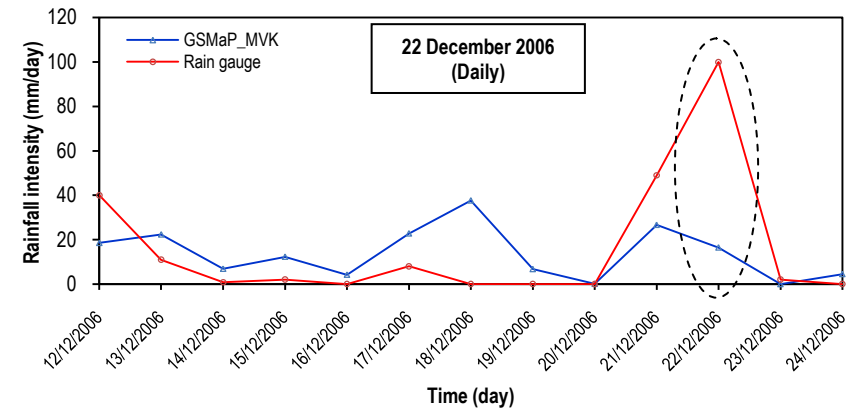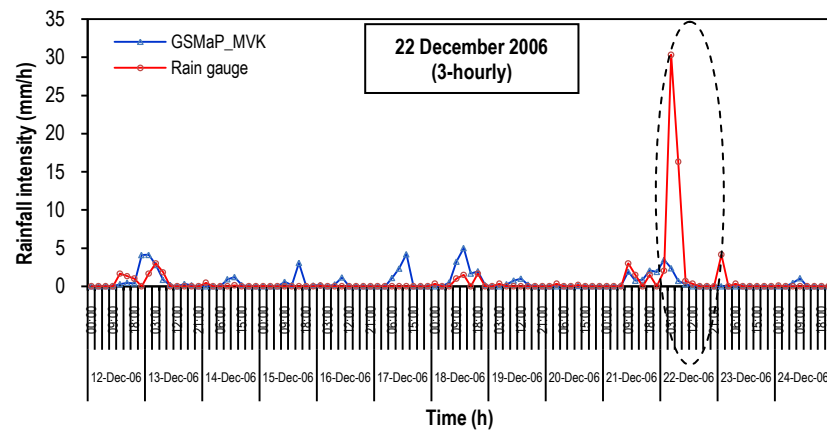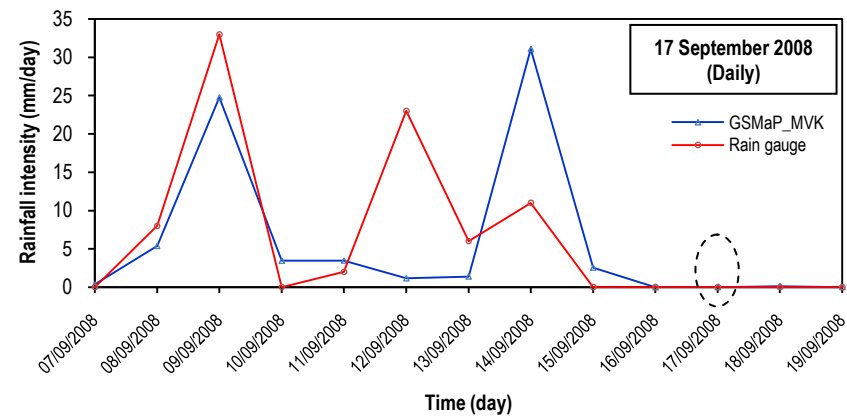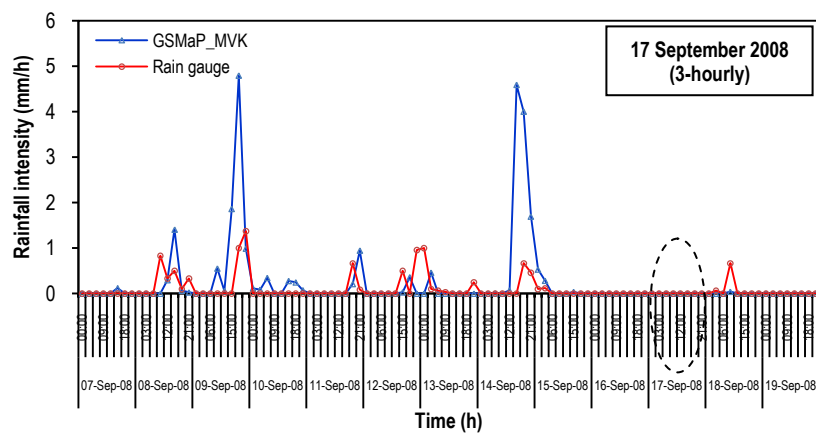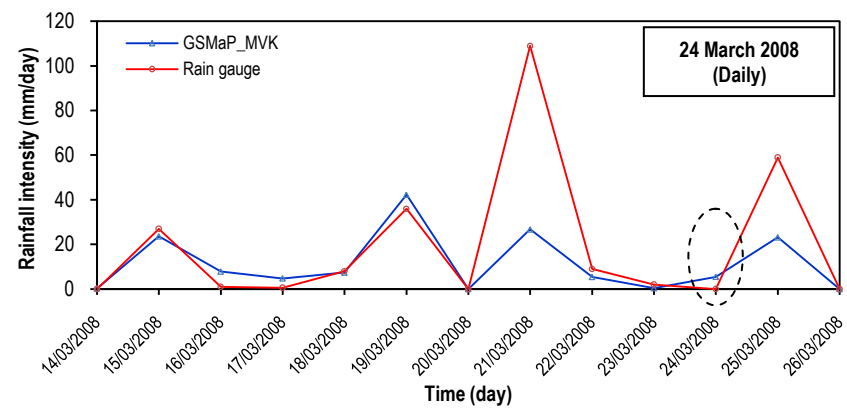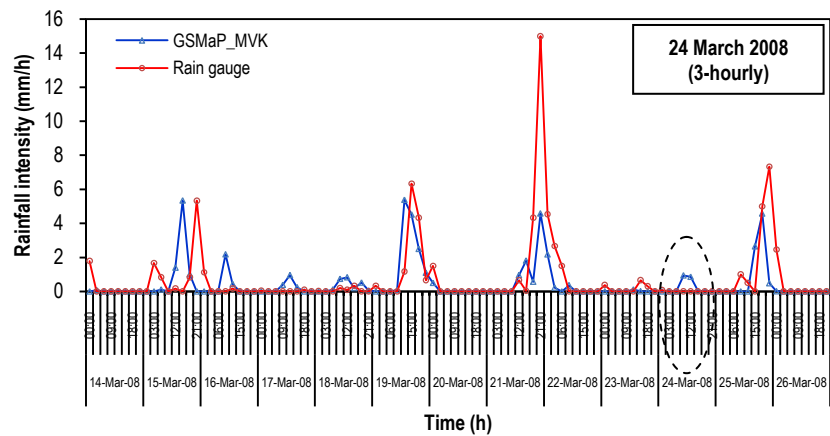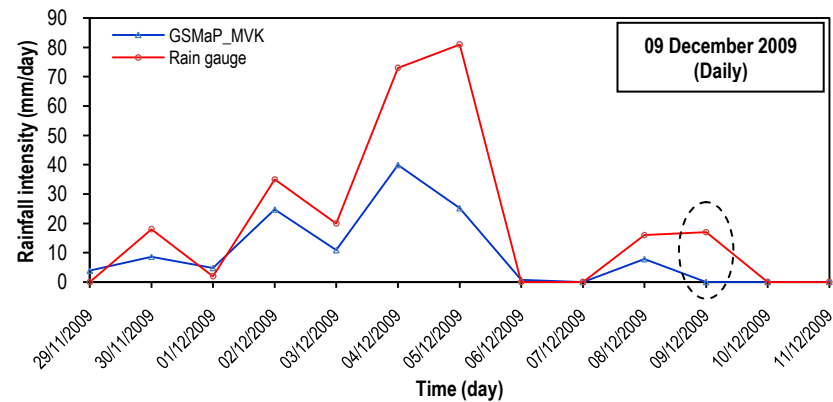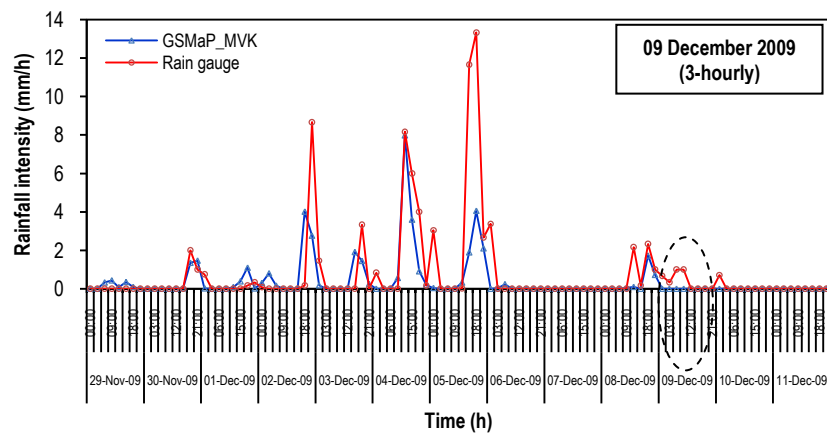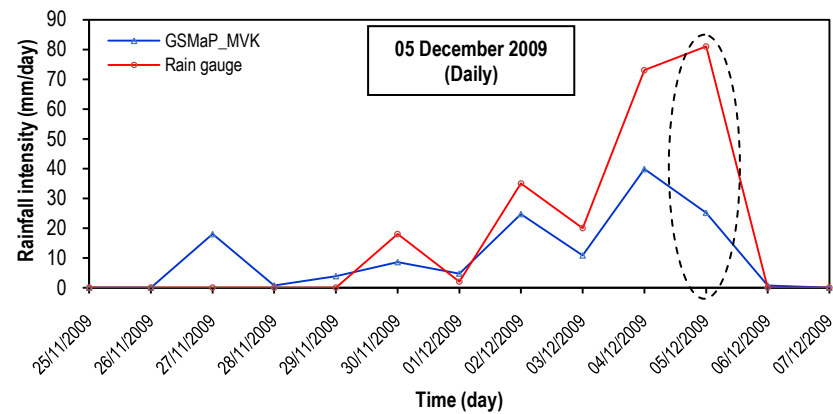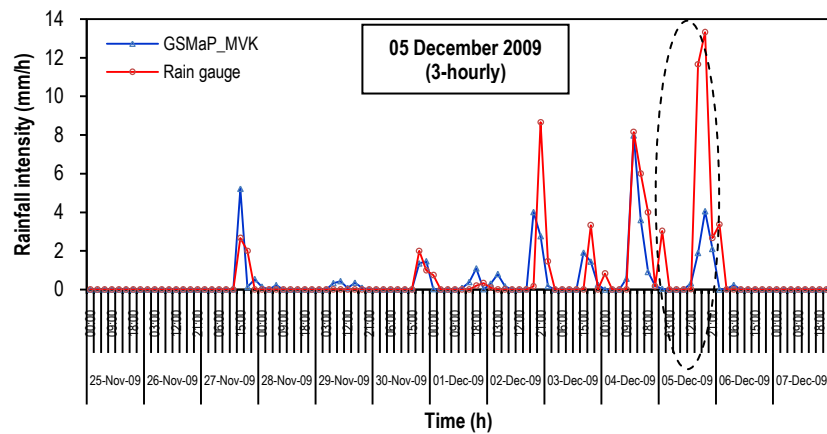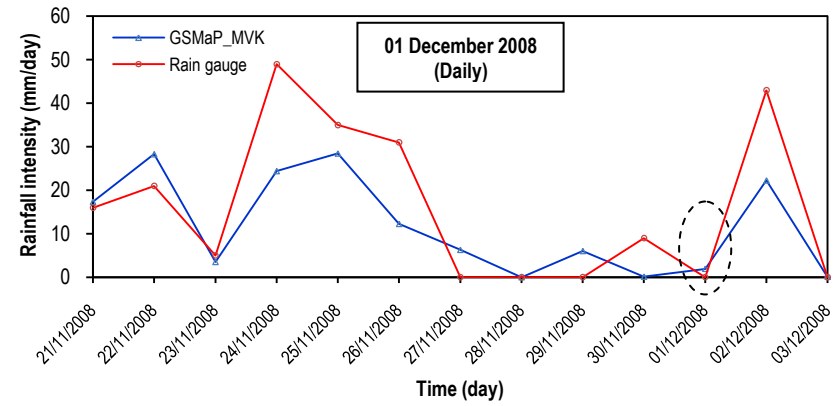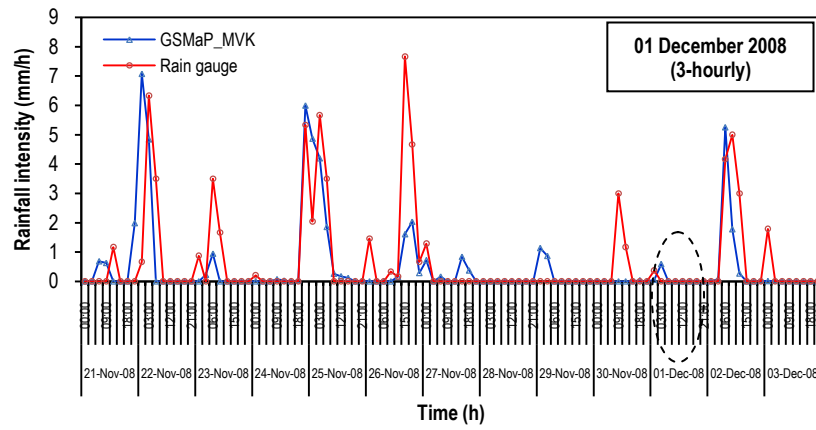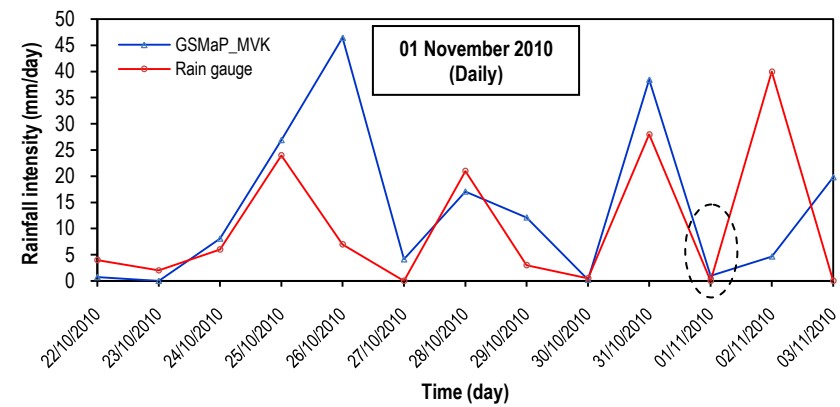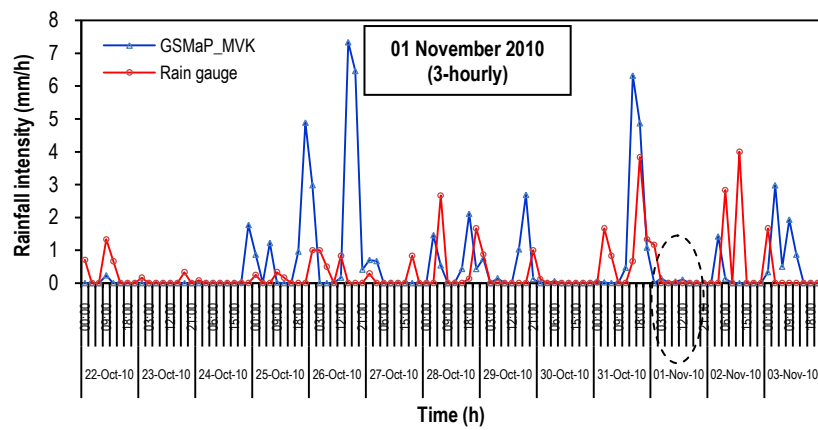
APPENDIX D   Time Series of 3-Hourly and Daily Rainfall Intensity for Flood Events in Samarinda City
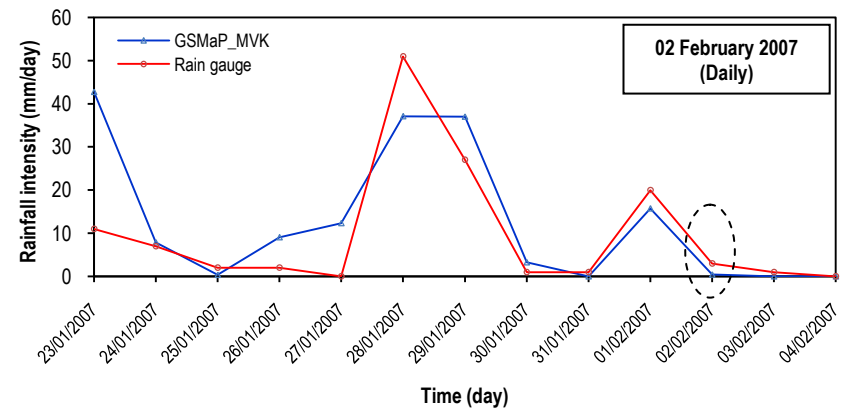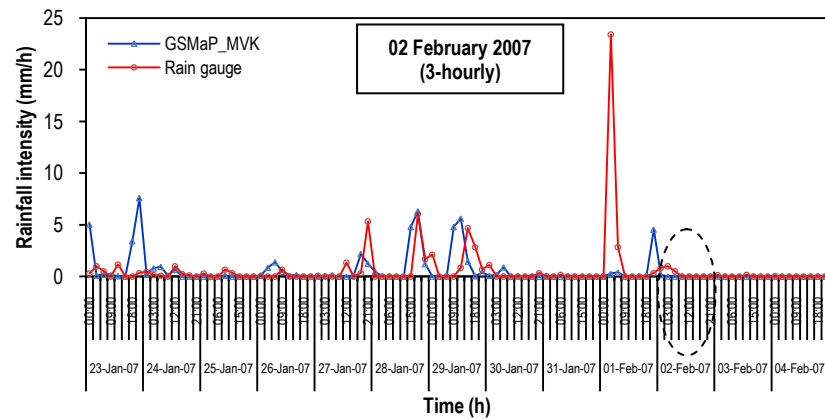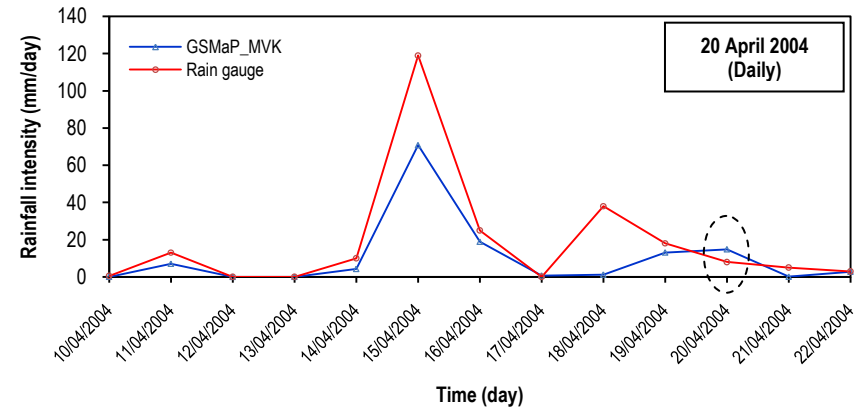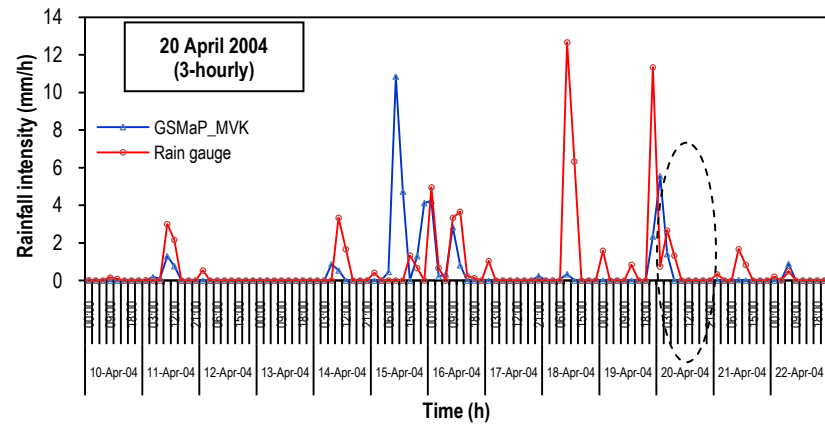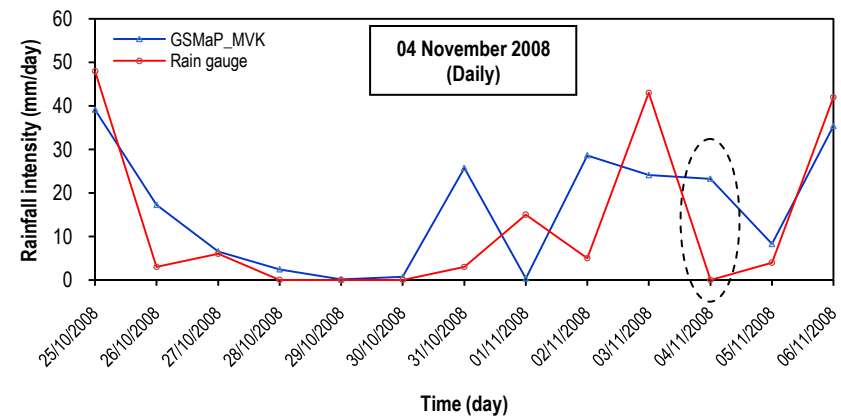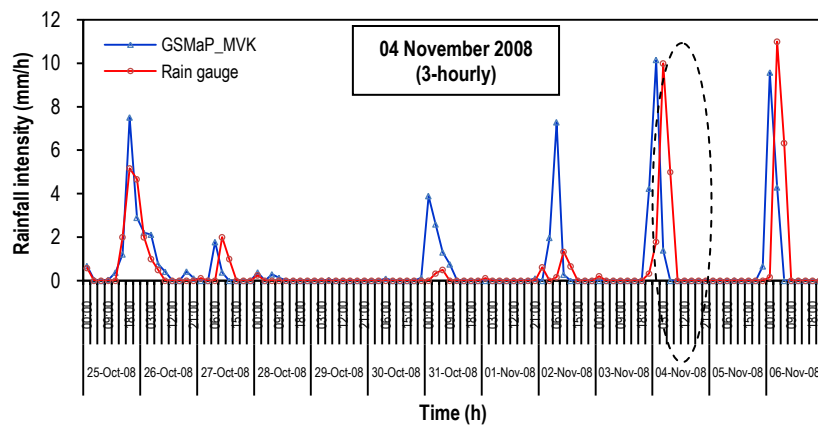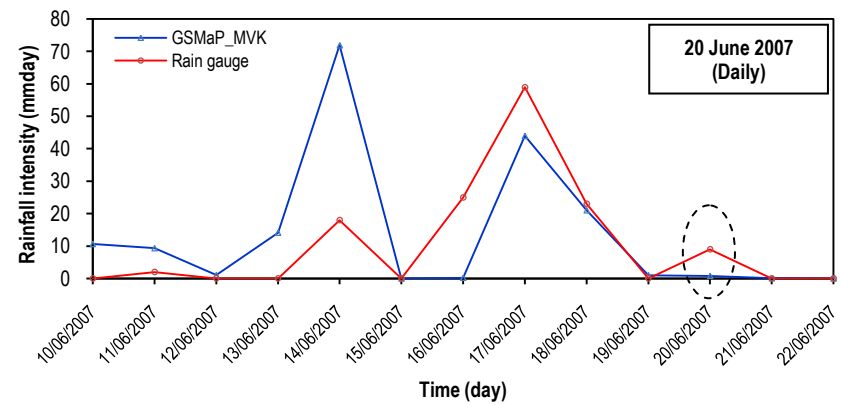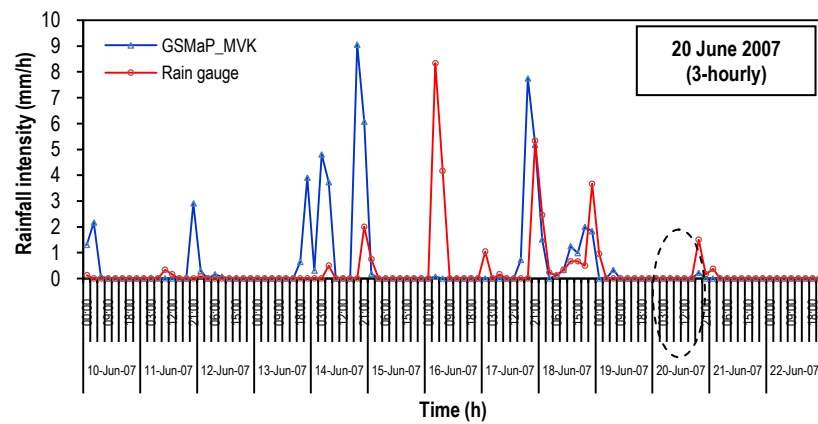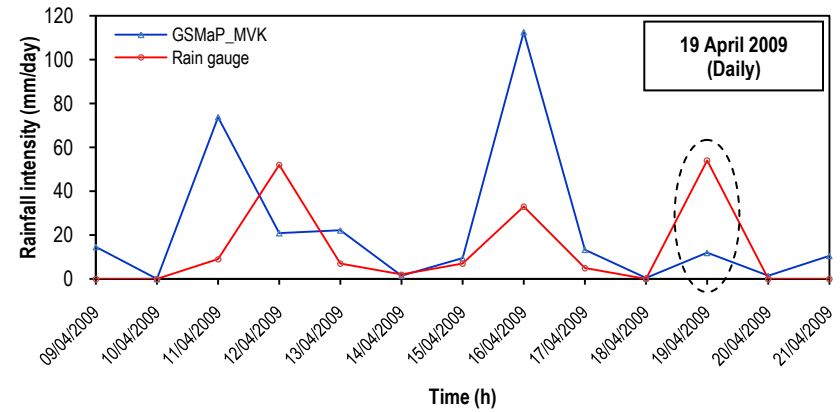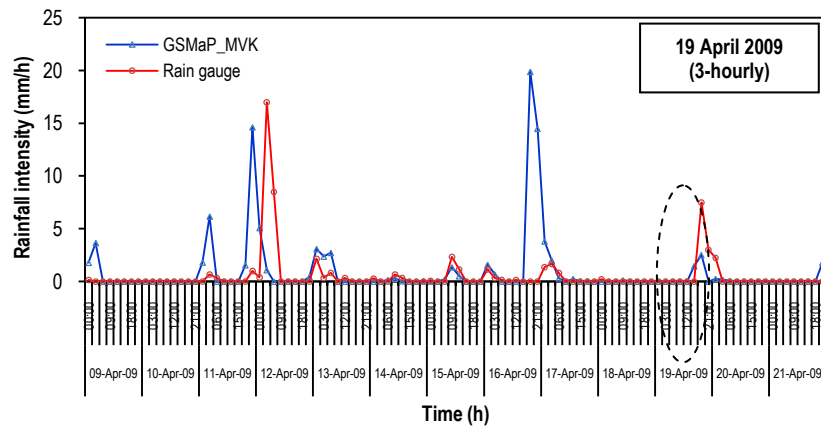
APPENDIX E   Time Series of 3-Hourly and Daily Rainfall Intensity for Flood Events in Manado City

116